

UNCLASSIFIED

AD NUMBER: AD0813989

LIMITATION CHANGES

TO:

Approved for public release; distribution is unlimited.

FROM:

Each transmittal of this document outside the Department of Defense must have prior approval of CG (April 1967), U.S. Army Electronics Command, Fort Monmouth, N. J. Attn: AMSEL-KL-EM.

AUTHORITY

ST-A USAEC LTR, 1 DEC 1967

AD

TECHNICAL REPORT ECOM-00264-9



AD813989

# STABLE FERRITES for R.F. APPLICATIONS

FINAL REPORT

by

C. O'NEILL and R. TENZER

APRIL 1967

CONTRACT DA-28-043-AMC-00264 (E)

INDIANA GENERAL CORPORATION

Keasbey, N. J.

#### Distribution Statement

Each transmittal of this document outside the Department of Defense must have prior approval of CG, U.S. Army Electronics Command, Fort Monmouth, N. J.  
Attn: AMSEL-KL-EM

# ECOM

UNITED STATES ARMY ELECTRONICS COMMAND · FORT MONMOUTH, N.J.

## NOTICES

### **Disclaimers**

The findings in this report are not to be construed as an official Department of the Army position, unless so designated by other authorized documents.

The citation of trade names and names of manufacturers in this report is not to be construed as official Government endorsement or approval of commercial products or services referenced herein.

### **Disposition**

Destroy this report when it is no longer needed. Do not return it to the originator.

TECHNICAL REPORT ECOM - 00264-9

STABLE FERRITES FOR R.F. APPLICATIONS

FINAL REPORT

1 July 1966 to 31 December 1966

Report No. 9

CONTRACT DA-28-043-AMC-00264 (E)

DA Task Number ICO-24401-A-348-00-03

Prepared by

C. O'Neill and R. Tenzer

INDIANA GENERAL CORPORATION

Keasbey, N. J.

Distribution Statement

Each transmittal of this document outside the Department of Defense must have prior approval of CG, U. S. Army Electronics Command, Fort Monmouth, N. J.

Attn: AMSEL-KL-EM

### ABSTRACT

Material MF-9003 originally investigated under a previous Government contract was further developed under the present one. The more or less normal development techniques improved the material somewhat but in regards to stability of  $\mu_0$  and Q, serious deficiencies existed. Silicate additives, notably bentonite, were found to generally improve the stability of  $\mu_0$  and Q; e.g., one material with 10.25 weight percent bentonite was found capable of yielding a temperature curve of  $\mu_0$  with a TF of 0.7 PPM/°C. This sort of success prompted extensive investigation into additions of the silicate type; and another silicate, lead silicate, was found to give useful and promising results. Evidence is presented supporting the theory that these silicate materials are actually two phase systems.

A major problem found associated with the silicate additions was a severe change of Q with temperature. This problem was studied thoroughly and it was found that divalent iron was very closely related to it. Too much divalent iron results in a considerable loss of Q with decreasing temperature and too little divalent iron results in a considerable increase in Q with decreasing temperature. The best Q behavior can be obtained by controlling both the total iron content and the amount of divalent iron. The hypothesis is made that there exists a loss mechanism dependent principally on the thermal energy of the ions and that a second loss mechanism exists which is related to the divalent iron content. The second loss mechanism is apparently dependent on the measuring frequency and total iron content.

The silicate containing materials were further improved by adding thorium nitrate. Q values were generally increased and the dependence of Q on temperature was lowered. In the case of lead silicate additions, the value of Q at frequencies below 5 Mc/s was greatly improved; sufficient in fact to make the material MF-9060 the most promising material investigated.

Cup core properties were evaluated in comparison with toroidal properties and a very favorable correlation was found.  $\mu_0$  and Q values equal to those of toroids can be attained in an ungapped cup core shape. Gapping was found to result in lower Q values and in lower inductances.

Overall, material MF-9060 (containing lead silicate and thorium nitrate), is probably the best material developed. Although MF-9060 hasn't been fully evaluated from a stability point of view, its  $\mu_0$  and Q properties are good; it has a relatively low temperature dependence of Q, which can undoubtedly be made smaller; and it has a temperature dependence of  $\mu_0$  which is relatively small and linear (96 PPM/°C). The fact that it is linear means that compensation techniques can be employed. In the case of the body discussed in the report, a ceramic capacitor with a temperature coefficient of -96 PPM/°C could be used.

While materials were developed which meet some of the contract requirements, none of the materials completely fulfill the requirements as specified.

## FOREWORD

This program was conducted under the guidance of the Electronic Parts and Materials Division, Electronic Components Laboratory, USAECOM, with Mr. William Skudera serving as project engineer initially, and Mr. Walter Malinofsky serving in the latter phase of the contract.

## TABLE OF CONTENTS

Abstracts	i
Foreword	ii
List of Graphs and Tables	v
I Purpose of Project	1
II Introduction and Definition of Terms Used	2
III Factual Data	4
Task A - Stable Ferrites for the Frequency Range 1 to 12 Mc/s	
Phase I - Development and Evaluation of Existing Materials	4
Part a - Studies on Formulation Variations and Forming Techniques on a Ni-Zn Ferrite	4
Part b - Overall Stability of $\mu_s$ and Q	11
Phase II- Development and Evaluation of New Materials	16
Part a - Silica Additions to MF-9304 Material	16
Part b - The Behavior of Q with Temperature	19
Part c - Physical and Chemical Composition	22
Part d - Investigation to Re- solve the Problem of the Change in Q with Temperature	26
Phase III- Investigations on the Geometry and Performance of Cup Cores	29

TABLE OF CONTENTS - (continued)

	Phase IV - Applicability of Materials Investigated toward Providing a Stable Radio Frequency Cup Core	33
	Task B - Stable Ferrites for the Frequency Range 8 to 32 Mc/s	35
IV	Conclusions	36
V	Appendices	38
	1 Magnetic Measurement Methods	38
	2 Calculation of Effective Initial Permeability	42

LIST OF GRAPHS

<u>GRAPHS</u>	<u>DESCRIPTION</u>
118	$\mu_o Q$ vs Frequency for Material MF-9003 with $Fe_2O_3$ Content Varied (Milling Time - 128 Hours)
119	$\mu_o Q$ vs Frequency for Material MF-9304 with $Fe_2O_3$ Content Varied (Milling Time - 128 Hours)
120	$uof \cdot \mu_o Q$ for MF-9003 and MF-9304 with $Fe_2O_3$ Content Varied
121	$\mu_o Q$ vs Frequency for a Ni-Zn Ferrite with $Fe_2O_3$ Content Varied (Air Atmosphere)
122	$\mu_o Q$ vs Frequency for a Ni-Zn Ferrite with $Fe_2O_3$ Content Varied (Oxygen Atmosphere)
123	$\mu_o Q$ vs Frequency for a Ni-Zn Ferrite with $Fe_2O_3$ Content Varied (Nitrogen Atmosphere)
124	$uof \cdot \mu_o Q$ vs $Fe_2O_3$ Content for a Ni-Zn Ferrite (Three Atmosphere Conditions)
125	$\frac{\Delta \mu_o}{\mu_o} \%$ vs DC Biasing Field for Material MF-9304
126	$\frac{\Delta \mu_o}{\mu_o} \%$ vs Applied Signal Voltage for Material MF-9304
127	Disaccommodation for Material MF-9304 $\frac{\Delta \mu_o}{\mu_o} \%$ vs Time at 25 C
128	$\frac{\Delta Q}{Q} \%$ vs Applied Signal Voltage for Material MF-9304
129	$\frac{\Delta Q}{Q} \%$ vs Temperature for Material MF-9304 and Powdered Iron
130	$\frac{\Delta \mu_o}{\mu_o} \%$ vs Temperature for Material MF-9353 with Additions of Bentonite, Kaolin and Silica
131	$\mu_o Q$ vs Frequency for Material MF-9353-S (Three Batches)
132	$\frac{\Delta \mu_o}{\mu_o} \%$ vs Temperature for Material MF-9353-S (Three Batches)

LIST OF GRAPHS - (continued)

<u>GRAPHS</u>	<u>DESCRIPTION</u>
133	Disaccommodation for Material MF-9353-S/1 $\frac{\Delta\mu_o}{\mu_o}$ % vs Time at 25°C (Fired: 1130°C/8 hours)
134	$\frac{\Delta\mu_o}{\mu_o}$ % vs DC Biasing Field for Material MF-9353-S/1 (Fired: 1130°C/3 hours)
135	$\frac{\Delta\mu_o}{\mu_o}$ % vs Driving Voltage at 5 Mc/s for Material MF-9353-S/1 (Fired: 1130°C/3 hours)
136	$\frac{\Delta Q}{Q}$ % vs Temperature for Material MF-9353-S
137	$\frac{\Delta Q}{Q}$ % vs DC Biasing Field for Material MF-9353-S/1 (Fired: 1130°C/8 hours)
138	$\frac{\Delta Q}{Q}$ % vs Driving Voltage at 5 Mc/s for Material MF-9353-S/1 (Fired: 1130°C/8 hours)
139	$\frac{\Delta Q}{Q}$ % vs Temperature for Material MF-9353-S with Fe <sub>2</sub> O <sub>3</sub> Content Varied
140	$\frac{\Delta\mu_o}{\mu_o}$ % vs Temperature for Material MF-9353-S with Fe <sub>2</sub> O <sub>3</sub> Content Varied
141	$\frac{\Delta Q}{Q}$ % vs Temperature for a Ni-Zn Ferrite with 49.94 Mol % Fe <sub>2</sub> O <sub>3</sub> for Six Firing Temperatures
142	$\frac{\Delta Q}{Q}$ % vs Temperature for a Ni-Zn Ferrite with 49.94 Mol % Fe <sub>2</sub> O <sub>3</sub> for Three Atmosphere Conditions and 1185°C Firing Temperature
143	$\frac{\Delta Q}{Q}$ % vs Temperature for a Ni-Zn Ferrite with 47.84 Mol % Fe <sub>2</sub> O <sub>3</sub> For Three Atmosphere Conditions and 1155°C Firing Temperature

LIST OF GRAPHS - (continued)

<u>GRAPHS</u>	<u>DESCRIPTION</u>
144	$\frac{\Delta Q}{Q}$ % vs Temperature for a Ni-Zn Ferrite with 51.96 Mol % Fe <sub>2</sub> O <sub>3</sub> for Three Atmosphere Conditions and 1195°C Firing Temperature
145	Magnetic Loss, $\mu''$ , vs Temperature at 5 Mc/s for a Ni/Zn Ferrite with Fe O Content Varied
146	Magnetic Loss, $\mu''$ , vs Temperature at 1 Mc/s for a Ni-Zn Ferrite with Fe O Content Varied
147	Magnetic Loss, $\mu''$ , vs Temperature at 10 Mc/s for a Ni-Zn Ferrite with Fe O Content Varied
148	Magnetic Loss, $\mu''$ , vs Temperature at 5 Mc/s for a Ni-Zn Ferrite
149	$\mu_o$ vs Temperature Through T <sub>c</sub> for Material MF-9353 with 0.0 and 1.1 Weight % Alumina
150	$\mu_o$ vs Temperature Through T <sub>c</sub> for Material MF-9353 with 2.8, 5.4 and 8.0 Weight % Silica
151	$\mu_o$ vs Temperature Through T <sub>c</sub> for a Ni-Zn Ferrite with 5.4 and 10.25 weight % of Bentonite
152	$\mu_o$ vs Temperature Through T <sub>c</sub> for Material MF-9353 with 5.4 and 10.25 Weight % Kaolin
153	$\mu_o Q$ vs Frequency for Materials MF-9622, -9632, -9633 and -9060
154	$\frac{\Delta \mu_o}{\mu_o}$ % vs Temperature for Materials MF-9622, -9632, -9633 and -9060
155	$\frac{\Delta Q}{Q}$ % vs Temperature for Materials MF-9622, -9632, -9633 and -9060

### LIST OF GRAPHS

<u>GRAPHS</u>	<u>DESCRIPTION</u>
156	$\mu_o Q$ vs Frequency for Materials MF-9055 and -9061
157	$\frac{\Delta \mu_o}{\mu_o} \%$ vs Temperature for Materials MF-9055 and -9061
158	$\frac{\Delta Q}{Q} \%$ vs Temperature for Materials MF-9055 and -9061
159	LQ vs Frequency for a Gapped Cup Core (1/4" O.D., 1/4" Height) Gap Varied with Shims of 0.0033", 0.0064" and 0.0098" Thickness (8 Turn Coil)
160	LQ vs Frequency for a Gapped Cup Core (1/4" O.D., 1/4" Height) Gap Varied with Shims of 0.0033", 0.0064" and 0.0098" Thickness (10 Turn Coil)
161	LQ vs Frequency for a Gapped Cup Core (1/4" O.D., 1/4" Height) Gap Varied with Shims of 0.0033", 0.0064" and 0.0098" Thickness (12 Turn Coil)
162	LQ vs Frequency for a Gapped Cup Core (1/4" O.D., 1/4" Height) Gap Varied Between Center Post Only: 0.004" and 0.008" (8 Turn Coil)
163	LQ vs Frequency for a Gapped Cup Core (1/4" O.D., 1/4" Height) Gap Varied Between Center Post Only: 0.004" and 0.008" (10 Turn Coil)
164	LQ vs Frequency for a Gapped Cup Core (1/4" O.D., 1/4" Height) Gap Varied Between Center Post Only: 0.004" and 0.008" (12 Turn Coil)

## LIST OF TABLES

<u>TABLES</u>	<u>DESCRIPTION</u>
20	Magnetic Data on MF-9003 and Related Materials
21	uuf, $\mu$ , Q and TF Values for Ni-Zn Ferrites with a Ni/Zn Mol Ratio = 1.5 with Fe <sub>2</sub> O <sub>3</sub> Content Varied
22	Temperature Factor in Relation to FeO Content
23	Magnetic and Stability Data for Materials MF-9304, MF-9353-S, MF-9060 and Powdered Iron
24	Change in $\mu$ , and Q After Vibration and Shock
25	Magnetic Data for a Ni-Zn Ferrite with Silicate Additions
26	Chemical Composition of a Ni-Zn Ferrite with 10.25 Weight Percent Bentonite
27	Chemical Composition of Principle Ferrite Materials
28	Experimental Data for Coils for 1/4" Cube Cup Cores
29	Dimensions of Ultrasonically Machined Cup Cores
30	Magnetic Properties of Gapped Cup Cores and Their Comparison with Toroids

## I - PURPOSE OF PROJECT

The purpose of this project is to develop radio frequency ferrite magnetic core materials with a high degree of stability and with a high value of initial permeability and Q for use in stable tuned circuit applications.

The specific purposes of the project are as follows:

- a. to develop for the frequency range 1 to 12 Mc/s a specified cup core shape ferrite which has: an effective permeability of at least 25, a Q of at least 190 up to 8 Mc/s and a Q greater than 130 over the whole frequency range; an overall instability of not more than 0.4% in effective initial permeability or 20% in Q when tested with respect to drive sensitivity, temperature, disaccommodation, D.C. fields, shock and vibration.
  
- b. to develop for the frequency range 8 to 32 Mc/s a specified cup core shape ferrite which has: an effective permeability of at least 15, a Q of at least 150 over the entire frequency range; an overall instability of not more than 0.4% in effective initial permeability or 20% in Q when tested with respect to drive sensitivity, temperature, disaccommodation, D.C. fields, shock and vibration.

## II - INTRODUCTION AND DEFINITION OF TERMS USED

Under Government Contract DA-36-039-SC-89222, which immediately preceded the present one, we investigated several ferrite materials in the nickel-zinc system. One of these materials, designated MF-9003, was considered promising enough to be further developed under this contract.

The effort to accomplish the development of material MF-9003 to meet the objectives of this contract was organized into two separate tasks, Task A and Task B. Task B was to be worked on after Task A was successfully completed. Task A is to provide a stable ferrite for the frequency range 1 to 12 Mc/s and Task B is to provide a stable ferrite for the frequency range 8 to 32 Mc/s. Task B was never begun.

Task A was suborganized essentially into four phases. The phases were not entirely independent of each other and much of the work was done simultaneously. Briefly, phase I was concerned with applying more or less normal development procedures to the MF-9003 formulation to get the most out of the material. These procedures included preparing different kinds of pressing powders; using different forming techniques; determining optimum iron content; investigating raw materials to use; determining optimum firing temperature and type of firing atmosphere; etc. Also, Phase I concerned a complete evaluation of the magnetic properties and stability characteristics of the developed material; this included developing suitable measuring procedures.

Phase II concerned the development of new materials. New ideas had to be applied to the basic formulation in order to overcome some serious shortcomings of the material. These new ideas led to materials with improved properties but at the same time generated other problems which had to be solved.

Phase III concerned a study of cup core properties. Included here were investigations on cup core geometry and coil design. The properties of cup cores were related to toroidal properties and the effect of introducing an air gap in the cup core assembly was determined.

Phase IV puts together everything that was done in the other three phases and examines what was learned and how it can be applied to the objectives of the contract.

### Definition of Terms Used

The following definitions, facts and statements are presented to facilitate the reading of this report:

$$\text{TC} = \text{Temperature Coefficient} = \frac{\Delta\mu_0}{\mu_0\Delta T} \quad (\text{PPM}/^\circ\text{C}) \quad \begin{array}{l} \text{Calculation based} \\ \text{on } \mu_0 \text{ at } 30^\circ\text{C} \end{array}$$

$$\text{TF} = \text{Temperature Factor} = \frac{\Delta\mu_0}{\mu_0^2 \Delta T} \quad (\text{PPM}/^\circ\text{C})$$

$$\text{DAF} = \text{Disaccommodation Factor} = \frac{\Delta\mu_0}{2\mu_0} \quad (\text{PPM}/10 \rightarrow 100 \text{ minute cycle})$$

$$\text{uuf} = \text{upper useful frequency} = \text{That frequency for which} \\ \mu_0 Q = \frac{\text{max. } \mu_0 Q \text{ between 1 and 12 Mc/s}}{2.72}$$

**IF = Instability Factor** = The sum of the instabilities due to temperature, a.c. drive variations, d.c. field exposure, disaccommodation, shock and vibration, expressed in %. The worst combination of events is figured.

For  $\mu_0$  and Q measurements, toroids are measured with a General Radio Bridge. Number 30 gauge enameled wire is wound on toroids which are approximately 6 mm in O.D. and 3 mm in I.D. The number of turns is dependent on the frequency of measurement, but initially 20 turns are wound on the toroid. The value of  $\mu_0$  measured is technically the effective  $\mu_0$ , but essentially it is the true value of  $\mu_0$ . The Q values measured are for coil and ferrite but are treated as apparent Q's of the material.

III - FACTUAL DATA

TASK A

STABLE FERRITES FOR THE FREQUENCY RANGE 1 TO 12 Mc/s

PHASE I - DEVELOPMENT AND EVALUATION OF EXISTING MATERIALS

Part a. - Studies on Formulation Variations and Forming Techniques on a Ni-Zn Ferrite

Work under a preceding Government Contract (see Final Report SC-89222) provided us with a basic composition which we felt could be developed to meet, using appropriate cup core designs and engineering techniques, the requirements of this contract. This material has the designation MF-9003. It is a nickel-zinc ferrite and it is characterized by three facts: 1) a molar Ni/Zn ratio of 1.5; 2) the pressing powder is a fine particle size powder made by milling a highly calcined (1200°C) material in steel ball-mills for ~ 128 hours; 3) cobalt oxide content is kept low. The latter fact requires inclusion in the characterization because in many high frequency nickel-zinc ferrites, cobalt oxide is added in varying amounts for the purpose of increasing the stability of  $\mu_o$  (initial permeability) with temperature and reducing the loss factor. The addition of cobalt, however, adversely affects the overall stability. Since the prime objective of our work was to improve the overall stability, the cobalt oxide content was kept to a minimum.

Table 20

Composition Number	Fe <sub>2</sub> O <sub>3</sub> (Mol %)	Ni/Zn (Mols)	6.4 Mc/s			12.8 Mc/s			DAF( $\mu_o$ )	
			$\mu_o$	Q	$\mu_o Q$	$\mu_o$	Q	$\mu_o Q$	TF( $\mu_o$ ) (PPM/°C)	PPM/cycle
Contract Requirements			25	190	4750	25	125	3125	1.2	1.2
MF-9003	53.88	1.478	106	112	11870	110	64.5	7110	23.7	29.9
-9012	56.90	1.709	58	132	7660	61.1	105	6420	14.0	43.7
-9013	56.19	1.928	52.9	146	7720	55.2	121	6680	15.5	48.8
-9003-SD	50.07	1.477	89	74	6590	92.5	35	3250	16.6	--
-9003-G(b)	50.07	1.477	77	128	9850	80	94	7510	15.1	32

The magnetic properties of MF-9003 as known at the beginning of this contract are listed in table 20, the second line. In the first line of table 20 are the values called for in the contract requirements. It is

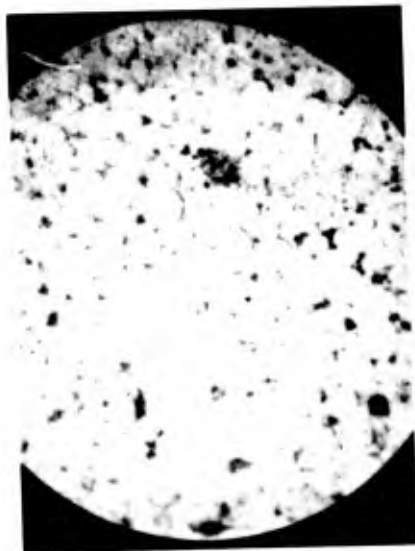
noted that the Q had to be increased by about 60% and the stability of  $\mu_0$  with temperature and time had to be improved by a factor of more than 25.

It was expected that the Q could be improved by increasing the nickel content of MF-9003. Although initial permeability becomes lower with increasing nickel content, the frequency at which the initial permeability curve goes through a dispersion becomes higher and this means that the magnetic losses are lower out to higher frequencies. To explore the effects of increased nickel content, two compositions, MF-9012 and 9013, were made with molar Ni/Zn ratios of 1.709 and 1.928 respectively. The best results obtained for their magnetic properties are shown in table 20. The Q was improved somewhat, particularly at the higher frequencies, and the TF values were lowered to about 2/3 of the value of MF-9003 material. The disaccommodation was higher but this was attributed to the higher iron content which could easily be lowered. The  $\mu_0 Q$  product of these two bodies at frequencies below 12 Mc/s was considered to be too low; so further development was not considered justified. It was felt at the time that a decrease in the  $\mu_0 Q$  product by a factor of 2 or more would be experienced in going from a toroidal to a cup core configuration and thus the toroidal  $\mu_0 Q$  product should be more than twice the value called for in the technical requirements of the contract. Development of MF-9012 and -9013 was thus terminated. We would concentrate on improving MF-9003 material instead.

Various ways to improve the properties of MF-9003 were tried. The forming process, for example, which is important in controlling shrinkage, pore size and reproducibility, was examined. There are many forming techniques, but one which is of principal importance is the technique in which dry powders coated with a small amount of some organic binder are poured into the cavity of a die and a top punch is lowered into the die cavity and a certain pressure is applied. Powders with very good flow characteristics are required with this method, so that the pressure will be uniform throughout the powder in the die cavity. If the pressure isn't uniform, the density of the pressed body will be inhomogeneous and strains will develop. These strains can result in physical defects, such as cracks and laminations, and in magnetic and electrical property changes, particularly in the Q.

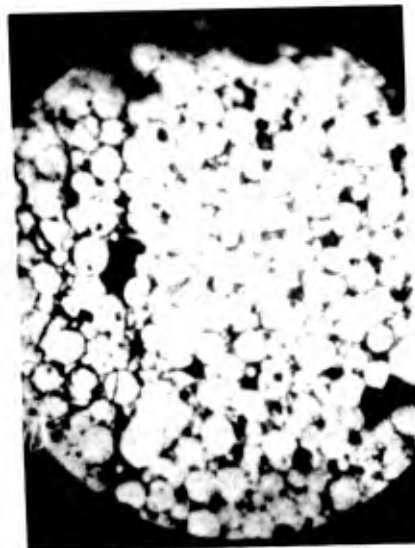
A very successful way to make a pressing powder with good flow characteristics is to spray dry the milled slurry to which has been added a small amount of an organic binder. This process yields a powder which consists of fine spherically shaped particles which flow almost like water. To make the flow properties even better, a material like zinc stearate can be added. This material is a light and very fine powder and is an excellent lubricant. It coats the spray dried particles with a thin film which reduces the friction between particles and allows them to glide easily over one another.

Applying spray drying techniques to MF-9003 material gave disappointing results (see table 20, 9003-SD). While there was some improvement in the temperature factor, the TF being lowered to 16.6 PPM/°C, the Q was reduced prohibitively. The reason for this is that higher firing temperatures are required in order to get a sufficiently sintered body. These higher firing temperatures result in large inhomogeneous grain growth. Work under the previous contract, SC-89222, demonstrated that magnetic losses are lower in nickel-zinc ferrites which have a fine, homogeneous grain structure. Why higher firing temperatures are required can be seen from the photograph in figure 12. The spray dried particles being very hard, because of the organic binder, do not compress well enough to fill the air spaces between them. Thus numerous large pores are present which cannot be removed by firing temperatures low enough to keep grain growth minimal. The poor compressibility of these spray dried particles is evident in the photograph where their identity is clearly visible even after firing. Spray dried powders were not considered suitable then for the purposes of this contract.



a  
Cup Core Centerpost  
Showing relatively closely packed  
spray dried aggregates with  
relatively small pore spaces

(X50)



b  
Cup Core Rim  
Showing loose packing of spray  
dried aggregates and large  
pore spaces.

(X50)

Figure 12

Dry granulations which form hard agglomerates, were also considered unsuitable for the same reason as the spray dried powders. A granular powder is one also made with organic binders but the milled slurry is dried in bulk quantities in a drying oven, and the dried cake is then pulverized and passed through an appropriate screen. This type powder yields somewhat better results inasmuch as the particles are more irregular and inhomogeneous in size and the resulting pores in the pressed body are smaller.

The obvious conclusion from all this was to try a soft powder and this was done with results that were very favorable. It should be understood that the powders we were working with in this evaluation of forming techniques were highly calcined, viz.  $\sim 1200^{\circ}\text{C}$ , and this means that the powder particles were quite hard to begin with. When organic binders are added in the slurry, all the particles tend to get a coating of binder and thus when the slurry dries, the powder becomes extremely hard and has to be crushed in a mortar with pestle in order to be screened. To prepare a soft powder, the slurry is dried and screened before adding binder. The powder at this stage is relatively soft. Now the organic binder can be added in a 10% water solution, and mixed in quickly and gently, forming a soft-moist powder. The moisture content can vary somewhat but its presence is beneficial in that less binder is required to hold the pressed piece together, and the pressing itself is easier due to its lubricating action. The powder should be immediately pressed while it is in the moist condition.

Using the same batch of MF-9003 from which the spray dried and dry granulation powders discussed above were made, a soft-moist powder was prepared. The first characteristic noted about the soft-moist powder was the improvement in green density (density was determined after binder was burned out of pressed bodies). The soft-moist powder gave green densities consistently in the range 2.9 to 3.0 g/cc whereas the spray dried and dry granulation powders gave densities in the range 2.4 to 2.8 g/cc. The best magnetic results obtained are listed in table 20 under MF-9003-G(b). The Q showed a definite improvement particularly in the neighborhood of 12 Mc/s, and the TF was reduced significantly, viz. 15.1 PPM/ $^{\circ}\text{C}$ . The increase in green density is considered an important factor in the improved magnetic results. The higher green density enabled lower firing temperatures to be used to attain the desired fired density. The success of this technique prompted us to employ it throughout the remainder of the contract.

To further improve the performance of MF-9003, particularly its overall stability, the nickel oxide raw material originally used was changed. In previous preparations a nickel oxide produced by Harshaw Chemical Co. was used. This nickel oxide contained a relatively high percentage of cobalt oxide and, as was noted in the first paragraph, cobalt has an adverse effect on the overall stability of  $\mu_0$  and Q. After performing

some experiments with the MF-9003 formulation, we determined that a more favorable raw material to use was a nickel oxide prepared from calcined nickel formate which was also obtained from Harshaw Chemical Co. This nickel oxide contains 0.1 weight percent or less of cobalt oxide and is a fine, more reactive powder. Subsequent formulations of MF-9003 were thus made with this nickel (formate) oxide, and to designate the fact that these were purer formulations (in reference to cobalt), a new composition number was assigned, namely MF-9304.

Undefined for the MF-9304 formulation has been the optimum iron content. Usually the ingredients of a material are specified to within 0.1% by weight or better, but in the case of MF-9304, this has been difficult. The difficulty stems from the fact that this material is milled for very long periods of time, ~ 128 hours, and the milling is done in steel ball mills with 5/8" steel balls. The result is that large inconsistent quantities of iron are milled into the material as a consequence of the abrasive action of the ferrite which has a high hardness due to its high calcining temperature. The batches that were initially studied all had different iron contents. Much experimental work was done in an effort to clarify this question.

The magnetic parameters considered in the study of iron content were the  $\mu_o Q$  product and the temperature behavior of  $\mu_o$ . It is not enough to study simply the iron content. Inasmuch as iron demonstrates two valence states in a ferrite, it is necessary to consider at the same time the oxygen content.

First we discuss the performance of  $\mu_o Q$  with frequency. If we evaluate the effect of iron on  $\mu_o Q$  versus frequency by considering the product  $uuf \cdot \mu_o Q$  ( $uuf$  = upper useful frequency), we find that this product seems to go through a minimum in the interval 50.5 to 52.5 mol %  $Fe_2O_3$ . In graph 118 and graph 119, the  $\mu_o Q$  vs. frequency curves for three bodies of formulation MF-9003 and five bodies of formulation MF-9304, prepared with various iron oxide contents, are shown. The  $uuf \cdot \mu_o Q$  products determined from these curves are plotted vs  $Fe_2O_3$  content in graph 120. Both series indicate a minimum between 50.5 and 52.5 mol %  $Fe_2O_3$ .

A third series, covering a range of  $Fe_2O_3$  content of ~ 48 to 52 mol %, was prepared and firings were made in atmospheres of air, 100% nitrogen and 100% oxygen. The best  $\mu_o Q$  vs frequency curves obtained from these materials are plotted in graphs 121, 122 and 123 for the air, oxygen and nitrogen firings respectively. In graph 124, the  $uuf \cdot \mu_o Q$  products are plotted vs  $Fe_2O_3$  content for the three atmosphere conditions. Again, the same trend as described in the previous paragraph is noted. In this case, however, the  $uuf \cdot \mu_o Q$  product is seen to drop again for values of  $Fe_2O_3$  content as low as 48 mol %. This is understandable since even though the  $Q$  improves with a deficiency of iron, there comes a point where the lattice becomes so deficient in iron that  $Q$  must drop

Table 21

uuf·μ<sub>o</sub>Q and TF Values for Ni-Zn Ferrites with a Ni/Zn Mol Ratio = 1.5  
With Fe<sub>2</sub>O<sub>3</sub> Content Varied

Material MF-	Fe <sub>2</sub> O <sub>3</sub> (Mol %)	FeO (Wt %)	Firing Temp. (°C)	uuf (Mc/s)	μ <sub>o</sub> Q	uuf·μ <sub>o</sub> Q	TF (PPM/°C)	Den. (g/cc)	5 Mc/s μ <sub>o</sub>
9029	47.84	0.08	1155		2575	41480	27.5	4.57	70
9029	47.84	0.08	1180	16.1			20.8	4.76	84
9031	49.10	0.07	1170	16.3	3460	56400	21.0	4.78	105
9032	49.54	0.10	1175	16.2	3990	64550	21.4	4.75	110
9033	50.13	0.17	1170	18.8	2612	49100	13.1	4.67	79
9030	51.96	0.31	1195	15.0	3717	55780	18.2	4.64	90
9029	47.84	0.08	1155	22.0	2870	63190	22.3	4.63	55
9031	49.10	0.09	1155	16.6	4855	80500	18.7	4.70	86
9032	49.54	0.10	1175	15.4	5515	85000	19.3	4.76	100
9033	50.13	0.27	1200	16.1	5200	51500	14.8	4.62	91
9030	51.96	0.54	1195	12.7	4415	56050	14.5	4.67	88
9029	47.84	0.85	1150	12.8	3098	39600	12.5	4.89	89
9031	49.10	0.81	1110	18.7	2650	49580	14.8	4.70	71
9032	49.54	0.83	1140	12.4	3717	46100	14.0	4.64	98
9033	50.13	0.72	1110	12.0	3900	46790	16.0	4.56	58
9030	51.96	1.95	1110	15.5	3863	59820	20.5	4.54	63
9030	51.96	2.01	1195					4.83	112

again and the permeability along with it. The data, as presented in table 21, indicates overall, that a formulation slightly deficient in iron and fired in an air atmosphere will yield the best values for  $\mu_o$  and Q. (For additional information, see Report No. 4, p. 14.)

In regards to the temperature behavior of  $\mu_o$ , the results are rather limited. Consider the data in table 21. Generally, the TF values for any combination of iron oxide content and firing atmosphere are high; the lowest value being only 12.5 PPM/°C. This is hardly a suitable value for the purposes of the contract but on the other hand, it is a relatively low value for this formulation. If the best TF value for a given composition, i.e., a given iron oxide content, is extracted from the table, then it can be seen that no matter what the iron oxide content (at least in the range studied ... 48 to 52 mol %), the same TF value can be obtained by controlling the oxygen content of the firing atmosphere. For example:

<u>Fe2O3 mol%</u>	<u>TF</u>	<u>Atmosphere</u>	<u>Q</u>
47.84	12.5	N2	58
49.10	14.8	N2	90
49.54	14.0	N2	76
50.13	13.1	O2	69
51.96	<u>14.5</u>	Air	78

Avg. 13.8

For deficient iron formulas, it would appear that a nitrogen atmosphere is most favorable and that a controlled amount of oxygen is needed for stoichiometric and excess iron formulas. Unfortunately, it is noted that for these relatively low TF values, the Q values are also quite low. It does not appear that nitrogen firings are compatible with high Q values. (See also Report No. 4, p. 14.)

Because of this apparent influence of the atmosphere during firing, particularly the oxygen content, it is reasonable to inquire about the influence of divalent iron. Under the varied experimental conditions, one could expect a variety of divalent iron contents in the materials studied. This is so, and a compilation of some of these results is shown below in table 22. Of primary interest here is the relation of divalent iron to TF, and this is the data accumulated in table 22. It is evident that other factors are involved in the temperature behavior of  $\mu_o$  besides the FeO content, and as a matter of fact, the data does not indicate that the FeO content is seriously involved. It appears rather that the total iron is important and that the iron oxide content should be such that the ratio of trivalent iron ions to divalent metal ions should be  $\sim 2:1$  (i.e. near stoichiometric).

Table 22

Temperature Factor in Relation to FeO Content

		Total Iron expressed in Mol % Fe <sub>2</sub> O <sub>3</sub>						TF (PPM/°C) FeO (Wt %)
		47.84		49.94		51.96		
Atm		TF	FeO	TF	FeO	TF	FeO	
	O <sub>2</sub>	27.5	0.08	13.0	0.14	18.2	0.31	
	Air	22.3	0.08	13.5	0.21	14.5	0.54	
	N <sub>2</sub>	12.5	0.85	15.9	1.29	18.7	2.01	
	Firing Temp.	1155°C		1185°C		1195°C		

The improvement of MF9304 was also sought from another direction; that is, small additions of various cations like Al, Ca, Cr, Ho, and Li. The results of these experiments indicated that there was little, if any, benefit to be derived from these additions although it must be noted that most of the additions were in small quantities. One possible exception is the addition of ~1.0 weight percent of lithium oxide which yielded a TF of 9.9 PPM/°C for a nitrogen atmosphere firing. For further discussion on these additions, see Report No. 4, p. 15 and Report No. 5, p. 13.

Part b. - Overall Stability of  $\mu_e$  and Q

We have discussed so far only the various preparative developments that have gone into the MF-9304 material. In this section, the overall magnetic stability of the material is considered. The methods of measurement used are described in appendix 1 and will not be detailed here.

The formulation of MF-9304 studied had an iron oxide content of 48.86 mol percent, the molar nickel to zinc ratio was 1.535. Also evaluated was a powdered iron toroid for purposes of comparison. The powdered iron sample was a TH-P material made by Arnold Company. The results of all the measurements made are compiled in Table 23. At the bottom of the table an instability factor (IF) is given. An immediate glance at the IF values reveals that both powdered iron and MF-9304 material do not meet the stability requirements of the contract and, furthermore, that MF-9304 is farthest from meeting the requirements. As regards initial permeability, the most serious instability is that in connection with temperature. This instability has been discussed already in the

Table 23

Magnetic and Stability Data

For Materials MF-9304, MF-9353-S, MF-9060 and Powdered Iron

	Contract Requirements		Powdered Iron		MF-9304	MF-9353-S	MF-9060	
	12 Mc/s	5 Mc/s	5 Mc/s	12 Mc/s				
$\mu_e$	25	9.4	9.4	9.4	92	53	55.9	
C	190	173	173	160	153	126	187	
$\mu_e Q$	4750	1620	1620	1300	14000	6670	10400	
uuf	15.0 Mc/s	20.5 Mc/s	20.5 Mc/s		15.4 Mc/s	19.7 Mc/s	32.5 Mc/s	
uuf $\mu_e Q$	26,300	13,000	13,000		99,200	59,000	125,000	
	$\mu_e$	Q	$\mu_e$	Q	$\mu_e$	C	$\mu_e$	Q
TC (PPM/°C)			36	(ii) 187	1830	133	96	11%
TF (PPM/°C)			3.8		22.5	2.5	1.7	
DA (PPM)			0		-180	1100		
DAF (PPM)			0		-1.8	20.8		
DC Field (%)			0.09	-2.4	2.6	1.2		+0.3
(0-190 oe)								
(a.c. demagnetized)								
AC Drive (%)			-0.02	-3.7	1.2			.22 -12.5
(.5-3 volts)					(See p. 14)			
Shock					(" " " ")			
Vibration								

Total Instability (-50-85°C) 0.4% 20% 1.4% 20.5% 11% 68% 2.4% 150%

(i) Toroid dimensions are for unwound condition. (ii) -50-85°C

previous section. From the results presented there, it would seem improbable that a temperature stability equivalent even to powdered iron could be developed in the strictly tri-component system  $\text{Fe}_2\text{O}_3\text{-NiO-ZnO}$ . There is some indication that a TF of 10 PPM/ $^{\circ}\text{C}$  or somewhat less could be obtained, however, possibly with a linear temperature curve. With these characteristics it would be feasible to consider compensating techniques. This idea will be discussed later on in the report.

Of the other instabilities, the influence of d.c. fields appears to be the more serious. Initial experiments determined that the worse condition for exposure of a toroid to a d.c. field was to magnetize it across its diameter. The experiments led to some very interesting results which unfortunately we have not had the time to satisfactorily interpret. The sample toroids before measurement were demagnetized by two different methods, a.c. field and thermal (i.e., heating the toroid slightly above the Curie temperature). The behavior of  $\mu_0$  was different for each case. Although several toroids were measured, only the curves in graph 125 are presented since they are indicative of the results obtained.

For the thermally demagnetized condition, the change in  $\mu_0$  is generally in the negative direction; sometimes there is a small increase at low field strengths. This result is consistent with what could be expected since exposure to a magnetic field tends to align the vector of magnetization of each domain and reduce the number of domain walls. These effects will contribute to a decrease in initial permeability and this is what is seen in the experiment. A curious characteristic of the curve is that it tends to flatten out or even rise again in some instances at a field strength somewhere above 120 Oersted. We have not established an explanation for this behavior.

For the a.c. demagnetized condition, initial permeability increases as the d.c. field to which the sample toroid has been exposed gets higher. This behavior is opposite to that of the thermally demagnetized condition. This curve, too, shows a noticeable break and sometimes two breaks. The first break will occur usually at 80 gauss or higher. An explanation for these characteristics has not been established yet either. (For further details on d.c. field effects, see Report No. 3, p. 11.)

The stability of  $\mu_0$  is further influenced by the voltage of the applied a.c. signal. In the range of measurement, 0.5 to 3 volts, an almost linear increase of about 1.2% was found. A curve showing this trend is plotted in graph 126. The curve represents the average of three measurements. Obviously improvement is required in this regard too.

Disaccommodation appears to be the least serious of the instabilities concerning  $\mu_0$ . A disaccommodation curve is shown in graph 127 which

is the average of measurements on five samples. Disaccommodation in the time interval 10 to 100 minutes, is only 0.018%, and this is well within the limit we are allowed.

Shock and vibration tests were run on several samples but the results were inconclusive. The services of the U. S. Testing Company in Hoboken, New Jersey, were secured in connection with these measurements. Their equipment and methods of shocking and vibrating the test samples are consistent with the requirements of the U. S. Government specifications. The difficulty in interpreting the results of the measurements derives from the fact that the reproducibility of measurements on the Boonton Rx-Meter on a single sample shows a greater margin of difference than the differences noted in the measurements after shock and vibration. The effects due to shock and vibration are thus obscured by the lack of refinement in the measurement. Table 24 shows the data obtained from the experiments. The initial permeability was found to increase by an average of 0.22% after vibration and decrease by 0.48% after shock treatment. The reproducibility test, which consisted of 50 measurements, i. e., ten repetitions on each of five samples, showed  $\mu_0$  to vary from the mean value by + 0.43% and - 0.93%. (The lower  $\mu_0$  values were averaged and the higher  $\mu_0$  values were averaged separately to determine this range.) Thus the variation in the reproducibility test was greater than the changes noted after shock and vibration. One conclusion that might be drawn from this result is that the shock and vibration treatment had a stabilizing effect on  $\mu_0$ . At any rate, this possibility cannot be overlooked.

As regards Q, the most serious effect was found for the circumstance under which the applied signal voltage is increased to values as high as 3 volts. The average change in Q noted under these conditions is a decrease of about 37.2%. A curve representing the average of three measurements is shown in graph 128.

The next most serious effect was the change of Q with temperature. For this material, MF-9304, the temperature curve, graph 129, shows a generally negative slope. The TF of Q is -10.9 PPM/°C. Over the temperature range -50 to 85°C, this represents a change in Q of about 22% which is also in excess of the allowable limit. Graph 129 also shows the temperature curve of Q for the powdered iron sample.

Moreover, Q was found to change after exposure to a d.c. field. In this case, the Q increased as the d.c. field to which it was momentarily exposed became stronger. The change was relatively small; about -2.8%. In the case of powdered iron, the change in Q was of about the same value, -2.4%.

Shock and vibration effects on Q are noted in table 24 and the results are subject to the same remarks as made above in the discussion on  $\mu_0$ .

In the case of Q, the reproducibility test gave a change in Q of + 9.7% and - 7.3% from the mean value. Changes in Q resulting from the shock and vibration effects are less than the variation found in the reproducibility test. Again the conclusion might be drawn that the shock and vibration treatment had a stabilizing effect.

In the overall view, it was apparent that the MF-9304 material had some serious instabilities. In all aspects but one, viz.  $\mu_0$ , MF-9304 was inferior to powdered iron. The total instability for MF-9304 as given by the instability factor IF was 11% for  $\mu_0$  and 68% for Q. This compared with 1.4% for  $\mu_0$  and 20.5% for Q for the powdered iron material.

The normal methods of approach to the development of MF-9304, i.e., investigating forming techniques, use of different raw materials, small variations in amounts of basic constituents, firing temperature and atmosphere conditions, resulted in a certain degree of progress. The capability of these methods, however, to provide a significantly greater improvement in MF-9304 material was questionable. New approaches were required in the formulation of the body to strengthen the probability for success in meeting the contract objectives.

TABLE 24

CHANGE IN  $\mu_0$  AND Q AFTER VIBRATION AND SHOCK

<u>AFTER VIBRATION</u>			<u>AFTER SHOCK</u>			
NO.	$\frac{\Delta\mu_0}{\mu_0} \%$	$\frac{\Delta Q}{Q} \%$	STRESS	NO.	$\frac{\Delta\mu_0}{\mu_0} \%$	$\frac{\Delta Q}{Q} \%$
5	.37	2.25	20 G's	25	-.31	.32
6	.47	-.50		26	-.25	2.96
7	.49	-.56		AVG.	-.28	1.64
8	.04	-4.14				
9	-.01	0	50 G's	22	-.19	.16
10	.13	-5.15		29	-.13	2.65
11	.04	-2.73		AVG.	-.16	-1.25
AVG.	.22	-1.69				
			80 G's	12	-1.85	3.39
				13	-.60	1.99
				17	-.03	2.75
				AVG.	-.83	2.71
			OVERALL AVG.		-.48	1.27

## PHASE II - DEVELOPMENT AND EVALUATION OF NEW MATERIALS

### Part a. - Silicate Additions to MF-9304 Material

Prior to the completion of the work presented in Phase I, it became quite apparent that only a limited amount of success could be hoped for in the development of a three component ferrite in the nickel-zinc system to satisfy the requirements of this contract. New approaches, therefore, in the formulation of the basic body MF-9304 were required. These new approaches constitute the efforts of Phase II and are the subject of discussion in this section.

Before proceeding with a discussion, we should put the work of this phase in the proper perspective. Investigations under the previous contract (DA36-039-SC89222, see Final Report) demonstrated that greatly improved Q values could be obtained by making a body with a fine homogeneous grain structure. Such a body was obtained by using a highly calcined ( $\sim 1200^{\circ}\text{C}$ ) pressing powder of a very fine particle size. The average particle size of the powder was in the neighborhood of 0.04 microns, and it was made by milling the calcined raw material for periods of up to 128 hours. The fine grain structure not only improves the Q but, equally important, it extends the frequency range of high Q values to higher frequencies. A fine grain, dense structure is thus a fundamental characteristic sought for in the ferrite body under development.

The method described in the preceding paragraph has been successful in providing dense fine grain structures but it has two major drawbacks; 1) it uses an excessively long milling time which, from a production point of view, is very undesirable; 2) the long milling introduces a considerable amount of iron into the body which makes control of the iron content a big problem. It was considered desirable to eliminate, or at least minimize, both of these problems.

Leading to the development of these new materials was an attempt to make a spray dried powder which could be used for cup cores. At the same time, the powder was prepared in a way to eliminate the drawbacks discussed above. This was done by making a new mix which was nearly stoichiometric in iron content; calcining it at a low temperature,  $\sim 750^{\circ}\text{C}$ , and then milling for only a 32 hour period. The results obtained from this powder, however, only verified the findings made under the previous contract. The fired bodies demonstrated low Q values in the frequency range 5 to 12 Mc/s when sintered to a dense enough condition and, when fired at lower temperatures, the densities dropped to around 4 gm/cc and the  $\mu_0 Q$  product dropped sharply above 8 Mc/s, giving a low uuf (upper useful frequency) value. Also TF values were high, around 28 PPM/ $^{\circ}\text{C}$ .

One of the advantages of a fine particle size powder is its increased reactivity and the consequent lower temperature required for sintering to the needed density. The powder as prepared above is not a fine particle size powder and doesn't have this kind of reactivity. In order to make the powder work, a densifying agent had to be added. The densifying agents selected were kaolin, bentonite and silicic acid. Kaolin and bentonite are ingredients which had been successfully used in the manufacturing of barium ferrite. Ordinarily, silica has a detrimental effect on the magnetic properties of soft ferrites but these detrimental results were associated with high firing temperatures and with high permeabilities. In this case, the initial permeability did not have to be very high and the firing temperatures consequently could be low, as long as the minimum  $\mu_0$  was attained.

These silicate additions accomplished the densification at lower temperatures, which was desired. Also higher uuf values were obtained. Of more importance was the fact that TF values were considerably lowered. The effect of these additions is illustrated by the data compiled in table 25. This data was obtained from cores fired at 1130°C for 8 hours in a periodic box type kiln. Also, graph 130 shows the temperature curves for the 5.4 wt.% addition of the three ingredients and the 10.25 wt.% addition of bentonite. The most striking data to observe in this table are the TF values. All additions improved the temperature behavior of  $\mu_0$  over the basic composition, but the bentonite addition of 10.25 wt.% gave the remarkable value of 2.3 PPM/°C and this without serious loss of initial permeability. At the same time Q was maintained at a level reasonable at least in comparison with the results described in Phase I.

Table 25

	Addition (Wt.%)	Density	uuf (Mc/s)	uuf· $\mu_0$ Q	5 Mc/s		12 Mc/s		TF PPM/°C
					$\mu_0$	Q	$\mu_0$	Q	
Kaolin	0.0	4.03	13.4	47300	72.1	123	80.9	57	28.6
	2.8	4.75	13.5	59600	96.6	88.4	101	55	17
	5.4	4.40	20.5	58150	62.0	88.0	64.8	71	18
	10.25	4.40	39.0	61700	35.5	100	39	93	9
Bentonite	2.8	4.69	19.2	62900	73.3	89.2	75.2	69	15
	5.4	4.69	21.5	68800	73.0	96.6	69.2	81	6.6
	10.25	4.67	22.1	66650	52.3	130	55.7	95	2.3
Silica	2.8	4.76	16.2	56000	79.1	87.3	83	63	15
	5.4	4.65	28.2	62300	53.6	88.3	57.6	65	10.4
	8.0	4.42	43.0	74450	44.6	93.3	47	75	12

A subsequent attempt to duplicate this result with the original and with a second batch of material using the same firing technique was not successful. Probably, however, further trials with small variations of the firing temperature would have yielded similar results. Fast firing techniques as used in the development work discussed in Phase I were employed instead and this technique was found to yield even better results than the slow firing technique although higher firing temperatures were needed, e.g.  $\sim 1200^{\circ}\text{C}$ . The  $\mu_0 Q$  versus frequency curves and the temperature curves of  $\mu_0$  for three batches of MF-9353-S (the designation given to the 10.25 wt.% bentonite material) are shown in graphs 131 and 132 respectively. The S/1, S/3, and S/4 means the first, third and fourth batches of material. The results shown in these graphs attest to the fact that the magnetic characteristics are reasonably reproducible. The TF values, for example, are -0.7, -2.0 and -3.1 PPM/ $^{\circ}\text{C}$ . The Q values obtained with the fast firing technique are also higher, sometimes reaching near 190 at 5 Mc/s.

Needless to say, material MF-9353-S looked quite promising. Measurements of the other stability factors, however, had to be made before a final judgment could be reached, and these measurements were subsequently made. The results are listed in table 23. As for  $\mu_0$ , stability was improved over MF-9304 by a factor of more than 4 times with only disaccommodation showing a higher instability. The disaccommodation is still small, however, and essentially negligible (see Report No. 6, p. 9). Graphs 133, 134 and 135 show curves for disaccommodation, d.c. field behavior and a.c. drive behavior. As for Q, the story was a little different. While d.c. field and a.c. drive effects were less detrimental to the Q of MF-9353-S, than they were to the Q of MF-9304, the temperature factor of Q, TF (Q), was five times worse for MF-9353-S. It was found to drop by as much as 70% as the temperature decreased from  $25^{\circ}\text{C}$  to  $-50^{\circ}\text{C}$ . Graphs 136, 137 and 138 describe the behavior of Q with temperature, d.c. field and a.c. drive.

When this drastic decrease of Q with decreasing temperature was discovered, efforts, as far as material development was concerned, were concentrated primarily on trying to understand this problem and to resolve it while still maintaining the other improved characteristics in the body.

## Part b. - The Behavior of Q with Temperature

The temperature behavior of Q for bodies containing 2.8, 5.4, 8.0 and 10.25 weight percent of kaolin, bentonite and silica was measured and the data examined. All bodies were found to exhibit the same drastic drop in Q (see Report No. 7, graphs 105 and 106). The behavior obviously was not peculiar to bentonite. Silica, being the common constituent of these three ingredients, attracted our first suspicions. Investigation of a body containing 1.1 weight percent of alumina quickly removed this suspicion, however, as it showed an almost 60% decrease of Q with decreasing temperature (see Report No. 8, graph 108). Commercial high frequency bodies also showed this decrease and they contain neither silic<sup>a</sup> nor alumina. These latter bodies do contain a significant excess of iron, however, and thus the iron content, particularly the amount of divalent iron, became the object of considerable investigation.

To begin with, a series of four compositions, previously prepared, each containing a 10.25 weight percent addition of bentonite and each having a different iron content was studied. The compositions in this series, designated MF-9375, -9376, -9353-S/4, and -9377, contained 41.08, 42.86, 43.45, and 44.67 mol percent iron oxide respectively in regard to all constituents. In regard only to the iron, nickel and zinc oxide content, the mol percent of iron oxide was 47.58, 49.37, 50.39, and 51.9 respectively. The behavior of Q with temperature of a representative toroid of each of these compositions was measured and the toroid then analyzed chemically for its divalent iron content. The Q versus temperature curves are shown in graph 139. The FeO content was found to be 1.1, 1.9, 1.8 and 2.6 weight percent for MF-9375, -9376, 9353-S/4 and -9377 respectively. The drop in Q with decreasing temperature is seen to be less as the FeO content increases. At the same time, the temperature curves of  $\mu_o$ , graph 140, show a change of slope from positive to negative with this increase in FeO content. It would seem at first glance that the increase in FeO content has improved the temperature curve of Q and that increasing the FeO content still more would improve the temperature curve further. But it is to be noted that the slope of the curve on the low temperature side for each body is very nearly parallel and that at the higher temperature side, the curve is moving toward a greater and greater negative slope. Thus the curve is apparently moving towards lower temperatures as the FeO content increases and at the same time is developing a narrower "peak". Actually the system involved here is too complicated to get a good understanding of the influence of iron since it contains seven different cations. In order to facilitate an understanding of the influence of iron, both divalent and trivalent, a simpler system was examined, i.e., the three component system  $Fe_2O_3-NiO-ZnO$ .

In the course of our material development, a Ni-Zn ferrite was made which had an  $\text{Fe}_2\text{O}_3$  content of 49.94 mol percent. Firings at several different temperatures had been made with this material and cores from six of them were selected for measurement of Q versus temperature and for chemical analysis of the FeO content. The temperature curves of Q for these six bodies are shown in graph 141. For three of these bodies the measurement was extended down to  $-196^\circ\text{C}$ . The FeO content in weight percent is recorded on the graph. The range of firing temperature was from  $1140^\circ$  to  $1245^\circ\text{C}$ , a difference of over  $100^\circ\text{C}$ ; the FeO content varied from 0.13 to 0.37 weight percent. The significant change in appearance of the temperature curves makes it seem unlikely that it could be related to the relatively small variations in the FeO content. It seems more likely that the change is related to the firing temperature or rather to structural factors influenced by the firing temperature.

In a subsequent set of experiments, the firing temperature was kept constant,  $1185^\circ\text{C}$ , and the FeO content was varied by firing in atmospheres of different oxygen content, e.g., 100%  $\text{O}_2$ , air and 100%  $\text{N}_2$ . The results of the Q versus temperature measurements are shown in graph 142. This time there is a dramatic difference in the curves as the FeO content varies from 0.14 to 1.29 weight percent; the change in Q at  $-50^\circ\text{C}$ , going from  $\sim +15\%$  to  $\sim -69\%$ . The amount of FeO present, in weight percent is 0.14 for the oxygen firing, 0.21 for air and 1.29 for nitrogen firings. The oxygen firing curve shows the same FeO content as the  $1155^\circ\text{C}$  firing curve on graph 140 and their temperature curves are almost identical even though the firing temperatures differ by  $30^\circ\text{C}$ . The difference in the percent change of Q between the oxygen and air curves is  $\sim -28\%$ . It seems incredible that 0.07 weight percent FeO could make such a difference. But this result was for the stoichiometric iron oxide case. Next, the deficient and excess iron oxide cases are examined.

In the deficient iron case, the results were much the same as found above. Curves corresponding to an oxygen, air and nitrogen firing atmosphere are plotted in graph 143 for a body with 47.84 mol percent  $\text{Fe}_2\text{O}_3$ ; the FeO contents are 0.08, 0.08 and 0.64 weight percent respectively. The oxygen and air curves are very similar to each other and the nitrogen curve shows about a 60% drop in Q at  $-50^\circ\text{C}$ .

In the excess iron case, the oxygen, air and nitrogen atmosphere firings gave FeO contents of 0.31, 0.54 and 2.01 respectively. The oxygen and air curves, graph 144, show the same trend noted in the stoichiometric and deficient iron cases. With the nitrogen firing, where the FeO content has gone over 2 weight percent, the trend is still followed but the high FeO content has apparently caused a considerable narrowing of the peak which is evident in most of the other curves but which is usually rather broad, and has caused the peak to move toward the lower temperatures. The effect is that in the temperature range  $25^\circ$  to  $-50^\circ\text{C}$ ,

the performance of Q is improved over the performance of the air firing in which the FeO content was only 0.54 weight percent.

From the information available in these graphs, we can form some idea of what is taking place. Assuming that, among other factors, magnetic loss,  $\mu''$ , is a function of the thermal energy,  $E_T$ , of the atoms, i.e.  $\mu'' = f(E_T, \dots)$ , then we could expect the magnetic losses to become less as  $E_T$  decreased, or, in other words, Q would increase with decreasing temperature. This situation is exemplified by the oxygen curve in graph 143, which represents a very low FeO content, and which shows an almost linear behavior of Q throughout the temperature range -196 to 85°C. In essence, we are assuming that this curve shows the basic behavior of Q with temperature. Since the other Q curves are severely non-linear, we can assume that another loss mechanism is active whose effect is superimposed on the basic behavior of Q. This loss mechanism we can relate to the FeO content.

To see a little better the relation of the FeO content to this other loss mechanism, we consider the curves showing magnetic loss,  $\mu''$ , versus temperature. The excess iron oxide bodies whose Q versus temperature curves are described in graph 144 are the ones for which  $\mu''$  values are available down to -196°C and their  $\mu''$  versus temperature curves are shown in graph 145; the measuring frequency is 5 Mc/s. For 0.31 weight percent FeO, the curve shows a sort of swelling in the low temperature region. At 0.54 weight percent, the swelling has become quite pronounced and a peak is discernible at  $\sim -140^\circ\text{C}$ ;  $\mu''$  at this point is more than double the  $\mu''$  of the lower curve. At an FeO content of 2.01 weight percent, the peak is very pronounced and still at  $\sim -140^\circ\text{C}$ , with  $\mu''$  at this point being about 10 times the value of  $\mu''$  for the 0.54 weight percent FeO curve.

The same set of curves is shown also for measuring frequencies of 1 and 10 Mc/s, graphs 146 and 147. The value of  $\mu''$  at the peak of the 2.01 weight percent FeO curve increases with increasing frequency, e.g.,  $\mu''$  is  $\sim 38, 43, \text{ and } 56$  for 1, 5 and 10 Mc/s respectively. Also the peak is apparently at the same point,  $-140^\circ\text{C}$ , for 1 and 5 Mc/s, but shifts to  $\sim -123^\circ\text{C}$  at 10 Mc/s; in addition, the peak at 10 Mc/s has become much sharper. The 0.54 weight percent FeO curve shows just the reverse effect with frequency but on a smaller scale, e.g.,  $\mu'' \simeq 41, 40 \text{ and } 29$  as the frequency goes from 1 to 5 to 10 Mc/s. The same behavior is noted for the 0.31 weight percent FeO curves where  $\mu'' \simeq 21, 19 \text{ and } 17$  for 1, 5 and 10 Mc/s respectively.

In graph 148, a curve of  $\mu''$  versus temperature (at 5 Mc/s) is described for an iron deficient body. This curve corresponds to the nitrogen firing curve in graph 143. The FeO content is 0.85 weight percent. In this case the apparent peak of the loss curve is shifted considerably

toward a higher temperature, i.e., to  $\sim -85^{\circ}\text{C}$ . Apparently an increase in the iron oxide content causes the loss peak to shift toward lower temperature. We do not have further data to support that conclusion but it probably is correct.

### Part c. - Physical Structure and Chemical Composition

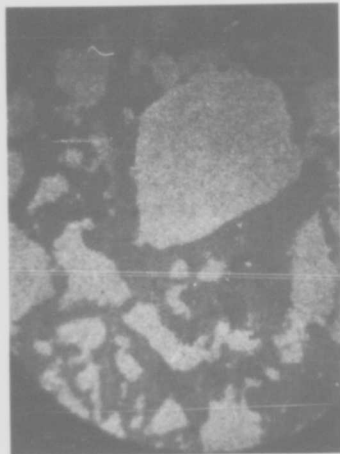
Before going on with the discussion of the behavior of Q in multi-component systems containing one kind of silicate addition or another, we will digress to discuss the physical structure and chemical composition of these silicate containing bodies. This discussion should aid in understanding the developmental steps taken in the last period of the contract.

Photomicrographs were made on a polished and etched sample of a large toroid of MF-9353-S (contains 10.25 weight percent bentonite). This toroid was one which had been fired for 8 hours at  $1130^{\circ}\text{C}$ . Four of these photographs are shown in figure 13. As is evident from photograph A, there was a heavy etching action over a large area of the surface. Within this area there are many crystallites of irregular shape and inhomogeneous size which were apparently unaffected by the etchant. It appears as if crystallites of a high nickel-zinc ferrite composition are imbedded in a matrix of a high silica content material. Photograph B shows the matrix at an edge of the large crystallite in photograph A; the magnification is 350X. A close look reveals that the structure of the matrix appears to consist of very fine crystallites and does not appear to be glassy. The fact that the matrix etched easily, and primarily, suggests that it is a high silica containing material. One could conclude then that MF-9353-S is a two phase system.

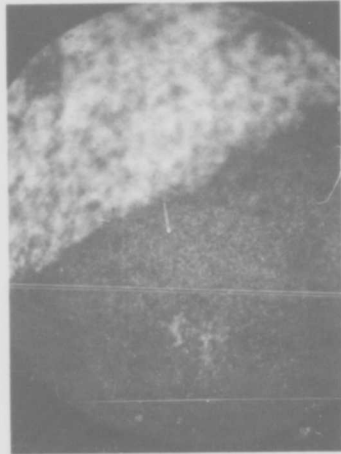
Photograph C is of the large crystallite in photograph A. This crystallite at 350X magnification does not show any clear, well-defined grain boundaries within itself but seems to show again on a smaller scale, the general structure shown in photograph A. Photograph D is of the polished surface before etching and it shows the body to be relatively dense.

A two phase system in soft ferrites would be a rather unique development. If this is the case, more evidence should be available to support it. Curie Temperature curves, using  $\mu_e$  as the measuring parameter, taken on several kaolin, bentonite, silica and alumina-containing bodies do provide some additional evidence. These curves also give some insight as to where the Al and Si ions are going.

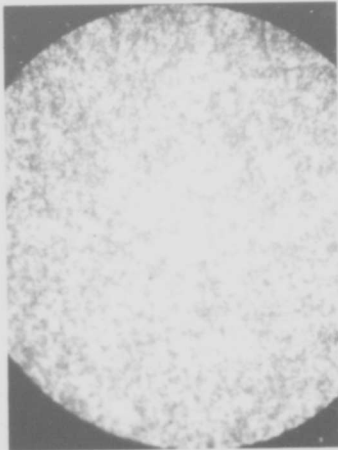
Consider first graph 149 and the Curie Temperature curve (curve A) for the Ni-Zn ferrite, MF-9353, to which the various additions were made. This curve shows a normal gradual increase of  $\mu_e$  with increasing temperature and then a peak and sharp drop off to a value near unity. There are no irregularities in the curve. The Curie Temperature determined from it is  $338^{\circ}\text{C}$ .



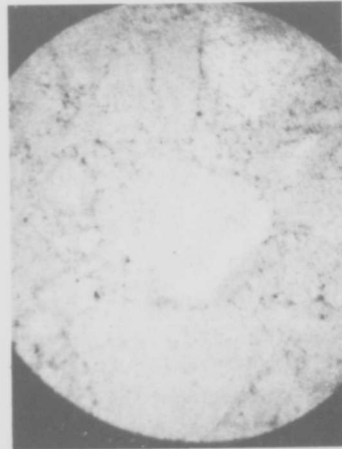
A(50X)



B(350X)



C(350X)



D(350X)

Fig. 13

Next, consider graphs 150, 151 and 152. These graphs show temperature curves for various additions of silica, bentonite and kaolin, respec-

and then three samples of the fine powder were treated with concentrated HF for 5, 10 and 15 minutes. The sample solutions were filtered and the filtrate and residue of each were chemically analyzed. The 15-minute sample was not completed. The FeO content was determined for the untreated powder and for the residue of the sample treated for 15 minutes. The data obtained is compiled in table 26.

Table 26

	<u>Residue</u> <u>(Crystallite Phase)</u>		<u>Filtrate</u> <u>(Matrix Phase)</u>	
	<u>(Wt %)</u>		<u>(Wt %)</u>	
	<u>5 min.</u>	<u>10 min.</u>	<u>5 min.</u>	<u>10 min.</u>
Fe <sub>2</sub> O <sub>3</sub>	66.35	66.72	52.48	51.11
NiO	18.04	17.85	12.19	13.99
ZnO	13.33	13.28	11.03	9.43
Al <sub>2</sub> O <sub>3</sub>	1.13	1.28	5.23	5.97
SiO <sub>2</sub>	.48	.30	18.42	18.70
Mg-CaO	.67	.57	.65	.80
	<u>FeO</u>			
	Whole sample		1.84 Wt %	
	Crystallite Phase		1.35 Wt %	

The two analyses are quite close, when comparing the 5-minute treatment to the 10-minute treatment. There are distinct differences in composition between the crystallite and the matrix phases. The principle differences are in the silica and alumina content wherein the matrix phase has by far a greater proportion of the Si and Al ions. This result is in agreement with the deductions made from the Curie Temperature curves. A contrary observation should be noted, and that concerns a sample sent to USAECOM for electron microprobe analysis. Its examination did not reveal to its examiners any more than a single phase system. The sample sent to them was the one from which the microphotographs shown on page 23 were made. X-ray diffraction studies were going to be performed and these would have been extremely helpful but there was not sufficient time available to do this.

Overall, the results support the idea that a two phase system exists in this ferrite. First of all, it is almost certain that six weight percent of silica could not have entered the spinel lattice; a consider-

tively. Seven curves are shown and their Curie Temperatures determined range from 318° to 328°C with an average value of 322°C. This is a very consistent result in view of the wide range of silica and alumina contents. Since only silica is the common ingredient in these three materials, and considering the drop in Curie Temperature associated with these additions, ~ 16°C, it would appear that some silica had entered the lattice of the crystallite material. Apparently only so much silica is allowed, however, or otherwise the Curie Temperature would have dropped progressively as the silica content increased.

Al ions are apparently present in both phases. Their presence is indicated in the matrix phase by the fact that the peak occurring at ~ 210°C in the  $T_C$  curves of silica is lowered as the alumina content increases. A  $T_C$  curve on MF-9353 to which 1.1 weight % alumina was added, showed no change in the Curie Temperature, see curve B, graph 149. This amount of alumina is equivalent to the amount in a 5.4 weight percent addition of bentonite. That no change occurred in the Curie Temperature would seem to preclude the possibility that Al ions entered the lattice of the crystallite phase but the change inherent to a 1.1 weight percent addition of alumina may only be 4 or 5°C. We don't have information available on this system to know for sure what the change should be. A strong indication that Al ions did enter the crystallite lattice is the fact that the FeO content of MF-9353 was increased from 0.37 to 1.2 weight percent upon the addition of 1.1 weight percent of alumina. A 100°C increase in firing temperature was required to sinter this body but the increase in FeO is not attributed solely to this. For another body whose iron content was near stoichiometric, the gain in FeO found for a 100°C increase in temperature was about 0.25 weight percent. So, the amount of FeO found in the alumina containing body is about twice that to be expected by the increase in firing temperature. This increase in FeO content also explains why the temperature curve of Q went from a positive slope to a severe negative slope (see graph 108, Report No. 8). The increase in FeO content would be due to the Al ions entering the octahedral sites of the spinel lattice and thus forcing trivalent iron ions to tetrahedral sites. Acquiring the Al ions results in a shortage of oxygen ions and a disruption of the electron balance. This situation is forthwith resolved by a change in valence of the iron from trivalent to divalent.

Further evidence in support of the idea of a two phase system is furnished by chemical analysis. To determine the chemical composition of each of the two phases presumed to be present, they should be separated. A mechanical separation would be difficult in view of the microscopic character of the constituents. A magnetic separation at an elevated temperature was tried but wasn't successful. A chemical separation was finally used. In the etching process, it was observed that the crystallites reacted very little, if at all, with a concentrated HF solution while the surrounding or matrix material reacted readily. Several fired toroids were thus crushed and ground to pass through a 325 mesh screen

able drop in Curie Temperature would have otherwise occurred. Secondly, the chemical analysis could not have shown such striking differences between filtrate and residue. As for the microprobe analysis, the beam has a finite dimension of the order of  $1 \mu$  in diameter, and it is unlikely that it has the resolving power necessary to detect a variation in composition in this ferrite. Going back to figure 13, photograph C shows in the large crystallite, a structure very much like the overall structure of the toroid; and from photograph B, we see that the easily etched area is undoubtedly composed of extremely fine grains  $\sim 1 \mu$  in size and the distance between grains is certainly not greater. The electron microprobe couldn't be expected to analyze this condition.

Part d. - Investigations to Resolve the Problem of the Change in Q With Temperature

Returning to the subject of the behavior of Q with temperature, we will discuss the effect of additions other than those of silica, bentonite and kaolin. The observations made in the preceding sections were considered in this work. Still of foremost concern was making a fine grain, dense ferrite and one with an appropriate amount of trivalent and divalent iron.

A dense, homogeneous, fine grain structure can be attained by firing a highly reactive powder at low temperatures. The powders prepared with a low temperature calcine and a relatively short milling time are not very reactive at low temperatures. Silicate additions as described earlier in this report were found to be effective in promoting sintering at lower temperatures. Improvement in the temperature behavior of  $\mu_o$  was also found, particularly for a 10 weight percent addition of bentonite. With kaolin, bentonite and silica, however, as previously described, the temperature behavior of Q was adversely affected.

In view of this something different had to be done. Either a different additive would have to be used but one which would hopefully yield the same benefits as the bentonite additive, or, some ingredient would have to be added with the bentonite which would modify its effect on the temperature behavior of Q.

One such additive in the first category is lead silicate and considerable experimentation was conducted to explore the effects of this ingredient. Lead silicate is a very effective fluxing agent. In this regard the monosilicate variety is more effective than the bisilicate variety in that it allows better sintering at lower temperatures. This is due to its much lower melting point. A ratio of  $PbO$  to  $SiO_2$  which is near the bisilicate ratio has given the best results from the point of view of magnetic properties, however. The amount of lead silicate which can be added to provide a beneficial effect is apparently in the range 6 to 11 weight percent. An amount of lead silicate less than this gives gradually increasing Q values but steadily worsening temperature curves of  $\mu_o$ , while higher amounts result in decreasing Q values and  $\mu_o$  values that are much too low.

High Q values are found, particularly at the higher frequencies, when the lead silicate content is between 6 and 11 weight percent. This is evident in the curves of  $\mu_o Q$  versus frequency which are plotted in graph 153 for three of the best bodies obtained from a strictly lead silicate addition; curves A, B and C. Q values in excess of 200 were measured at frequencies as high as 30 Mc/s. The Q tends to drop off a little at the lower frequencies, e.g. below 5 Mc/s, but their values are still reasonably good.

The temperature curves of  $\mu_o$  for two of these bodies, MF-9622 and -9633, are very good, see graph 154, curves A, B and C, particularly for MF-9633 which shows a TF of 0.0 PPM/°C within a tolerance of -0.2%. The low TF is probably due to the SiO<sub>2</sub> content. From the chemical formulas in table 27, it is seen that the SiO<sub>2</sub> content is 2.69, 3.22, and 4.0 weight percent for MF-9632, -9622, -9633 respectively and this can be correlated with the TF values which are respectively 7.4, 0.4 and 0.0 PPM/°C. For a similar body without SiO<sub>2</sub> but with ~ 5.3 weight percent PbO, the TF was found to be over 14 PPM/°C.

Unfortunately the temperature behavior of Q is not as good as that of  $\mu_o$ . For MF-9633, e.g., which is an iron deficient material, Q shows a more or less linear increase of ~ 45% as the temperature drops from 85 to -50°C, see graph 155. This behavior of Q is opposite to that of the bentonite containing bodies. For iron excess materials with a lead silicate addition, the Q versus temperature curves have a severely positive slope. Thus again it is found that an excess iron condition which leads to higher divalent iron content is associated with a severe drop in Q with decreasing temperature.

An attempt to reduce this large variation of Q and at the same time improve the low frequency response of Q, was made by adding iron oxide and thorium nitrate to the MF-9632 formula, making material MF-9060. The results were encouraging but there was insufficient time to study the system thoroughly. The thorium nitrate caused the firing temperature to be much higher than without its addition and it is not likely that the optimum firing conditions were discovered. Anyway, the behavior of Q with temperature was found to be changed significantly as curve D in graph 155 shows, the total variation is ~ 11%. The  $\mu_o Q$  performance for MF-9060 is shown in graph 153, curve D, and it is seen to be improved at the lower frequencies as hoped. The temperature behavior of  $\mu_o$ , curve D, graph 154, is a little worse as far as the TF is concerned, the value being 1.7 PPM/°C, but on the other hand, it is linear to a 0.1% tolerance.

Another attack on the problem of the severe change of Q with temperature was made by adding thorium nitrate and iron oxide to the bentonite containing material MF-9353-S/4. This modification resulted in a material, MF-9055, which demonstrated very high Q values and  $\mu_o Q$  values which were in excess of 10000 throughout the frequency range 1 to 12 Mc/s, see graph 156, curve A. The best of these bodies showed a temperature change of Q of 20% and a TF of  $\mu_o$  of ~ 1.7 PPM/°C. Time did not permit a more complete study. The temperature curves of  $\mu_o$  and Q are shown respectively in graphs 157 and 158, curve A.

Finally, a last composition was prepared, MF-9061, which contained a 10 weight percent addition of bentonite and a thorium nitrate addition and whose nickel and zinc oxide constituents were present in a mol ratio equal to 2.5. The increase in nickel content was made in order to try to further flatten the temperature curve of  $\mu_0$ . Increasing the nickel content lowers  $\mu_0$  but since lower nickel content bodies had more than enough  $\mu_0$ , it was felt that a certain amount of  $\mu_0$  could be sacrificed in order to gain further temperature stability. The increased nickel content also tends to increase the frequency range of the material. Curve B in graphs 156, 157, and 158 show  $\mu_0 Q$  versus frequency,  $\mu_0$  versus temperature and  $Q$  versus temperature, for the MF-9061 material.

Table 27

Chemical Composition of Principle Ferrite Materials

(Mol %)

MF-	Fe <sub>2</sub> O <sub>3</sub>	NiO	ZnO	SiO <sub>2</sub>	Al <sub>2</sub> O <sub>3</sub>	PbO	MgO	CaO	ThO <sub>2</sub>
9304	48.86	30.89	20.25	--	--	--	--	--	--
9375	41.13	26.38	18.21	10.38	2.79	--	.87	.29	--
9376	42.54	26.42	17.77	9.80	2.60	--	.66	.22	--
9353-S	43.49	25.39	17.42	10.18	2.64	--	.65	.23	--
9377	44.75	24.73	16.84	10.26	2.52	--	.67	.22	--
9622	44.99	28.03	18.70	--	--	2.05	--	--	--
9632	44.70	28.66	19.24	--	--	2.20	--	--	--
9633	42.58	27.58	18.64	--	--	3.41	--	--	--
9055	44.75	21.65	14.75	8.98	2.21	--	.59	.19	6.88
9060	48.31	23.35	15.67	5.71	--	1.79	--	--	5.16
9061	*36.65	32.50	13.46	8.44	1.85	--	.73	.25	6.22

\*Iron oxide content in raw mix; before milling for 42 hours in vibration mill.

PHASE III - INVESTIGATIONS ON THE GEOMETRY AND PERFORMANCE OF CUP CORES

The contract requirements for a radio frequency magnetic material are stated in terms of a cup core shape, which is expected to be the shape used in most applications. The maximum dimensions of the cup core to be used in our work is specified to be a 1/4 inch cube. Up till now all discussions on material properties have concerned toroidal configurations. This section presents the information we have accumulated on cup core properties and their relationship to toroidal properties.

Initially, measurements were made on cup cores which were less than half the volume and mass of a cup core of a size allowed in the specification. The results obtained from these small cup cores were rather poor. Not only was the ratio of the mass of ferrite to copper in the winding very low, but the cup cores themselves were structurally poor. Spray dried powders were used to press the cup cores and their hard, nearly incompressible (at reasonable pressing pressures) nature made a very porous structure inevitable (see photographs, figure 13); and furthermore, they made an inhomogeneously dense structure. Non-uniformity in density causes strains in a body which increase the magnetic losses and lower the Q.

Following these initial experiments, the results of which are not worth discussing, we had a die built by the tool and die shop of I.G.C., which made a cup core fulfilling the required 1/4 inch cube dimensions. For a description of the cup core and die, see Report No. 5, pages 9 and 10. Attempts to make good cup cores from this die were not successful. We experimented with materials MF-9353-S (the 10.25 weight percent bentonite containing material) and MF-9304 as soft-moist powders and were able to press cup cores which could be fired at low temperatures to a good density. The cup cores invariably warped on firing, however, and it was not possible to get a good evaluation of the material. Further development on pressing cup cores was curtailed at this point inasmuch as it would have required too much time and it was felt that the time could be more profitably spent on material development, and magnetic measurements.

In preparing to study the cup cores made with the above die, an investigation was made on the properties of small coils to determine the most suitable design for use in these small cup cores. The results of this investigation are given in table 28. About three dozen coils, using two types of wire of various sizes, were made and tested. The two types of wire used were single strand enameled and Litz. The length of the coils was kept constant at about 0.19 inches. With the enameled wire, the size was varied from 24 to 40 gauge and the number of turns ranged from 10 to 100. With Litz wire, various kinds were

tried: 72/44, 20/44, 10/44, 6/44, 7/41, 10/40, and 3/36; the number of turns ranged from 10 to 38. All coils were tested on a Boonton Q-meter at 5 Mc/s. The coils with the better Q's (Q's in the neighborhood of 30) were further tested in a cup core assembly of a MF-9353-RS material (containing 8.6 weight percent bentonite) made from the die discussed above. The Litz wire coils emerged clearly superior to the single strand enameled wire coils. Number 10/44 Litz with windings ranging from 20 to 30 turns gave the best results.

TABLE NO. 28  
EXPERIMENTAL DATA FOR COILS FOR 1/4" CUBE CUP CORES

Coil length 0.190 inches, I.D. 0.077 inches								
Enameled Wire				Litz Wire				
Number of Turns	Wire Size	Q Coil 5 Mc/s	Q/with Cup Core 5 Mc/s	Number of Turns	Wire Size	Q Coil 5 Mc/s	Q/with Cup Core Q-Meter 5 Mc/s	Q/with Cup Core G.R. Bridge 5 Mc/s
10	24	24	76	10	72/44	24.5	73	
18	35	22	64	16	20/44	26		
20	30	26	89	18	10/44	24	85	
20	35	25.5		20	10/44	30	94	106
30	35	28	84.5	22	10/44	30	92.5	109
40	30	19	64	24	10/44	30	96	103
50	30	17		27 <sup>1</sup>	10/44	29	94	113
50	40	25.5	71	27 <sup>2</sup>	10/44	29		
100	40	28.5		30 <sup>1</sup>	10/44	30.5		
				30 <sup>2</sup>	10/44	30	94	110
				24	20/44			
				24	6/44	28	96	103
				30	6/44	32	95	105
				34	6/44	34	96.5	101
				36	6/44	34	96.5	96.5
				38	6/44	33	96	97.5
				24 <sup>1</sup>	7/41	22.5	88.5	
				24 <sup>2</sup>	7/41	22.5	87.5	
				27	7/41	22	91	
				30	7/41	21.5	84.5	
				22	7/41	23	87.5	
				22	10/40	18		
				24	10/40	18		
				35	10/40	30.5	94	100.5
				24	3/36	20		
				27	3/36	18.5		

Although the work on developing a technique for pressing cup cores was terminated, the idea of measuring cup cores was not given up. Instead, fired slabs of MF-9304 material were sent out to Ultrasonics Machining Co. in Long Branch, New Jersey, and toroids and cup cores of various dimensions were ultrasonically machined. The dimensions to which the cup cores were machined are shown in table 29. Toroidal properties were measured and are compared with the properties of some of the cup cores.

Table 29

Dimensions of Ultrasonically Machined Cup Cores (in inches)

<u>Height</u>	<u>O.D.</u>	<u>I.D.</u>	<u>CP (Center Post) Diameter</u>
0.125	0.250	0.200	0.120
"	"	"	0.110
"	"	"	0.100
"	"	"	0.090
"	"	"	0.080
"	"	"	0.070
"	"	0.190	0.090
"	"	0.180	0.090

The number of measurements we were able to make on the cup cores was limited by time. But some interesting and useful results were obtained nevertheless, and these results are shown in table 30. First of all, as regards  $\mu_e$  and Q for toroid versus ungapped cup core shapes, the comparison is very favorable. Incidentally, our procedure for calculating effective initial permeability is detailed in appendix 2. The Q of the cup core can apparently be even a little higher than that of a toroid. Upon gapping the cup core, however, Q as well as  $\mu_e$  were found to drop; the drop being greater as the gap increased. The cup cores were gapped in one set of conditions in the center post and outer rim by inserting a shim and in another set of conditions in the center post only. Under both sets of conditions, Q and the LQ product decreased; the center-post-only gapping resulted in much the poorer values of Q and LQ product. The LQ data discussed here is also described in graphs 159 thru 164.

The important result derived from this data is that the technique of gapping a cup core will not yield higher Q values. That is, contrary to what was originally hoped, the LQ product does not remain constant with gapping; it rather was found to decrease with increasing gap length. The other important result derived is that cup core properties can be equivalent to toroidal properties in the ungapped condition. Thus if we provide a material with the desired  $\mu_e$  and Q values over the frequency range, we can be assured that these properties will be available from a cup core shape.



PHASE IV - APPLICABILITY OF MATERIALS INVESTIGATED TOWARD  
PROVIDING A STABLE RADIO FREQUENCY CUP CORE

During the course of this contract we have investigated a great many materials which were modifications of the basic Ni-Zn ferrite MF-9003. The most significant modifications we have discussed pointedly in this final report. The last question to consider is whether any of these modifications fulfill the requirements of the contract or whether they can be applied in a way to meet the objectives of the contract, i.e., providing a stable high frequency cup core. The answer to the first part of the question is no. None of the modifications meet the requirements in full. It must be stated though that the developments accomplished during the life of this contract exceed in some respects what was considered likely to be accomplished. This is true principally in regards to the temperature stability of  $\mu_0$  and in regard to the value of Q over the required frequency range. The answer to the second part of the question is that a compensating technique can be used to help fulfill part of the requirements.

Concerning compensation, during the course of the contract, experiments were conducted on a special compensating technique which involved varying the inductance of a gapped cup core assembly by changing the air gap length. The gap length was changed by affixing a piece of plastic, in one way or another, to the cup core assembly and the expansion or contraction of the plastic with temperature would lengthen or shorten the air gap. Experiments verified the fact that this technique could work but inasmuch as the temperature behavior of  $\mu_0$  has been improved to below 10 PPM/°C, i.e., in the range where compensation with ceramic capacitors is allowed, this technique is no longer considered. For details on the work that was done, see: Report No. 1, p. 8; Report No. 2, p. 14; Report No. 3, p. 14; Report No. 5, p. 18.

Magnetic data for the most promising materials are included in table 23, p.12. Unfortunately, complete stability data is not available for the materials made during this last period. Thus an overall comparison is not possible. But we can compare their overall usefulness in terms of  $\mu_0$ , Q and the temperature behavior of  $\mu_0$  and Q. First of all, it is noted that every material which displayed a nearly flat temperature curve of  $\mu_0$ , i.e., a TF  $\leq$  1 PPM/°C, also displayed a temperature change of Q which far exceeds the limits allowed. This is not meant to imply that a flat temperature curve of  $\mu_0$  is inseparably related to a large deviation in the temperature behavior of Q. It just means that the materials made so far have had that combination of characteristics. The evidence rather indicates that a small temperature change of Q can be associated with a nearly flat temperature curve of  $\mu_0$ . The understanding which would enable us to achieve this was unfortunately acquired too late in the contract and only a minimal number of experiments could

be performed to exploit this knowledge. So the materials with  $TF \leq 1.0$  PPM/ $^{\circ}C$ , i.e., MF-9353-S, -9622 and -9633, cannot be considered useful to the purpose of the contract unless the temperature instability of Q can be tolerated. But even if this condition were acceptable, the  $\mu_0 Q$  performance of MF-9622 and -9633 is too low at frequencies below 5 Mc/s; and with MF-9353-S, the Q is well below the 190 value required. So MF-9353-S, -9622 and -9633 are not satisfactory in the overall consideration.

MF-9632 fails for at least three reasons; low  $\mu_0 Q$  at frequencies below 5 Mc/s, high TF value (7.4 PPM/ $^{\circ}C$ ), and too great an instability of Q with temperature. The modification of MF-9632, i.e., MF-9060, which has an increased iron content and a thorium nitrate addition, shows a marked improvement in these characteristics. The  $\mu_0 Q$  performance through the frequency range 1 to 12 Mc/s is good, except for the region 1 to 2 Mc/s where the Q appears to drop. The temperature curve of  $\mu_0$  is linear within 0.1% and gives a TF of 1.7 PPM/ $^{\circ}C$ , and the temperature curve of Q shows a total change of  $\sim -11\%$ . These characteristics are obtained, it must be remembered, with no development work on this material and they could undoubtedly be improved.

With the MF-9060 material, compensation techniques can be considered in order to make a device with an essentially temperature independent inductance. The temperature curve of  $\mu_0$  of MF-9060 is quite linear and a ceramic capacitor meeting the MLL-C-20 specifications with a linear temperature coefficient of  $-95$  PPM/ $^{\circ}C$  would provide a system with a temperature independent inductance. The temperature coefficient of the ceramic capacitor was determined on the basis of an effective initial permeability of the cup core assembly of 56.

TASK B

STABLE FERRITES FOR THE FREQUENCY RANGE 8 TO 32 Mc/s

Development work on a material for the frequency range 8 to 32 Mc/s was contingent upon our successfully completing Task A. Thus no work was done specifically for this Task.

#### IV - CONCLUSIONS

None of the materials developed under this contract completely fulfill the requirements as specified. Much has been accomplished, however, toward meeting these requirements in full. Materials have been developed which meet some of the requirements: e.g., MF-9633 has a flat temperature curve of  $\mu_n$  and good Q values from 5 to 20 Mc/s; MF-9060 has good  $\mu_n$  and Q values from 2 to 20 Mc/s, a reasonably stable Q with temperature, and a linear temperature curve of  $\mu_n$  with a TF of 1.7 PPM/°C which is less than powdered iron; MF-9353-S which has nearly a flat temperature curve of  $\mu_n$  and an overall instability of 2.4% which is only a little greater than the 1.4% instability of  $\mu_n$  of powdered iron. All of these materials either have some characteristic which is unfavorable or have not been evaluated completely.

Considerable knowledge has been gained in our investigations these past thirty months. Knowledge which, if sufficient time were available, could undoubtedly be applied to yield a material quite satisfactory to the purpose of this contract. Materials MF-9060 and MF-9061 were, so to speak, single shot experiments in the last days of the contract applying this knowledge. The success attained with these formulations attests to the possibility of attaining even better results under a comprehensive development program.

What we have learned is briefly summarized as follows:

- 1) A fine homogeneous grain structure, grains  $\leq 1\mu$ , is necessary. This grain structure together with a density in the neighborhood of 90% theoretical will contribute toward high Q values and good initial permeabilities. Also, a fine grain structure is found invariably associated with a low TF value.
- 2) The total iron content should be near stoichiometric; probably slightly excess in relation to the nickel and zinc content. A deficiency of iron results in either very high TF values of  $\mu_n$  or nonlinear temperature curves. An excess of iron results in the formation of divalent iron ions. Divalent iron in excessive amounts is responsible for the severe temperature instability of Q. An excessive amount of divalent iron in terms of FeO may be around 0.5 weight percent.
- 3) That significant amounts (e.g., 6 to 11 weight percent) of silicate additions like bentonite and lead result in flat or nearly flat temperature curves of  $\mu_n$ . The silicate apparently forms a second phase with some of the other ingredients in the ferrite, and this second phase acts as a sort of matrix in which the fine grains of the basic ferrite are imbedded.

- 4) Silicate additions allow sintering processes to take place at lower temperatures.
- 5) Thorium nitrate, when added, appears to act as a grain growth inhibitor. It also apparently retains oxygen in the structure, which holds down the amount of divalent iron that can be formed.
- 6) There is apparently a temperature dependent magnetic loss mechanism which is related to the divalent iron content. The peak of the loss is a function of the total iron content and also apparently of the measuring frequency.
- 7) That cup core assemblies can be made which have the same  $\mu_0$  and Q that toroidal shapes have. The cup cores must not be gapped, however, as this leads to lower Q's as well as to lower inductance values.

## APPENDIX I

### MAGNETIC MEASUREMENT METHODS

#### Initial Permeability and Q

Initial permeability and Q measurements were done using standard equipment and methods. The equipment used consisted of: RF Bridges (General Radio Co.), RX-Meter (Boonton) and a Boonton 260A Q-Meter. The absolute accuracy attainable with this equipment is  $\pm 2.0\%$  for  $\mu_0$  and  $\pm 3.0\%$  for Q.

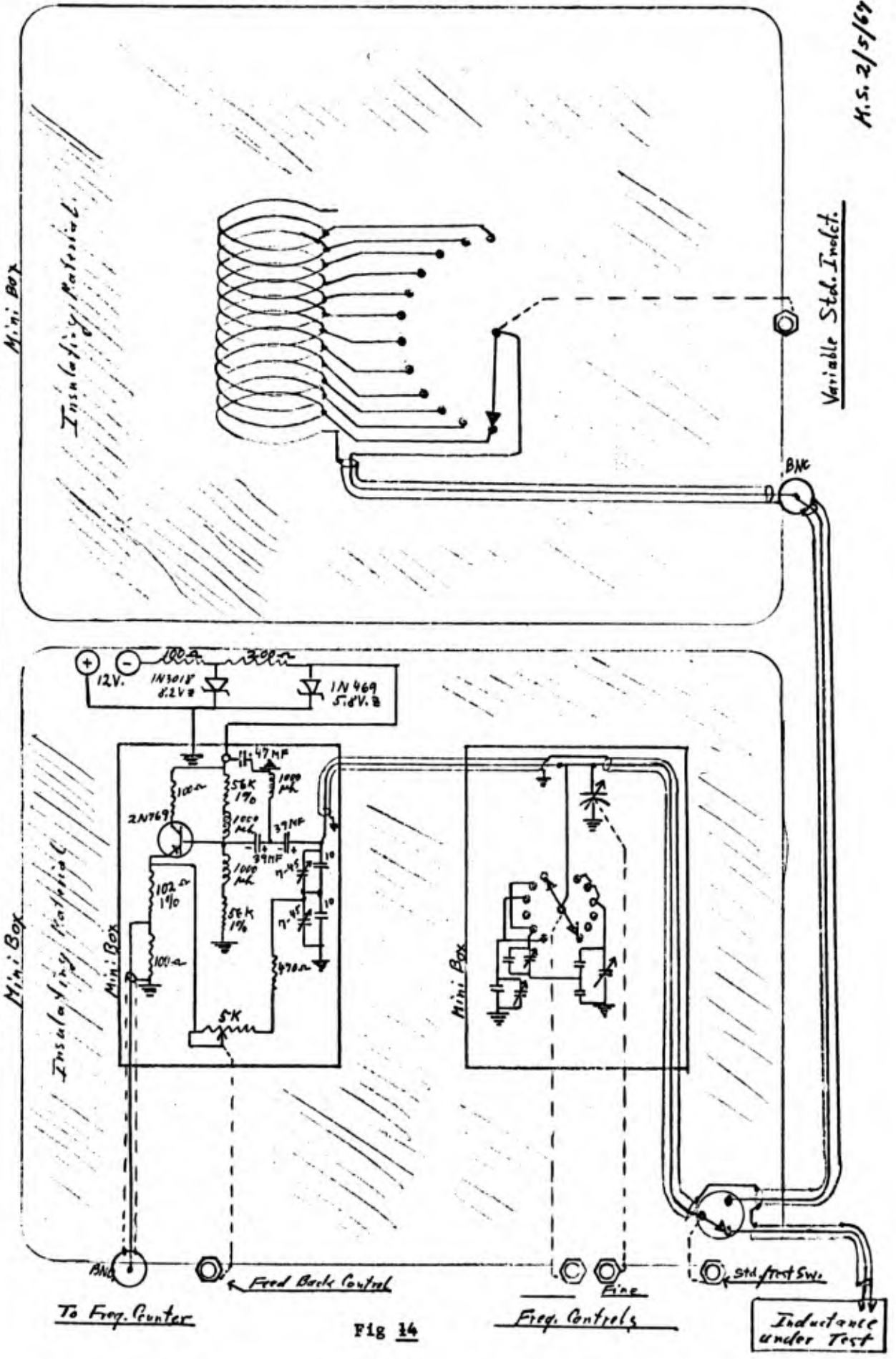
#### Temperature Coefficient of $\mu_0$

This measurement was based on a resonant frequency method employing the sample toroid as an inductance in an oscillating circuit. The toroids ( $\sim 6$  mm O.D.) were wound with a sufficient number of turns of 30 gauge enameled wire to allow the oscillator to resonate at a frequency near 5 Mc/s. A circuit diagram for this set-up is shown below in fig. 14. The sample toroid is clamped on a terminal strip which is mounted in a temperature chamber. The terminal strip has ten positions and each position is connected to an external switch by a coaxial cable (all ten cables have the same inductance). The measurement itself is accomplished simply by reading the resonant frequency directly from the frequency counter at each test temperature. The change in  $\mu_0$  is calculated then from the value of the resonant frequencies at  $30^\circ\text{C}$ .

#### Disaccommodation

The disaccommodation measurement was accomplished in the same way and with the same equipment as the temperature coefficient measurement, except that a demagnetizing step was included prior to the initial measurement. A two-way switch was connected to the ten position switch on the terminal strip mentioned above. This switch allowed an a.c. demagnetizing signal to be applied to the sample toroid without interfering with the oscillator circuit. The demagnetizing circuit is shown in fig. 15. It consists of a capacitance C, inductance L and the sample toroid in series with the contact of a mercury wetted relay. The contact of the relay is normally open. The coil of the relay is energized during the retrace of a Tektronix oscilloscope through a special gate output provided in the scope. When the relay contact is open, the capacitance C becomes slowly charged through the resistor R. During the retrace of the scope the contact closes, thus discharging capacitance C. This sets up a damped oscillation with a frequency of 200 Kc/s and a time constant of 30  $\mu\text{sec}$ . This damped oscillation demagnetizes the ferrite core.

Free Running 5 Meg. Cycle Oscillator (Temperature Stable)



M.S. 2/5/69

Fig 14

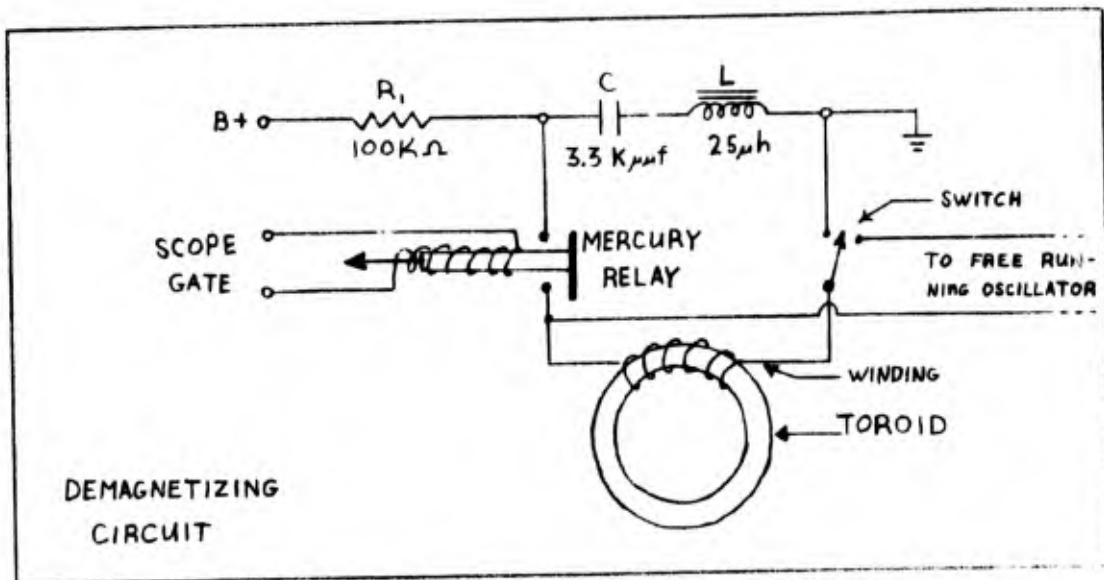


Fig 15

#### Direct Current Field Measurements

A toroidal sample ( $\sim 6$  mm O.D.) was wound with 20 turns of No. 28 gauge insulated copper wire and mounted on a glass rod with its diameter parallel to the length of the glass rod as shown in fig. 16. The wire leads were taped to the rod to prevent movement and the pinned ends were inserted into a fixed receptacle also mounted on the rod. The leads from the receptacle were taped to the rod and extended through the rubber stopper holding the glass rod; the ends were pinned and inserted into the binding posts of a 260-A Boonton Q-meter. The glass rod was inserted into the solenoid in such a way that the toroid was in the center of the solenoid. A dc power supply (Power Designs Inc.) was used to energize the solenoid. A frequency counter (Hewlett-Packard 5244L Electronic Counter) was connected into the oscillator

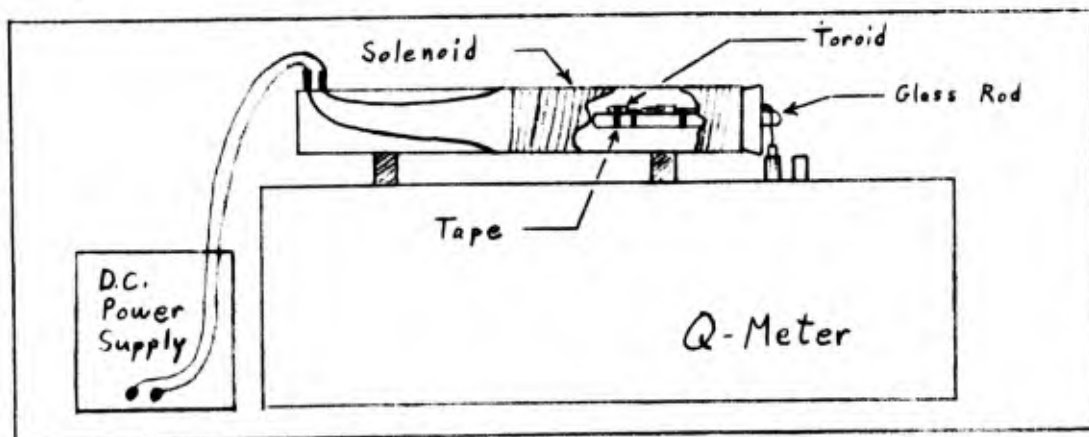


Fig 16

circuit with a T connector and was used to monitor the frequency. At zero field, i.e., with the power supply off, the circuit was tuned to a frequency of 5 Mc/s. The exact frequency was read on the frequency counter to six places. After this initial measurement, a d.c. current was applied to the solenoid for 15 seconds and then the current was disconnected and the circuit was retuned with the frequency control, and the frequency was recorded. The percent change in  $\mu_0$  after exposure to each new field condition was calculated from the zero field reading.

#### A.C. Drive Measurement

The oscillator circuit of a 260-A Boonton Q-Meter was separated from the thermocouple unit by an external switch. The oscillator signal was then fed through a 0.5 ohm resistor to the winding on the sample toroid, see fig. 17. The input voltage ( $V_i$ ) to the core was read on an RF voltmeter and the output voltage ( $V_o$ ) was read on the voltmeter of the Q-Meter. The ratio  $V_o/V_i$  was calculated to determine the Q. Initially the Q-Meter was tuned to  $\sim 5$  Mc/s. Then the input voltage for the first measurement was set at  $\sim 0.005$  volts. The frequency of the initial measurement was read exactly to 5 figures on a frequency counter. For subsequent measurements, the input voltage was increased in several steps until, for the final measurement, a voltage of about 3 volts was impressed across the core. For these measurements the circuit was retuned with the frequency dial and the frequency on the counter was recorded. The change in  $\mu_0$  was calculated from the change in the resonant frequency of the circuit.

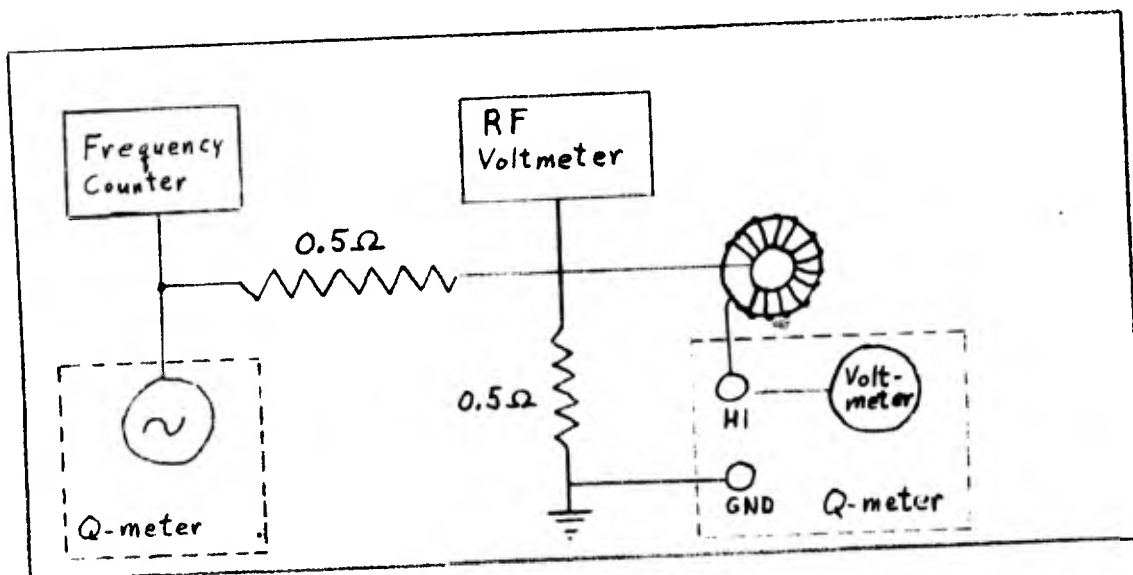


Fig 17

APPENDIX 2

CALCULATION OF EFFECTIVE INITIAL PERMEABILITY

In regards to the magnetic evaluation of cup cores, our procedure for calculating effective initial permeability,  $\mu_o$ , is as follows:

The inductive reactance ( $X_L$ ) and resistance (R) of a cup core are measured at a given frequency (F) on a General Radio Bridge. From  $X_L$  and the measuring frequency, F, the inductance L is found from the relation,

$$L = \frac{X_L}{2\pi F}, \text{ where F is in Mc/s}$$

The effective permeability  $\mu_{eff}$ , for zero air gap<sup>1</sup>, is given by,

$$\mu_{eff} = \frac{L}{L_o}, \text{ where } L_o \text{ is a constant determined from the geometry of the cup core and the number of turns (N) in the coil winding, viz,}$$

$$L_o = \frac{4\pi N^2 (10^{-9})}{\sum_{i=1}^5 \frac{L_i}{A_i}}$$

The summation  $\sum_{i=1}^5 \frac{L_i}{A_i}$  is found from the relations:

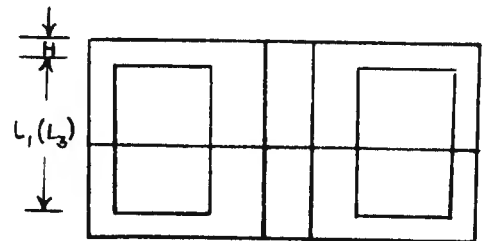
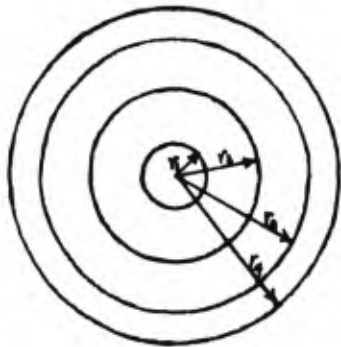
$$\frac{L_1}{A_1} = \frac{L_1}{(r_4 - r_3)(r_4 + r_3)\pi}, \quad \frac{L_2}{A_2} = \frac{0.7330}{H} \log \frac{r_3}{r_2}$$

$$\frac{L_3}{A_3} = \frac{L_3}{(r_2 - r_1)(r_2 + r_1)\pi}, \quad \frac{L_4}{A_4} = \frac{.5 \left[ H + 2 \left( \sqrt{\frac{r_3^2 + r_4^2}{2}} - r_3 \right) \right]}{(r_4^2 - r_3^2 + 2r_3H)}$$

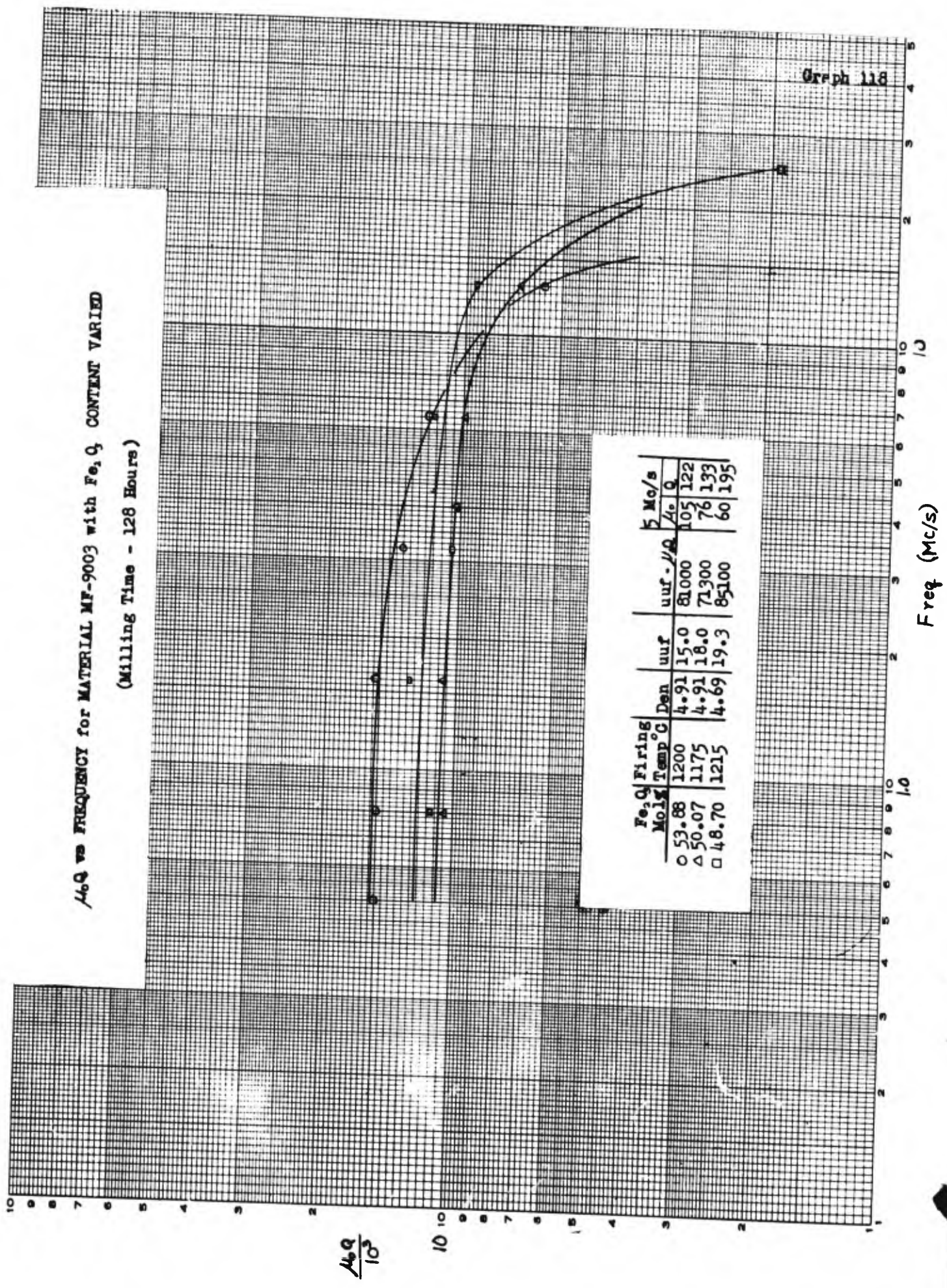
<sup>1</sup> For the zero air gap condition  $\mu_{eff} = \mu_o$ . When an air gap is introduced the above calculation for  $\mu_{eff}$  must be modified. The measurements reported on are for the zero air gap condition.

$$\frac{L_5}{A_5} = \frac{.5 \left[ H + 2 \left( r_2 - \sqrt{\frac{r_2^2 + r_1^2}{2}} \right) \right]}{(r_2^2 - r_1^2 + 2r_2H)}$$

$r_1, r_2, r_3, r_4, L_1, L_3$  and  $H$  are dimensions obtained from the cup core, i.e.,



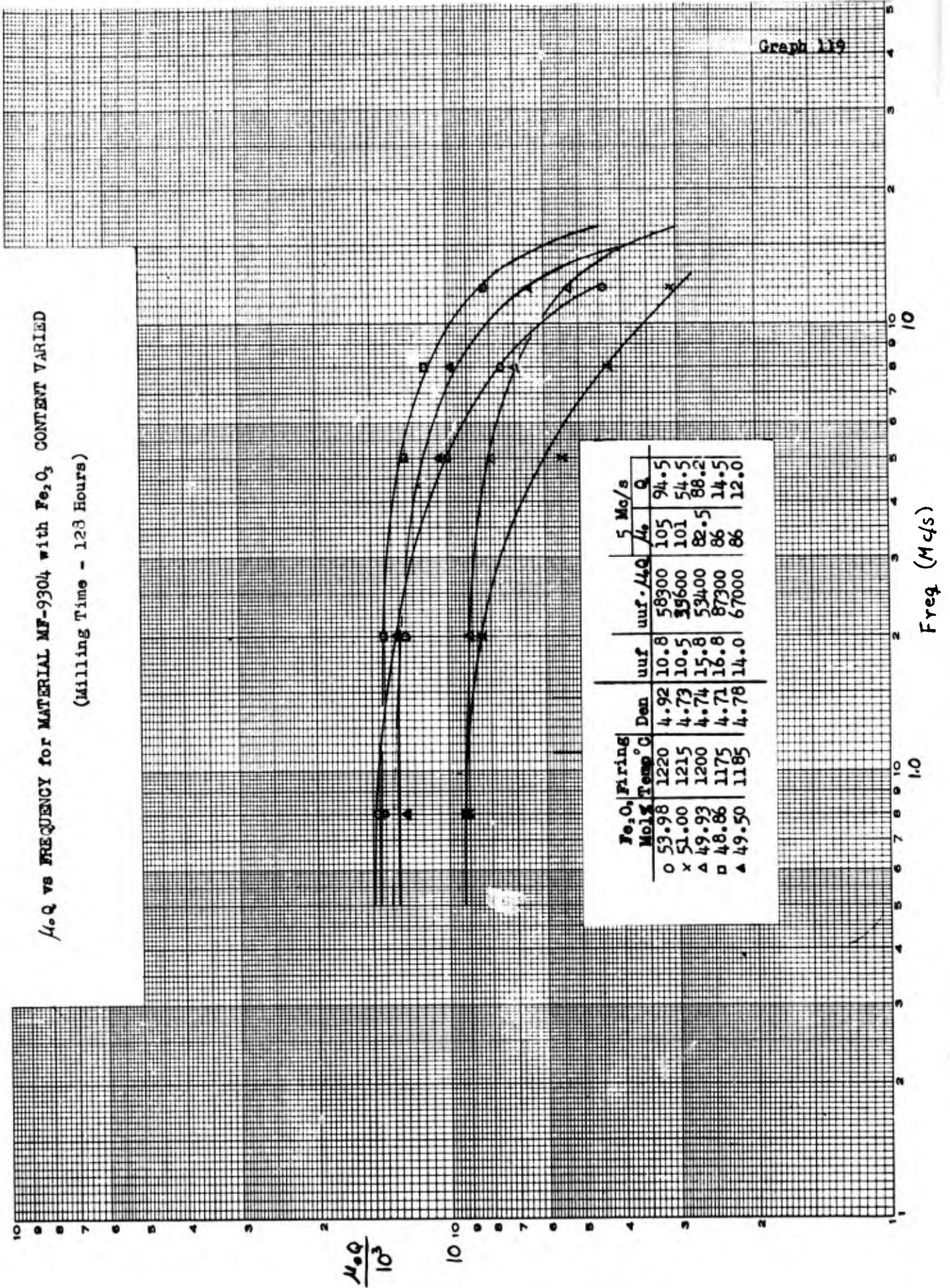
**$\mu_0$  vs FREQUENCY for MATERIAL MF-9003 with  $Fe_2O_3$  CONTENT VARIED**  
 (Milling Time - 128 Hours)



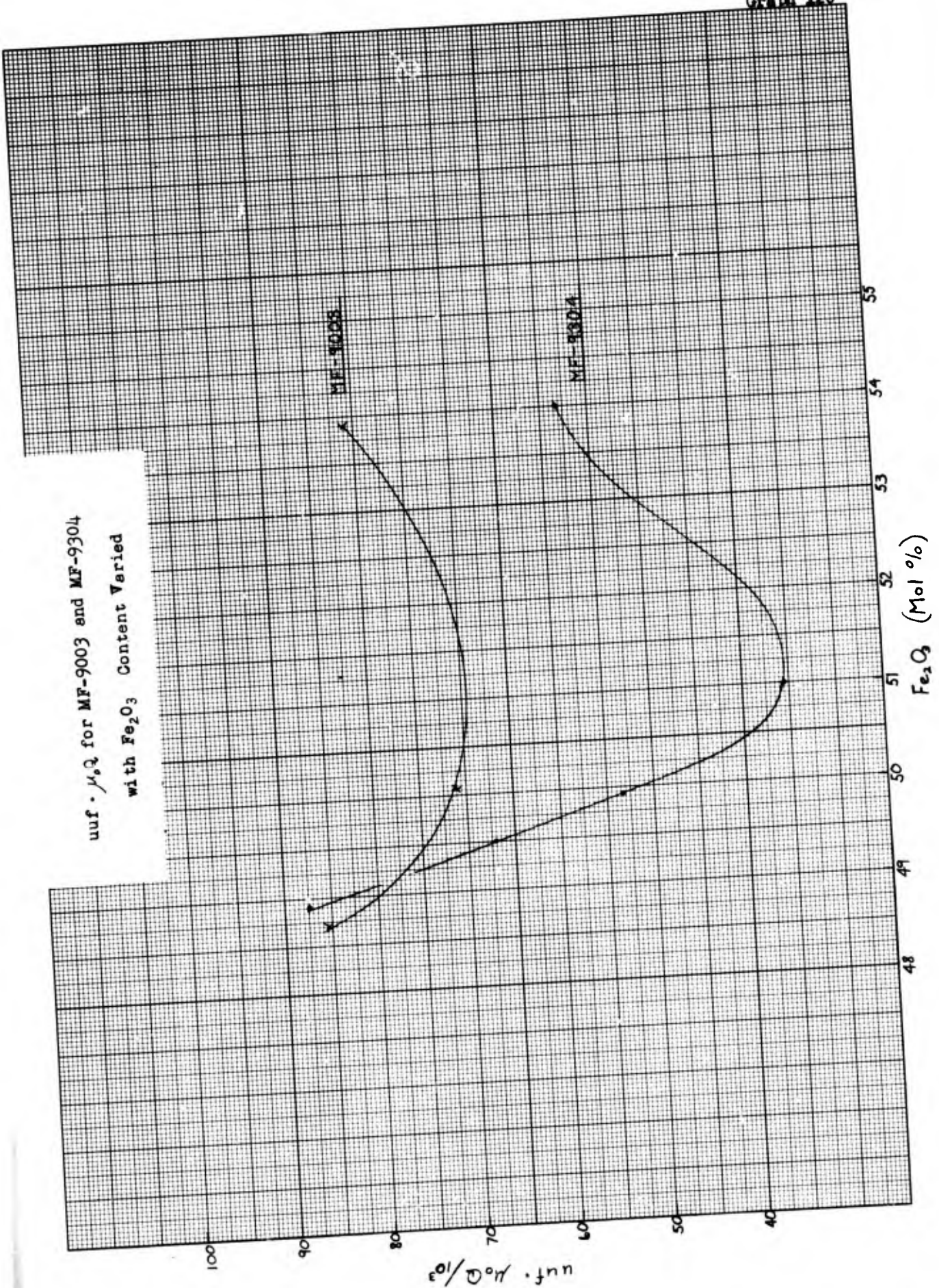
$Fe_2O_3$ Mols %	Firing Temp °C	Den	unf	unf. $\mu_0$	$\mu_0$ / 10 <sup>3</sup>	5 Mc/s
○ 53.88	1200	4.91	15.0	81000	105	122
△ 50.07	1175	4.91	18.0	71300	76	133
□ 48.70	1215	4.69	19.3	85100	60	195

Graph 118

$\mu_o Q$  vs FREQUENCY for MATERIAL MF-9304 with  $Fe_2O_3$  CONTENT VARIED  
 (Milling Time - 123 Hours)



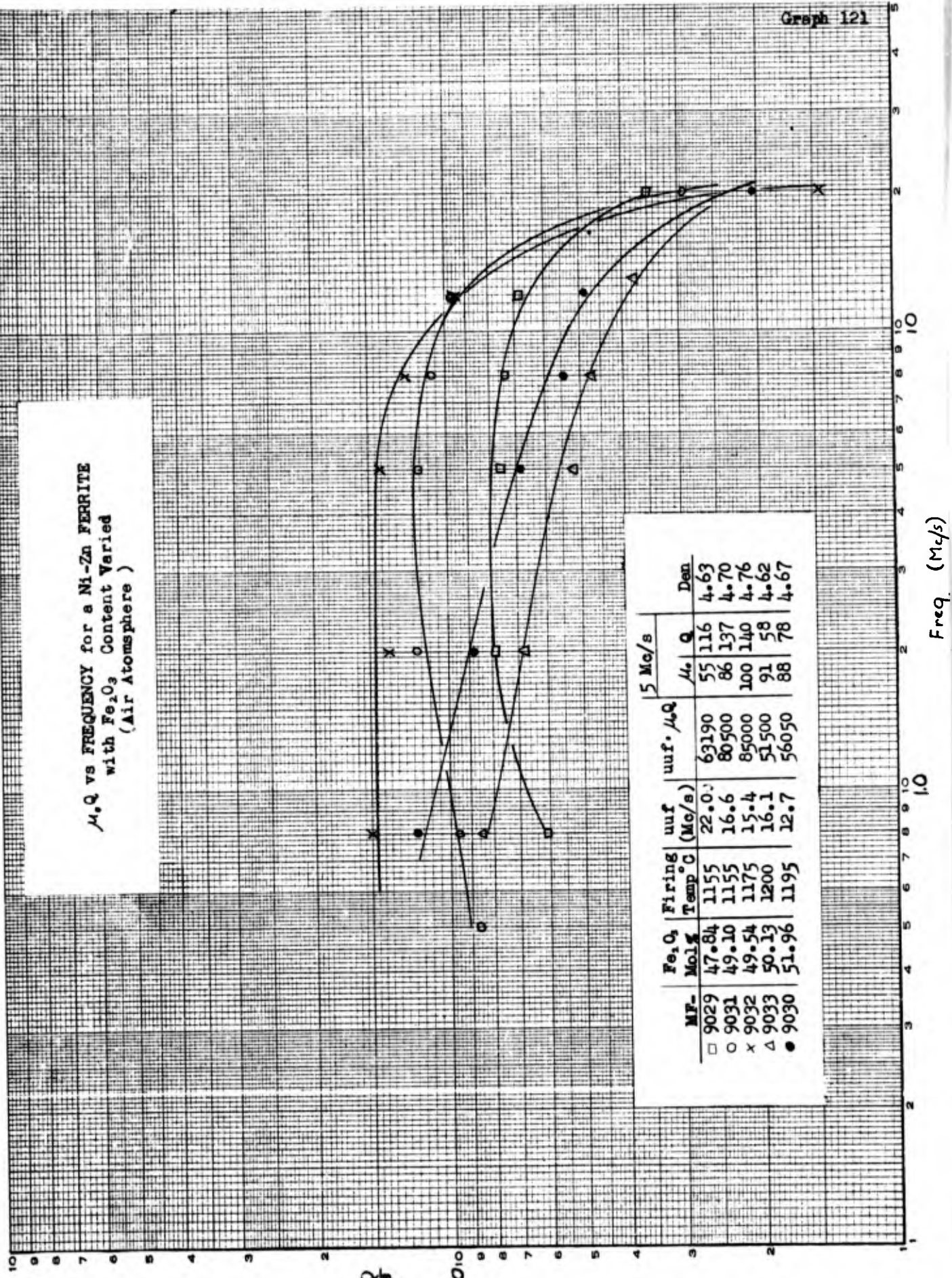
uuf ·  $\mu_2 Q$  for MF-9003 and MF-9304  
with  $Fe_2O_3$  Content Varied



$\mu_r Q$  vs FREQUENCY for a Ni-Zn FERRITE  
with  $Fe_2O_3$  Content Varied  
(Air Atmosphere)

Graph 121

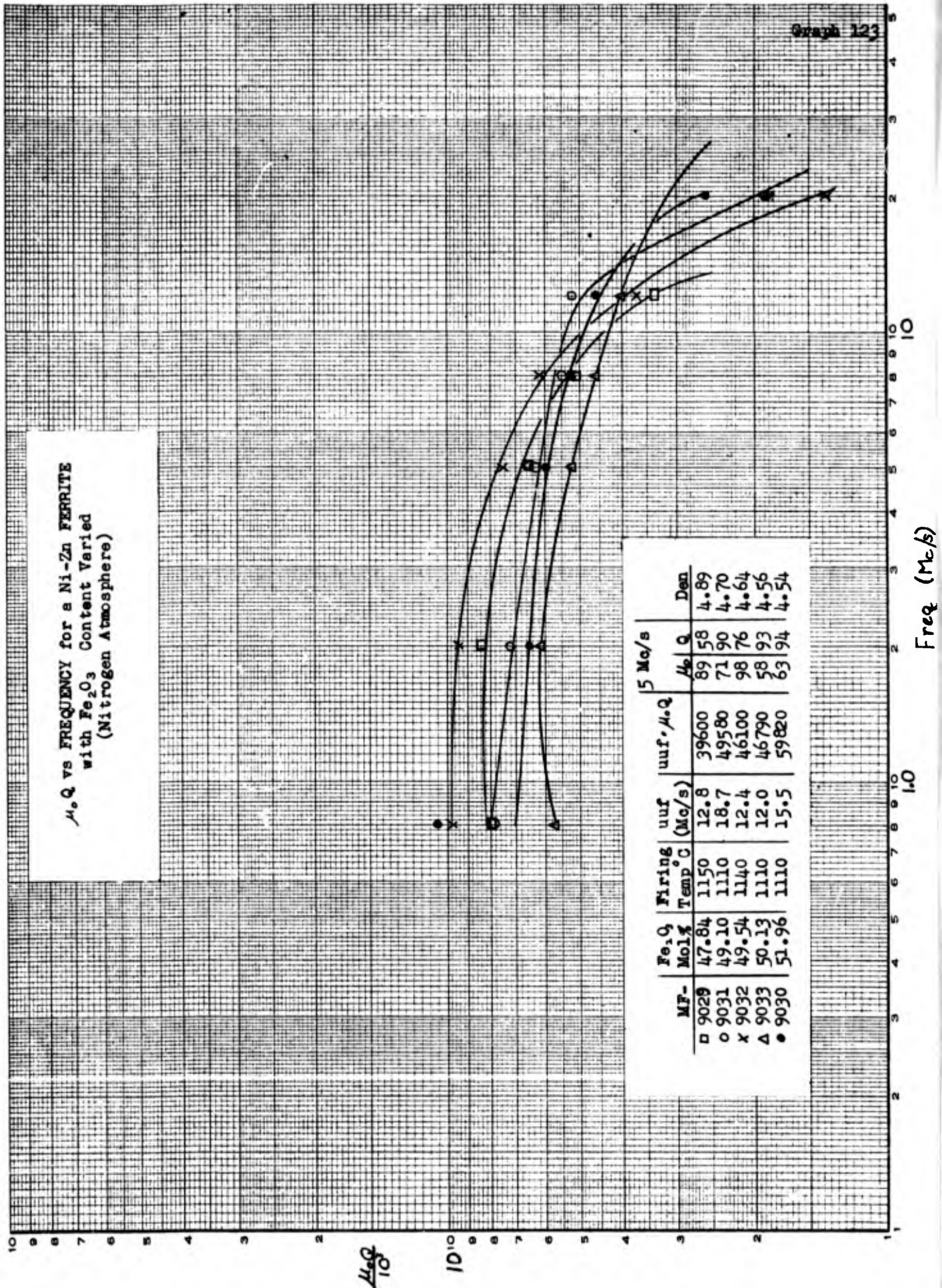
$\frac{40}{10}$



MF-	$Fe_2O_3$ Mol%	Firing Temp °C	uuf (Mc/s)	uuf. $\mu_r Q$	5 Mc/s		Den
					$\mu_r$	Q	
□ 9029	47.84	1155	22.0	63190	55	116	4.63
○ 9031	49.10	1155	16.6	80500	86	137	4.70
× 9032	49.54	1175	15.4	85000	100	140	4.76
△ 9033	50.13	1200	16.1	51500	91	58	4.62
● 9030	51.96	1195	12.7	56050	88	78	4.67

Freq. (Mc/s)

$\mu_o Q$  vs FREQUENCY for a Ni-Zn FERRITE  
with  $Fe_2O_3$  Content Varied  
(Nitrogen Atmosphere)



MF-	Fe <sub>2</sub> O <sub>3</sub> Mol%	Firing Temp °C	unf (Mc/s)	unf. $\mu_o Q$	5 Mc/s $\mu_o Q$	Den.
9029	47.84	1150	12.8	39600	89.58	4.89
9031	49.10	1110	18.7	49580	71.90	4.70
9032	49.54	1140	12.4	46100	98.76	4.64
9033	50.13	1110	12.0	46790	58.93	4.56
9030	51.96	1110	15.5	59820	63.94	4.54

$\frac{\mu_o Q}{10}$

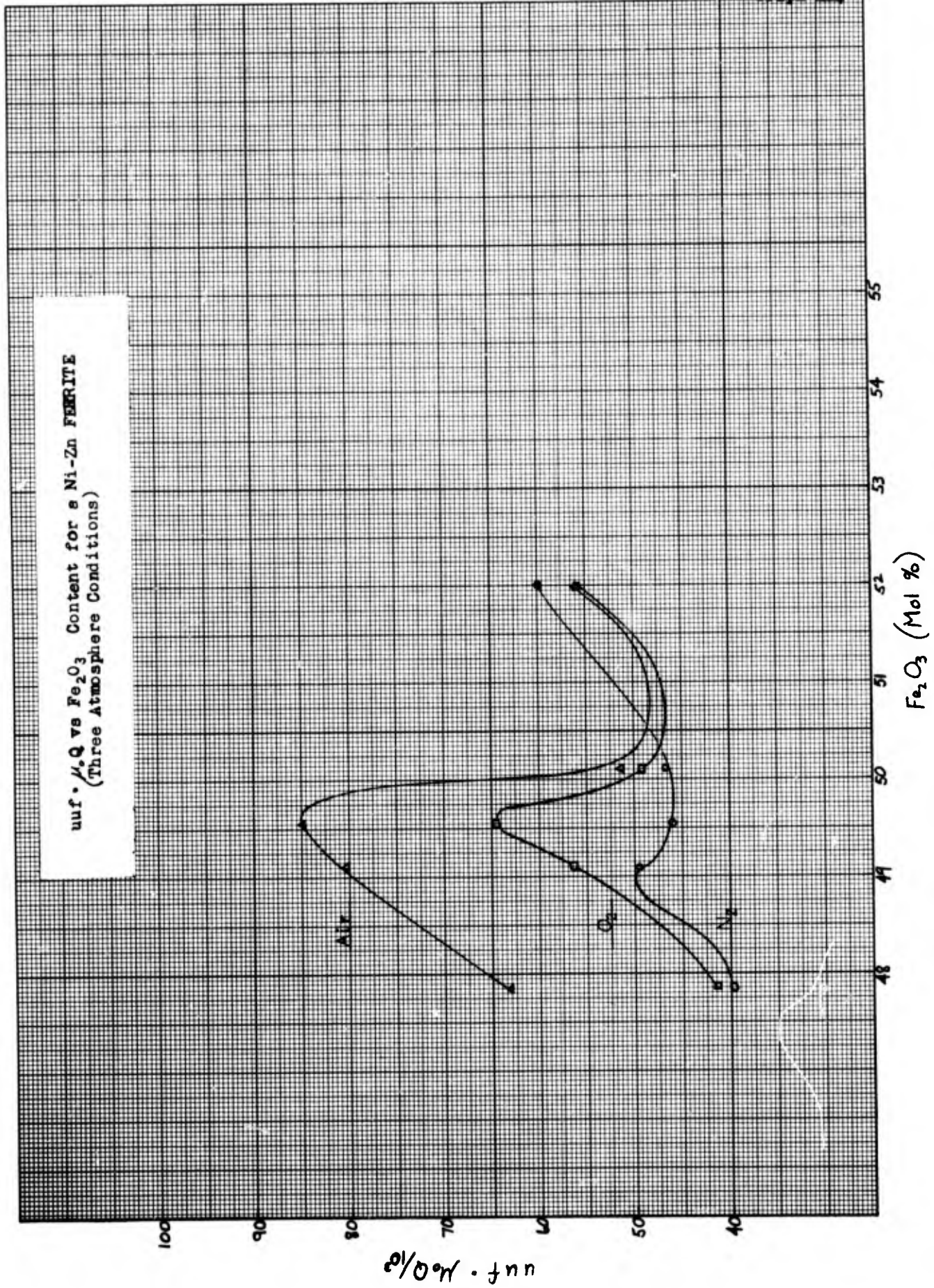
10<sup>10</sup>

1.0

10

Freq (Mc/s)

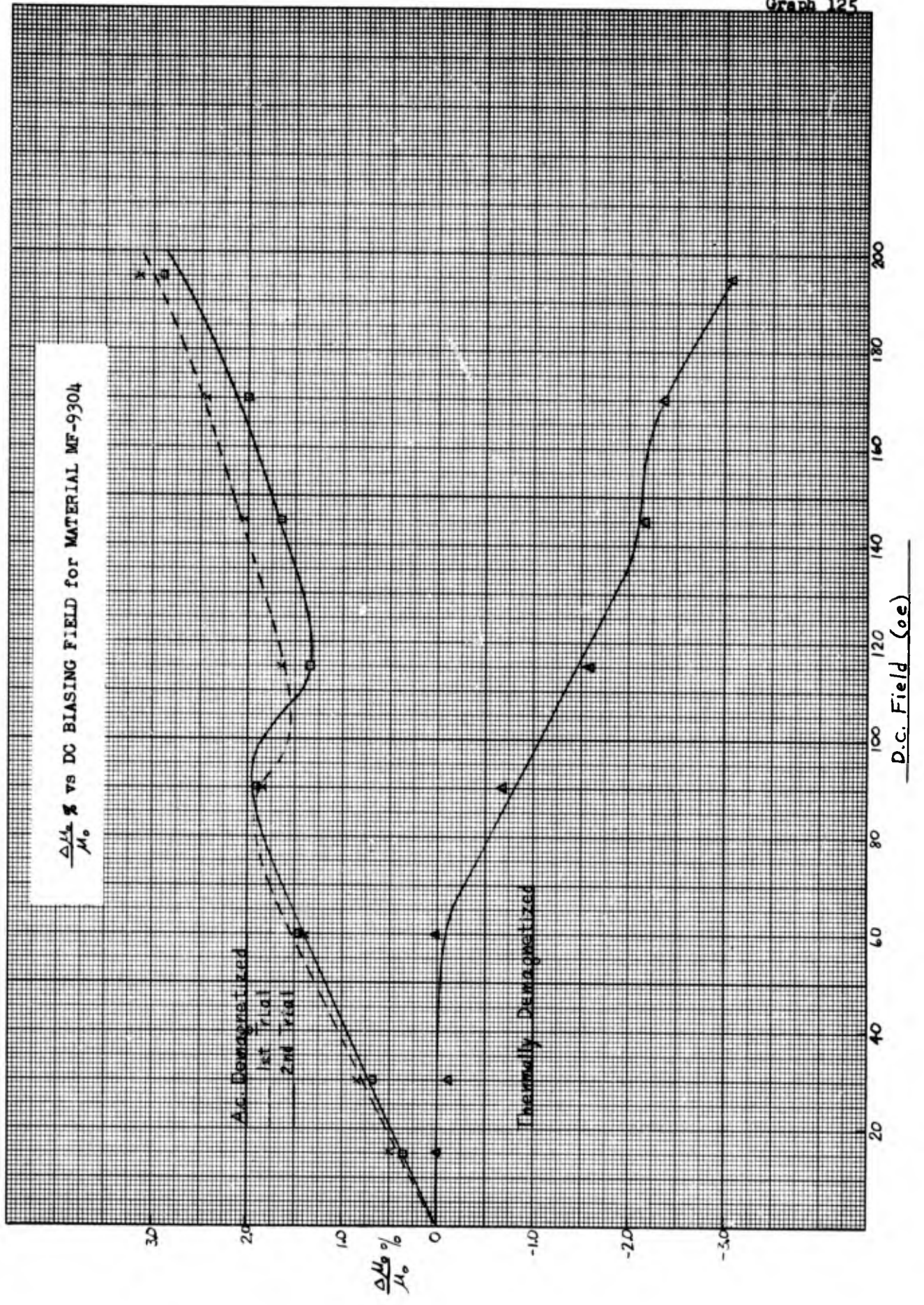
unf. %Q vs Fe<sub>2</sub>O<sub>3</sub> Content for a Ni-Zn FERRITE  
(Three Atmosphere Conditions)



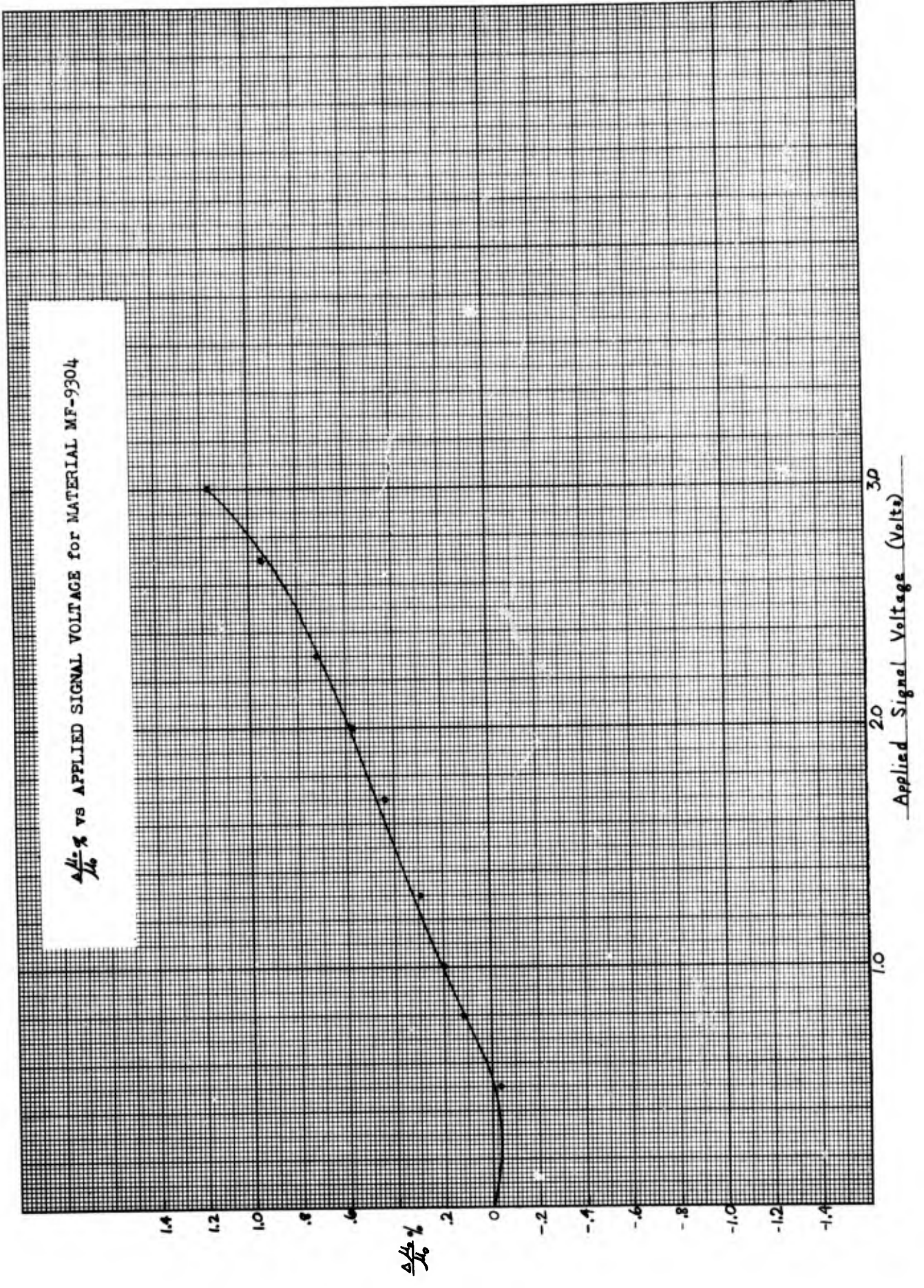
unf. %Q vs Fe<sub>2</sub>O<sub>3</sub>

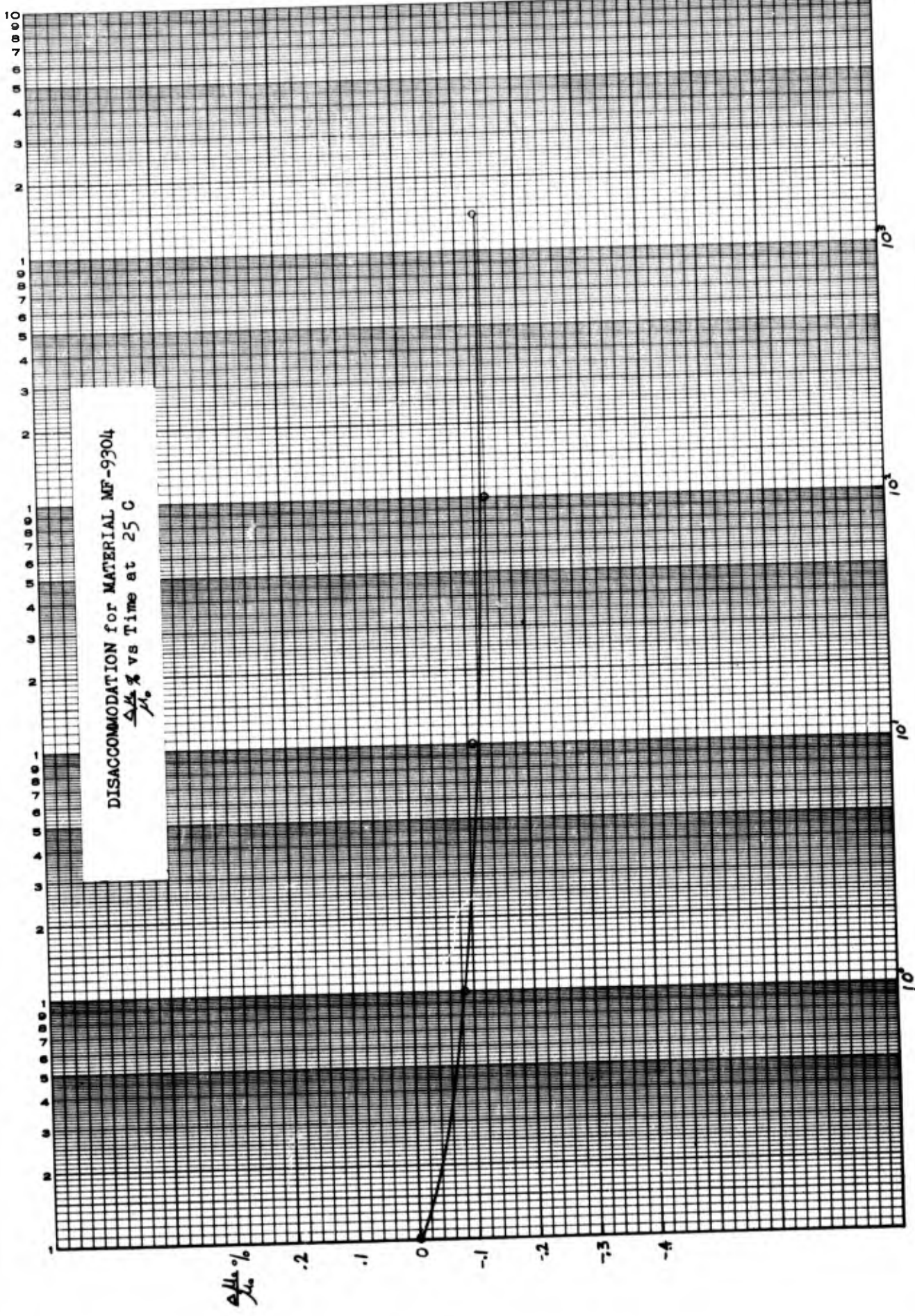
Fe<sub>2</sub>O<sub>3</sub> (Mol %)

$\frac{\Delta \mu_0}{\mu_0} \%$  vs DC BIASING FIELD for MATERIAL MF-9304

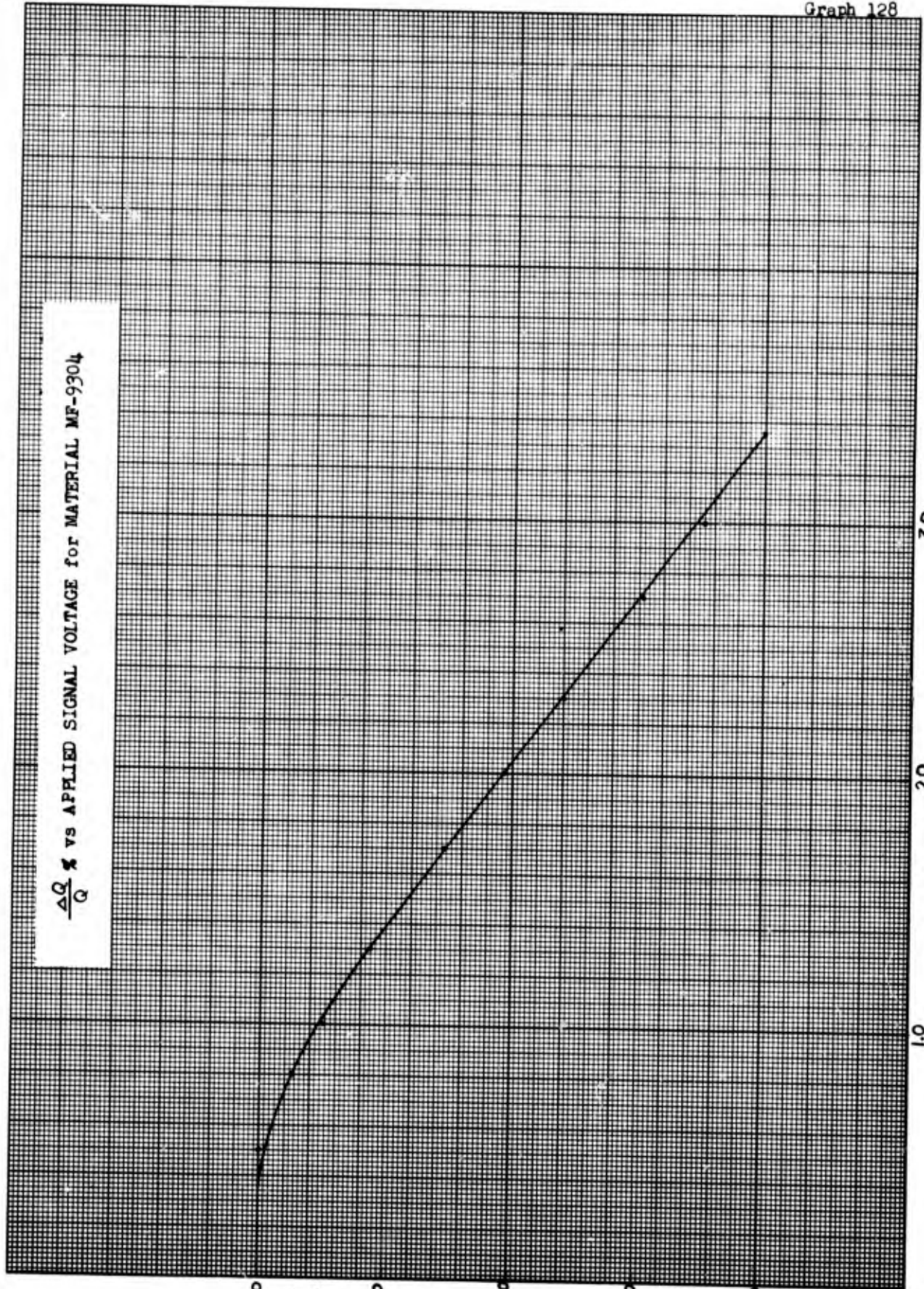


$\frac{\Delta L_c}{L_c} \%$  vs APPLIED SIGNAL VOLTAGE for MATERIAL MF-9304





$\frac{\Delta Q}{Q} \%$  vs APPLIED SIGNAL VOLTAGE for MATERIAL MF-9304



$\frac{\Delta Q}{Q} \%$

-10

-20

-30

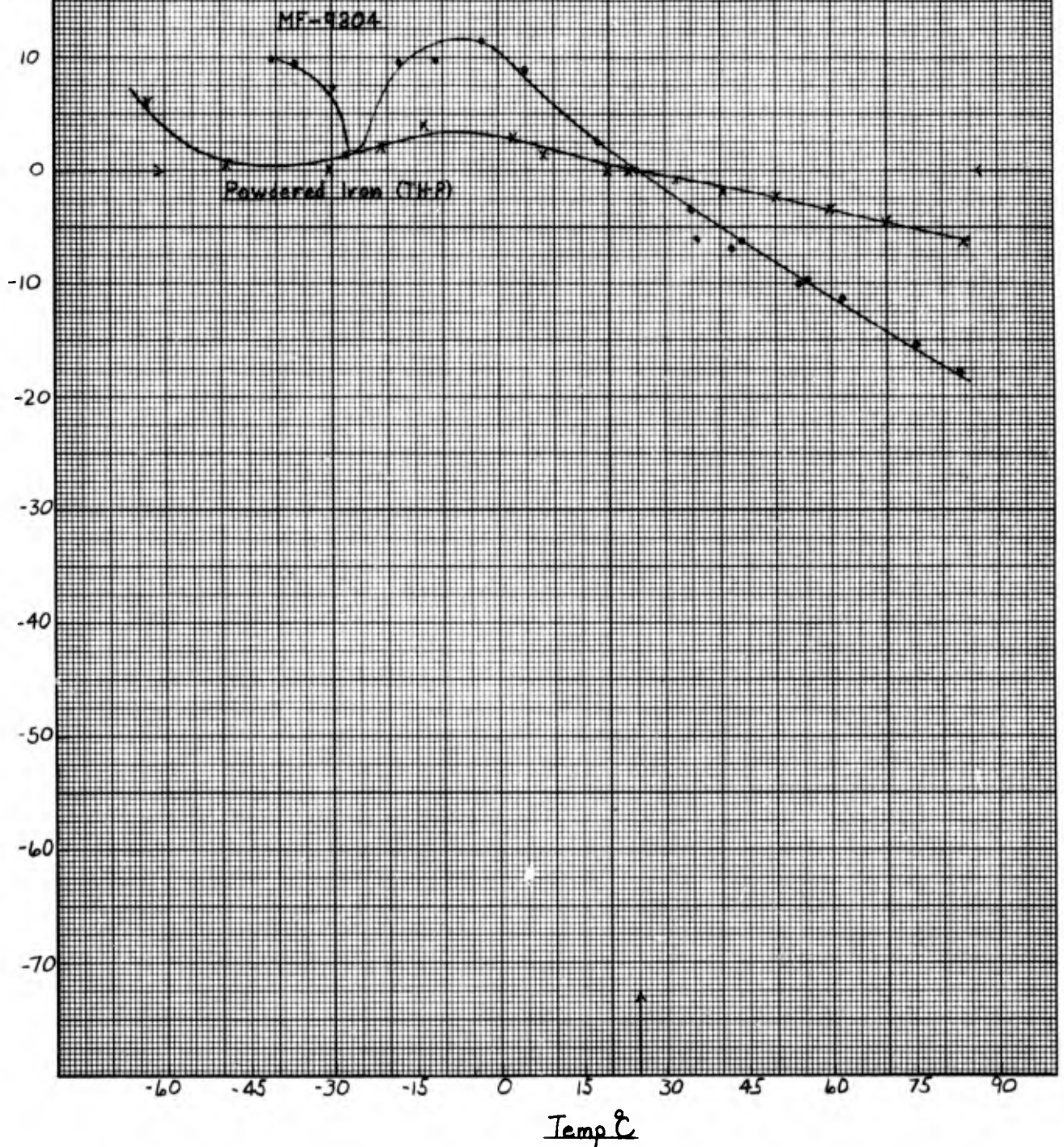
-40

1.0

2.0

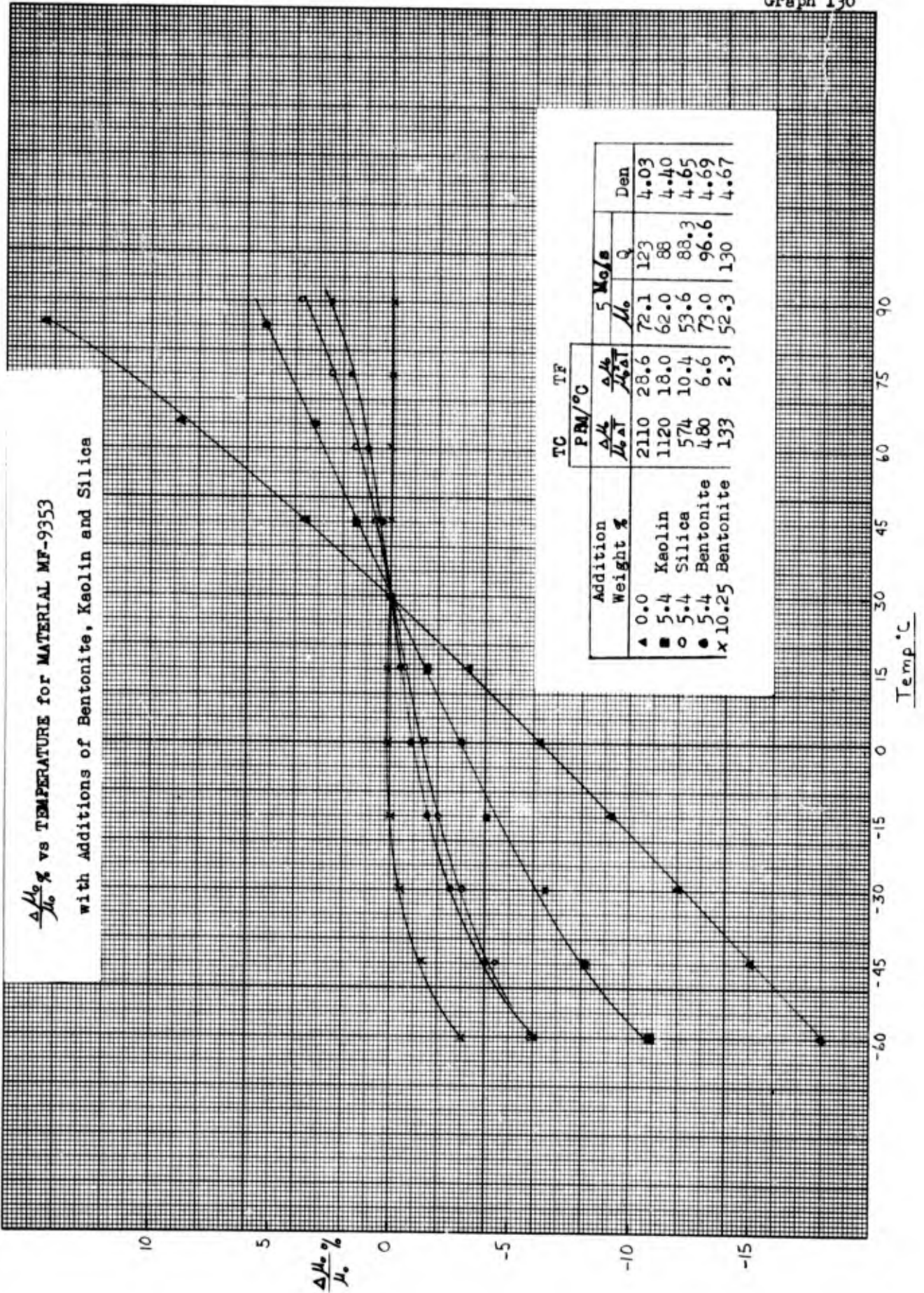
3.0

Signal Voltage (Volts)

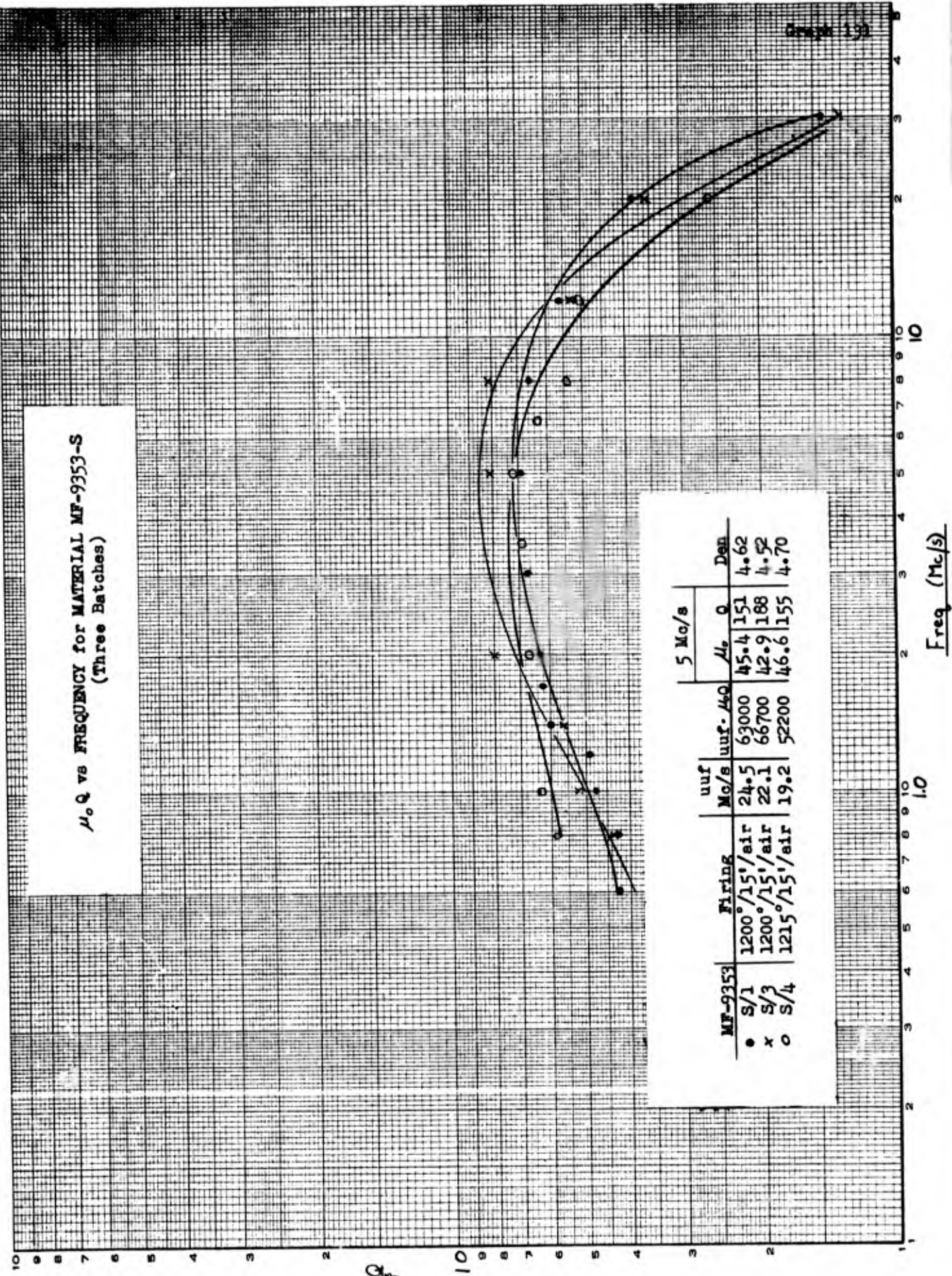
$\frac{\Delta Q}{Q} \%$  vs TEMPERATURE for MATERIAL MF-9304 and POWDERED IRON $\frac{\Delta Q}{Q} \%$ 

$\frac{\Delta \mu_0}{\mu_0} \%$  vs TEMPERATURE for MATERIAL MF-9353

with Additions of Bentonite, Keolin and Silica



$\mu_0 Q$  vs FREQUENCY for MATERIAL MF-9353-S  
(Three Batches)

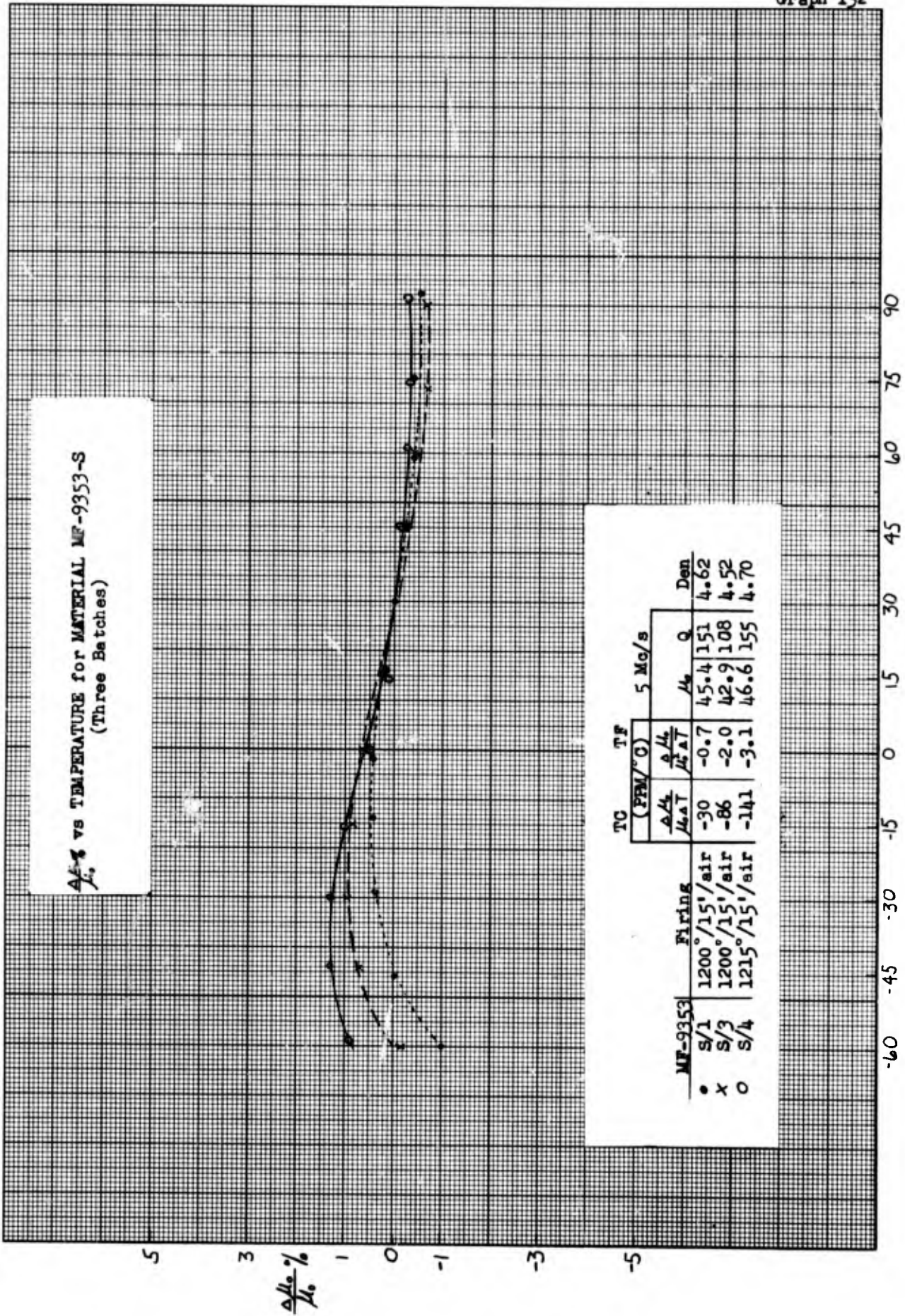


MF-9353	Firing	unf		5 Mc/s	
		Mc/s	unf. 460	$\mu_0 Q$	Den
● S/1	1200°/15'/air	24.5	63000	45.4	151
× S/3	1200°/15'/air	22.1	66700	42.9	188
○ S/4	1215°/15'/air	19.2	52200	46.6	155

$\frac{\mu_0 Q}{10}$

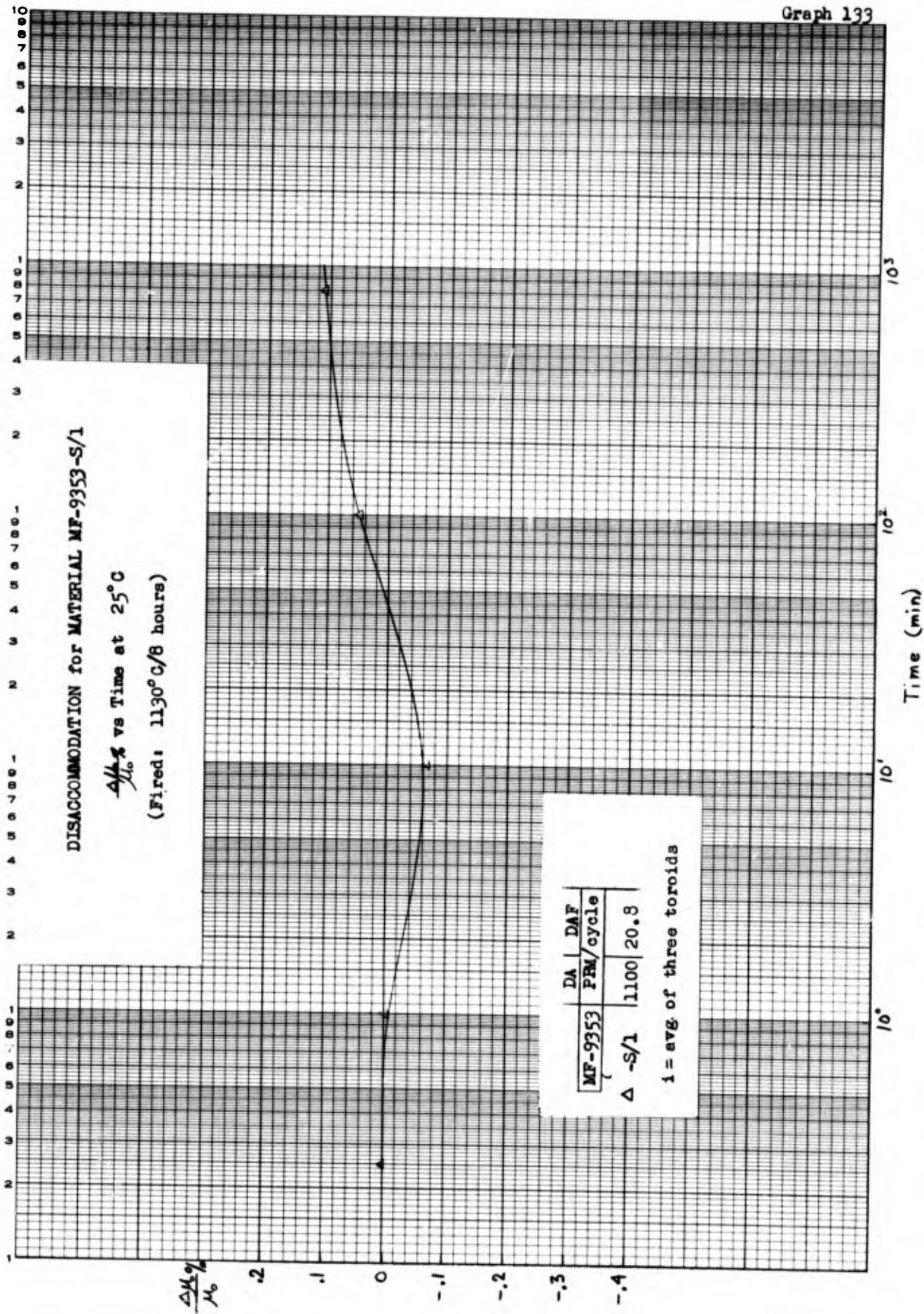
Freq (Mc/s)

$\Delta \mu_0$  vs TEMPERATURE for MATERIAL MF-9353-S  
(Three Batches)



MF-9353	Firing	TC			TF			Den
		$\frac{\Delta \mu_0}{\mu_0 \Delta T}$	$\frac{\Delta \mu_0}{\mu_0 \Delta T}$	(PPM/°C)	$\frac{\Delta \mu_0}{\mu_0 \Delta T}$	$\frac{\Delta \mu_0}{\mu_0 \Delta T}$	(PPM/°C)	
• S/1	1200°/15'/air	-30	-0.7		45.4	151	4.62	
x S/3	1200°/15'/air	-86	-2.0		42.9	108	4.52	
o S/4	1215°/15'/air	-141	-3.1		46.6	155	4.70	

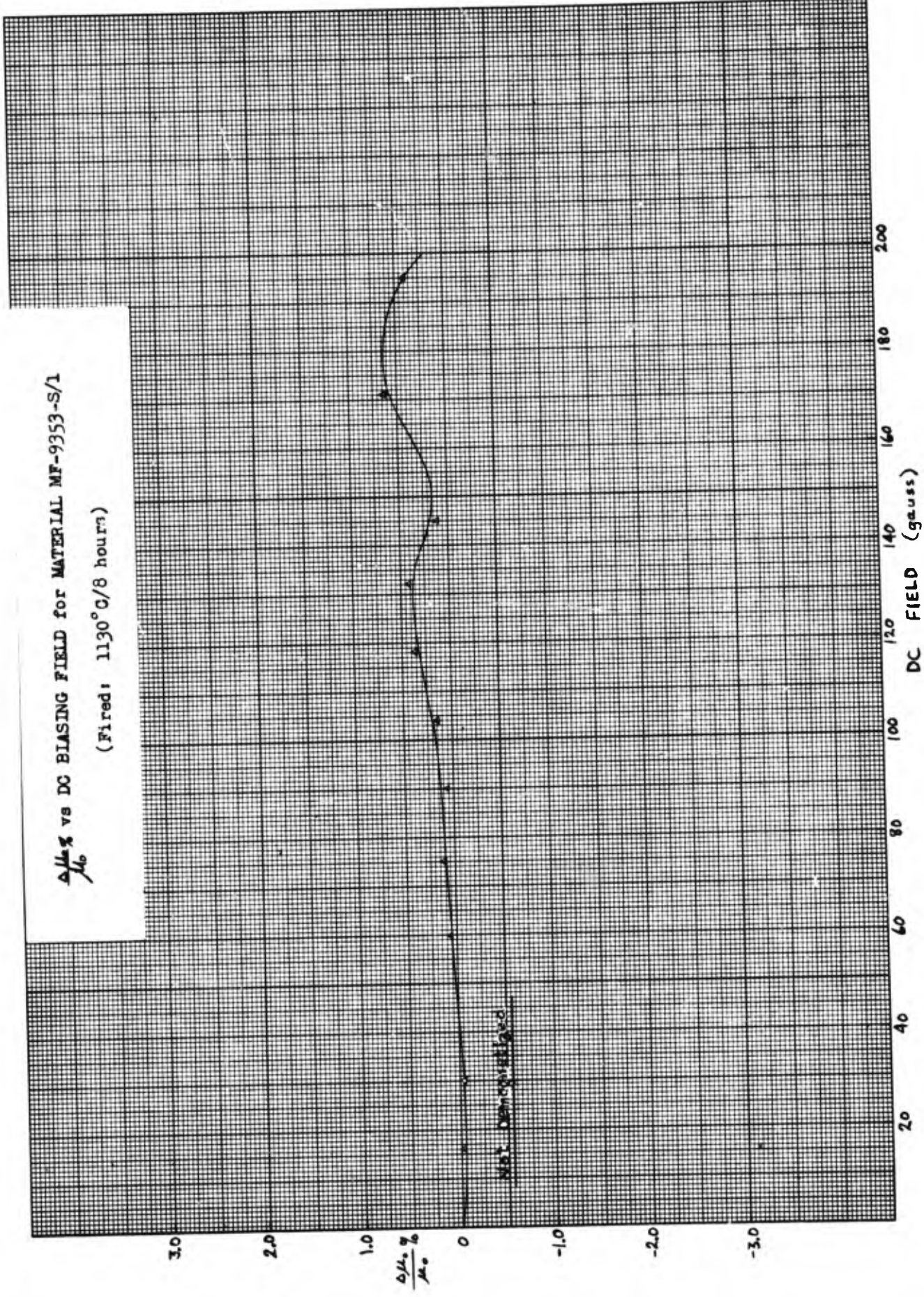
Temp °C



DISACCOMMODATION for MATERIAL MF-9353-S/1

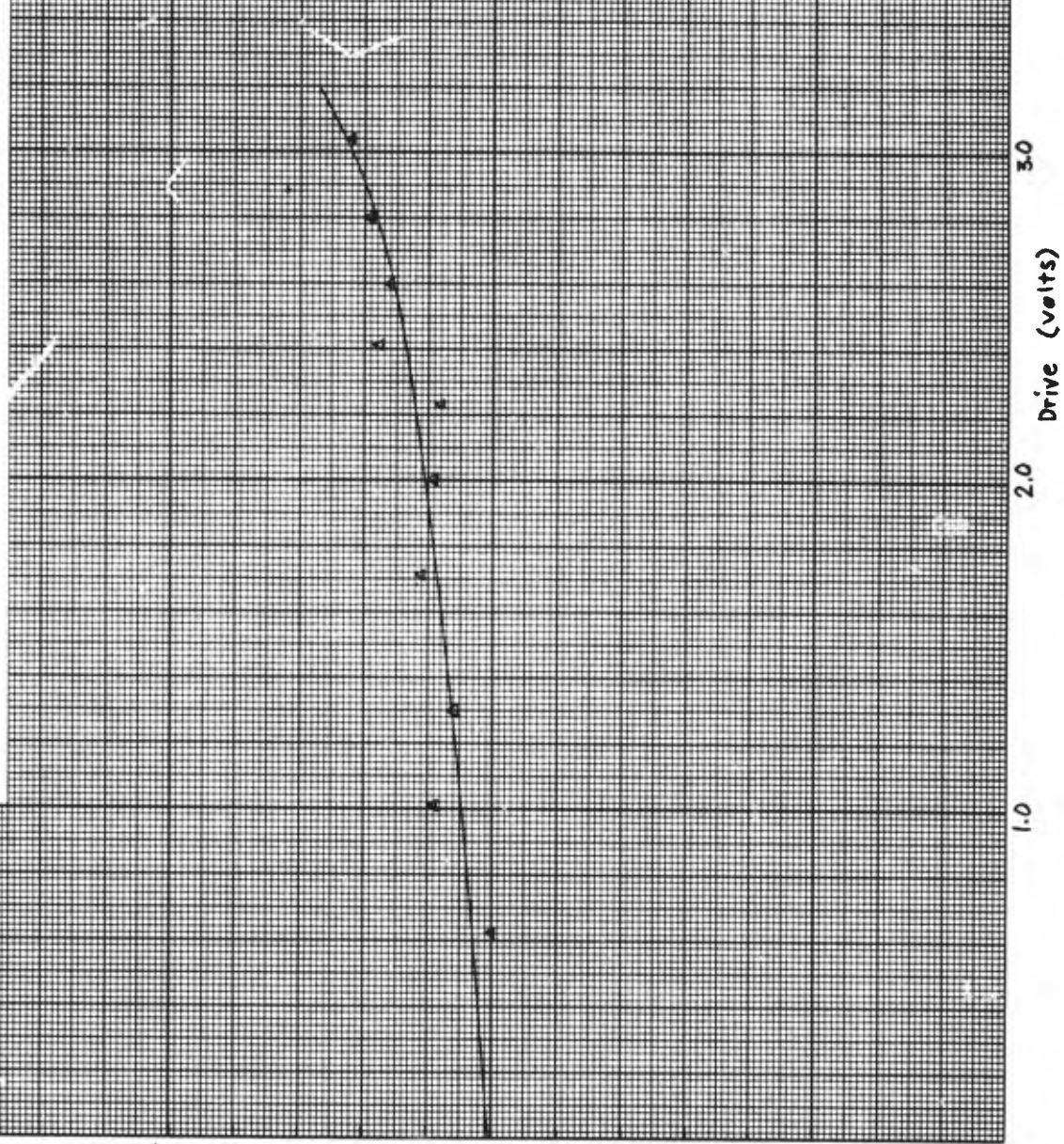
$\frac{\Delta H_0}{M_0}$  vs Time at 25°C  
 (Fired: 1130°C/8 hours)

$\frac{\Delta\mu_g}{\mu_0}$  vs DC BIASING FIELD for MATERIAL MF-9353-S/1  
(Fired: 1130°C/8 hours)

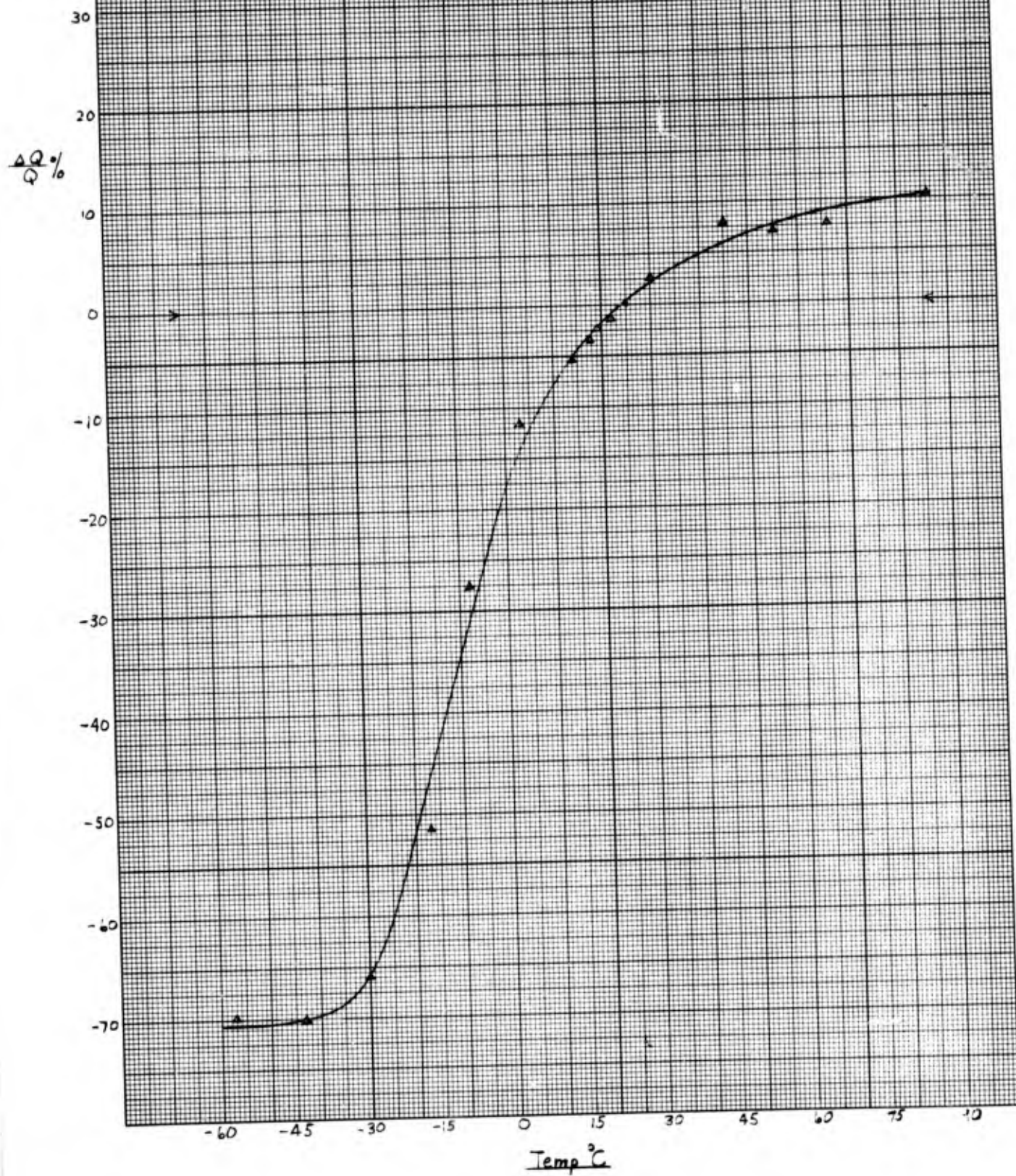


$\frac{\Delta \mu_0}{\mu_0} \%$  vs DRIVING VOLTAGE at 5 Mc/s for MATERIAL MF-9353-S/1  
 (Fired: 1130°C/8 hours)

$\frac{\Delta \mu_0}{\mu_0} \%$

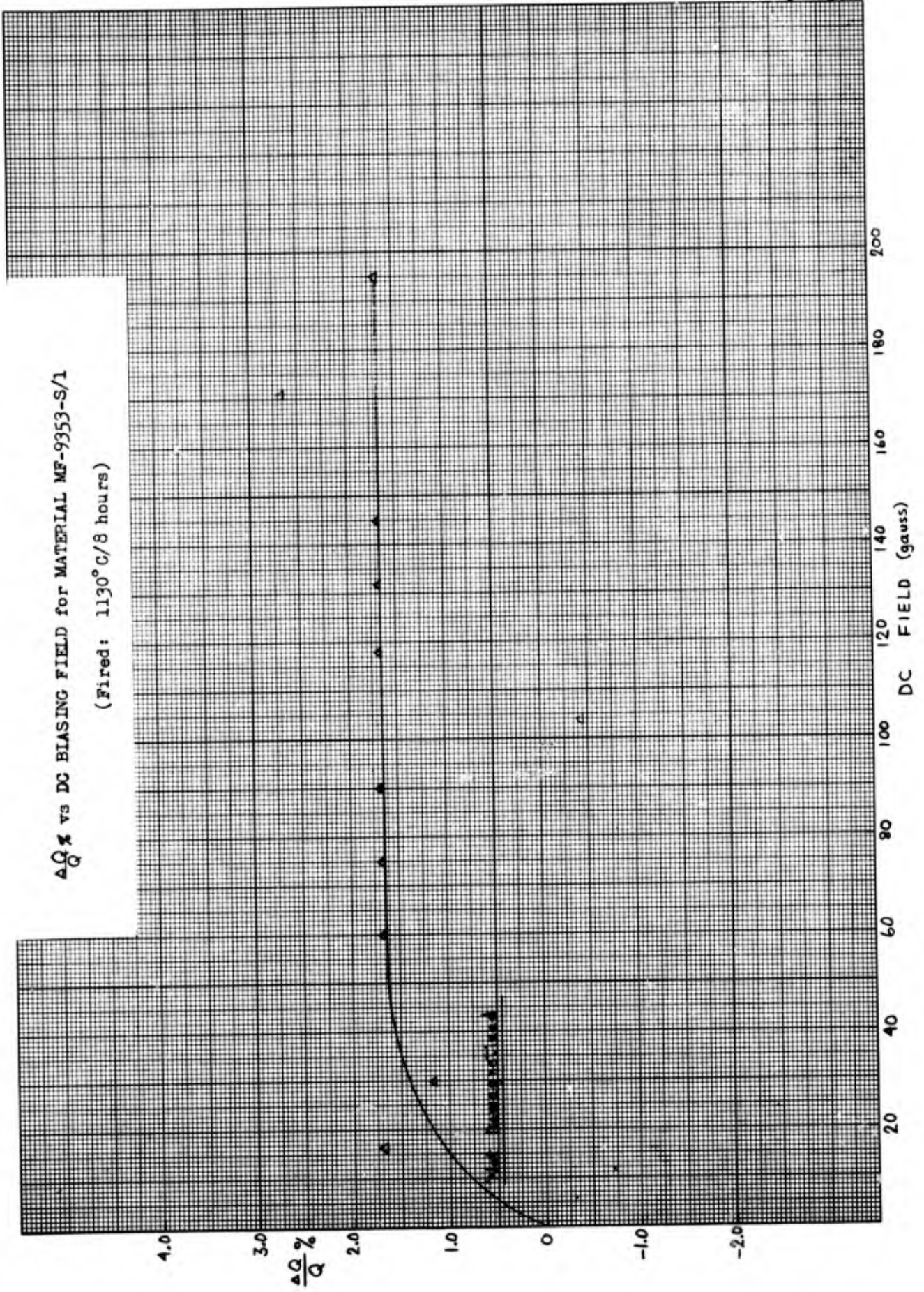


$\Delta$	$\frac{\Delta \mu_0}{\mu_0} (\% / \text{volt})$	Tol (%)	$\mu_0$
	0.09	0.05	52.3

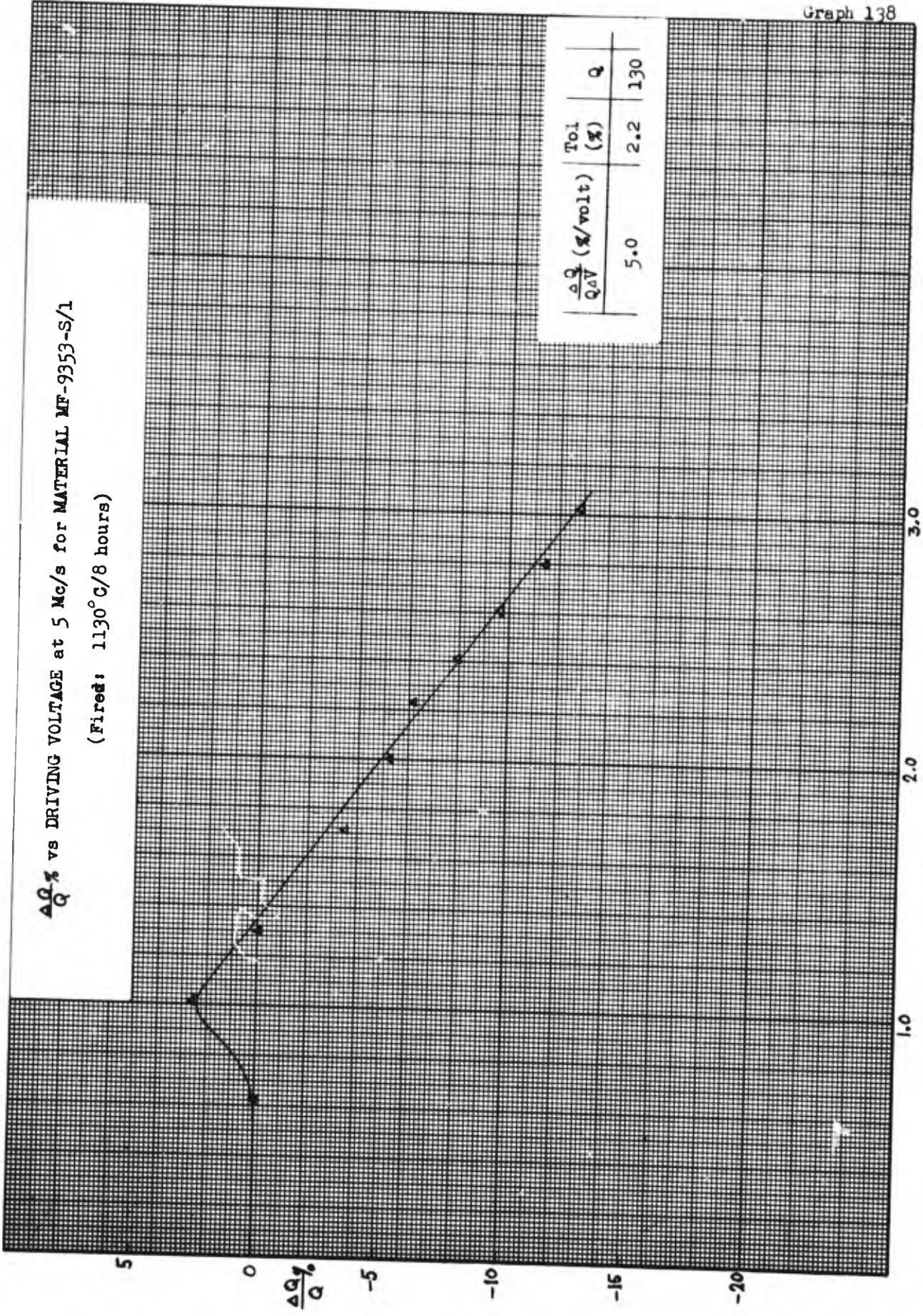
$\frac{\Delta Q}{Q} \%$  vs TEMPERATURE for MATERIAL MF-9353-S

$\frac{\Delta Q}{Q} \%$  vs DC BIASING FIELD for MATERIAL MF-9353-S/1

(Fired: 1130° C/8 hours)



$\frac{\Delta Q}{Q}\%$  vs DRIVING VOLTAGE at 5 Mc/s for MATERIAL MF-9353-S/1  
 (Fired: 1130° C/8 hours)



$\frac{\Delta Q}{Q}\%$ (g/volt)	Tol (%)	Q
5.0	2.2	130

$\frac{\Delta Q}{Q} \%$  vs TEMPERATURE for MATERIAL MF-9353-S  
with  $Fe_2O_3$  Content Varied

$\frac{\Delta Q}{Q} \%$

10

0

-10

-20

-30

-40

-50

-60

-70

-60

-45

-30

-15

0

15

30

45

60

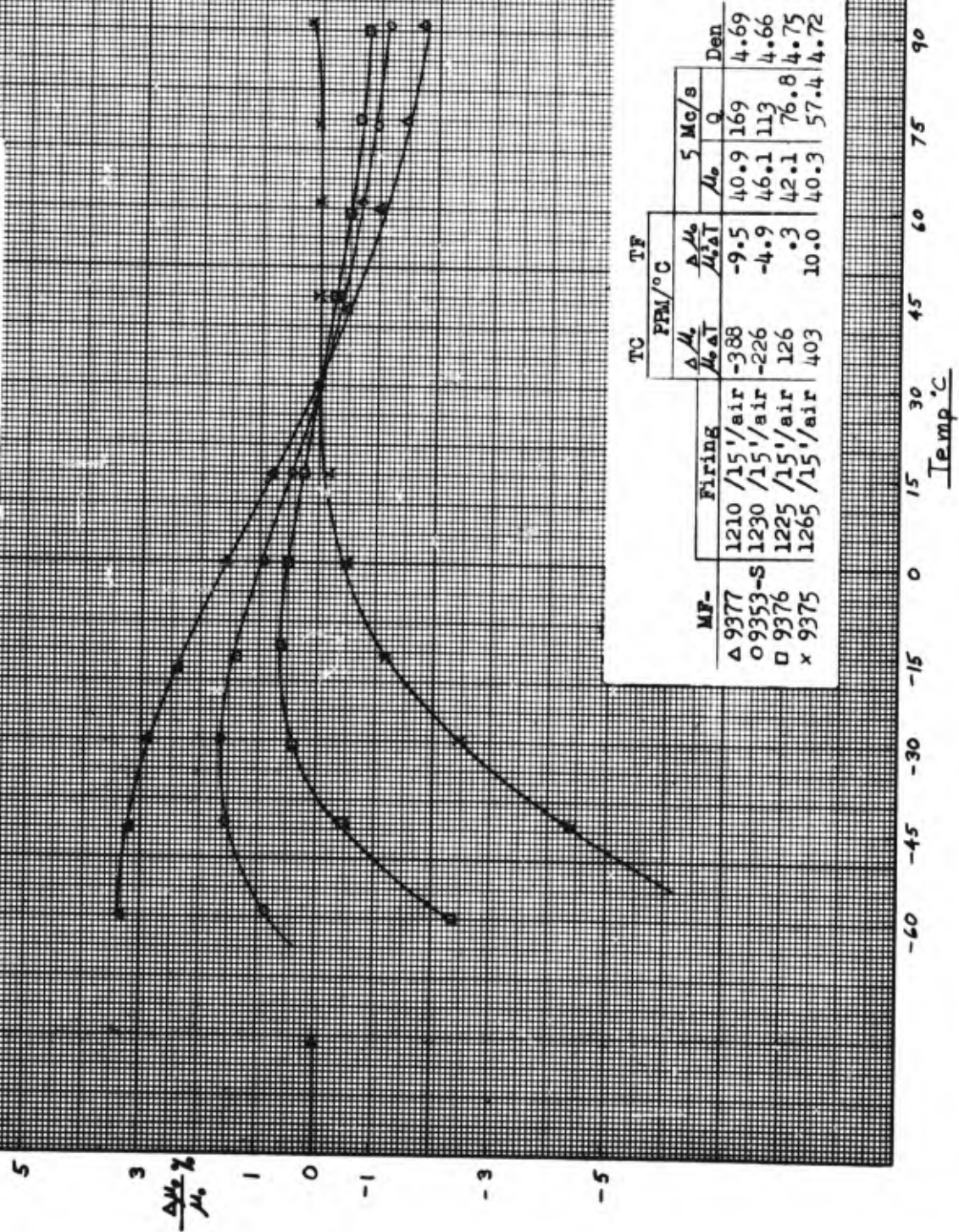
75

90

Temp °C

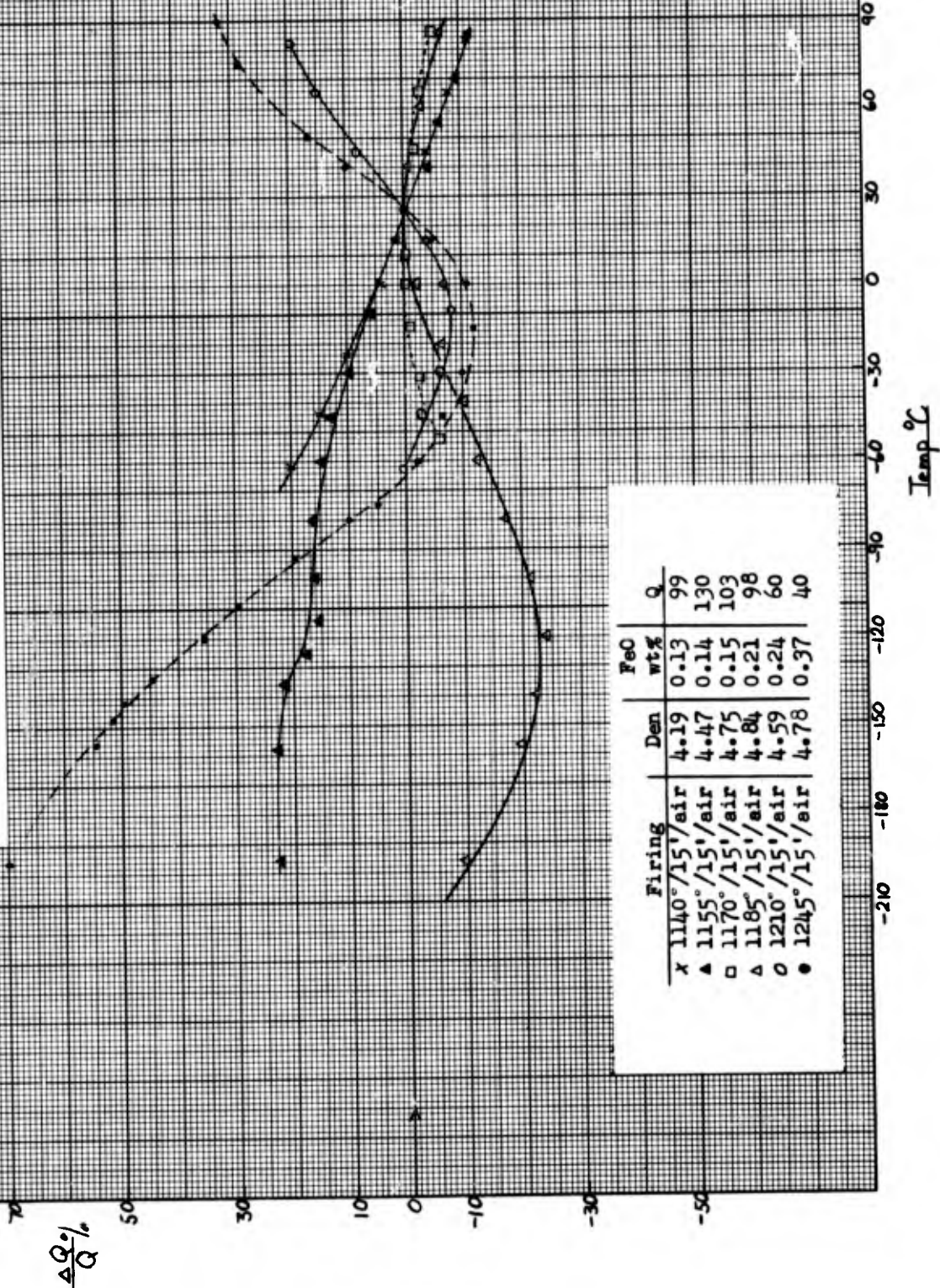
MF-	Firing	$Fe_2O_3$ (Mol%)	Den	FeO Wt%
Δ 9377	1210/15'/air	44.67	4.69	2.6
○ 9353-S	1230/15'/air	43.45	4.66	1.8
□ 9376	1225/15'/air	42.86	4.75	1.9
x 9375	1265/15'/air	41.08	4.72	1.1

$\frac{\Delta \mu_0}{\mu_0} \%$  vs TEMPERATURE for MATERIAL MF-9353-S  
with Fe<sub>2</sub>O<sub>3</sub> Content Varied



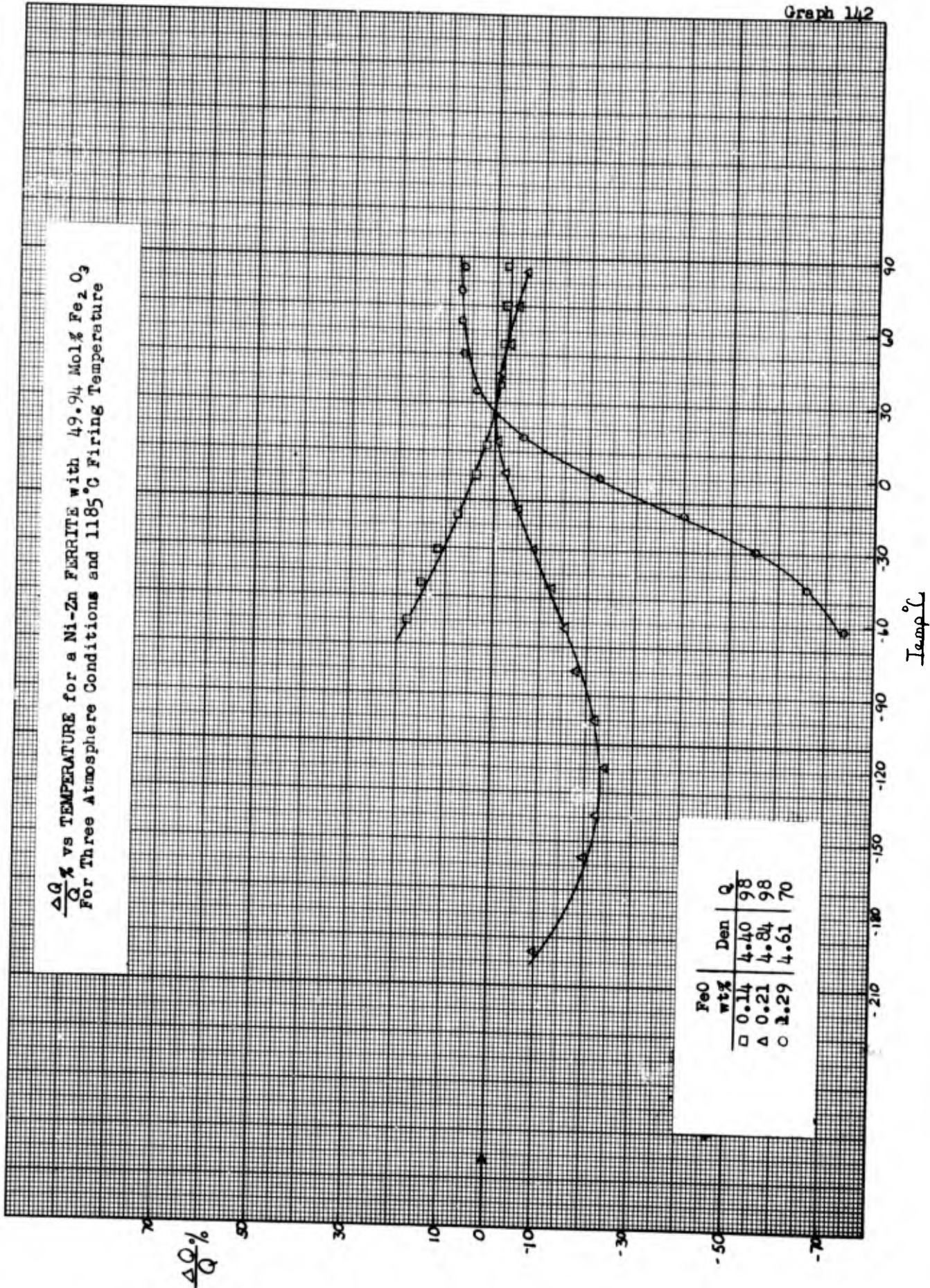
MF-	Firing	TC		TF		5 Mc/s		Den
		$\frac{\Delta \mu_0}{\mu_0 \Delta T}$	PPM/°C	$\frac{\Delta \mu_0}{\mu_0 \Delta T}$	PPM/°C	$\mu_0$	Q	
Δ 9377	1210 / 15' / air	-388	-9.5	40.9	169	4.69		
○ 9353-S	1230 / 15' / air	-226	-4.9	46.1	113	4.66		
□ 9376	1225 / 15' / air	126	.3	42.1	76.8	4.75		
x 9375	1265 / 15' / air	403	10.0	40.3	57.4	4.72		

$\frac{\Delta Q}{Q}\%$  vs TEMPERATURE for a Ni-Zn FERRITE with 49.94 Mol% Fe<sub>2</sub>O<sub>3</sub>  
for Six Firing Temperatures



Firing	Den	FeO wt%	Q
x 1140°/15'/air	4.19	0.13	99
▲ 1155°/15'/air	4.47	0.14	130
□ 1170°/15'/air	4.75	0.15	103
△ 1185°/15'/air	4.84	0.21	98
○ 1210°/15'/air	4.59	0.24	60
● 1245°/15'/air	4.78	0.37	40

$\frac{\Delta Q}{Q} \%$  vs TEMPERATURE for a Ni-Zn FERRITE with 49.94 Mol% Fe<sub>2</sub>O<sub>3</sub>  
 For Three Atmosphere Conditions and 1185°C Firing Temperature

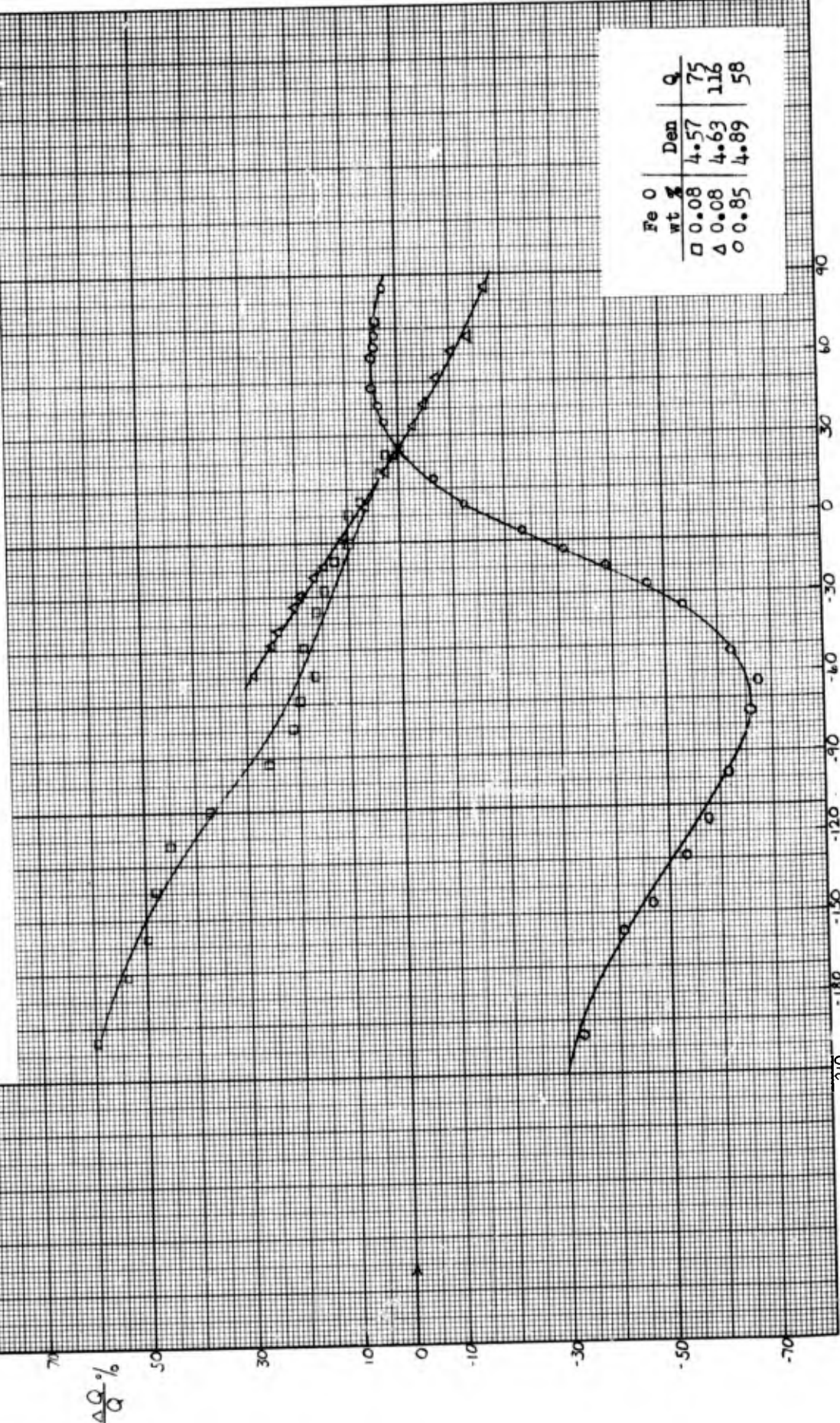


FeO wt%	Den	Q
□ 0.14	4.40	98
△ 0.21	4.84	98
○ 2.29	4.61	70

$\frac{\Delta Q}{Q} \%$

Temp °C

$\frac{\Delta Q}{Q}$  vs TEMPERATURE for a Ni-Zn FERRITE with 47.84 Mol% Fe<sub>2</sub>O<sub>3</sub>  
 For Three Atmosphere Conditions and 1155°C Firing Temperature

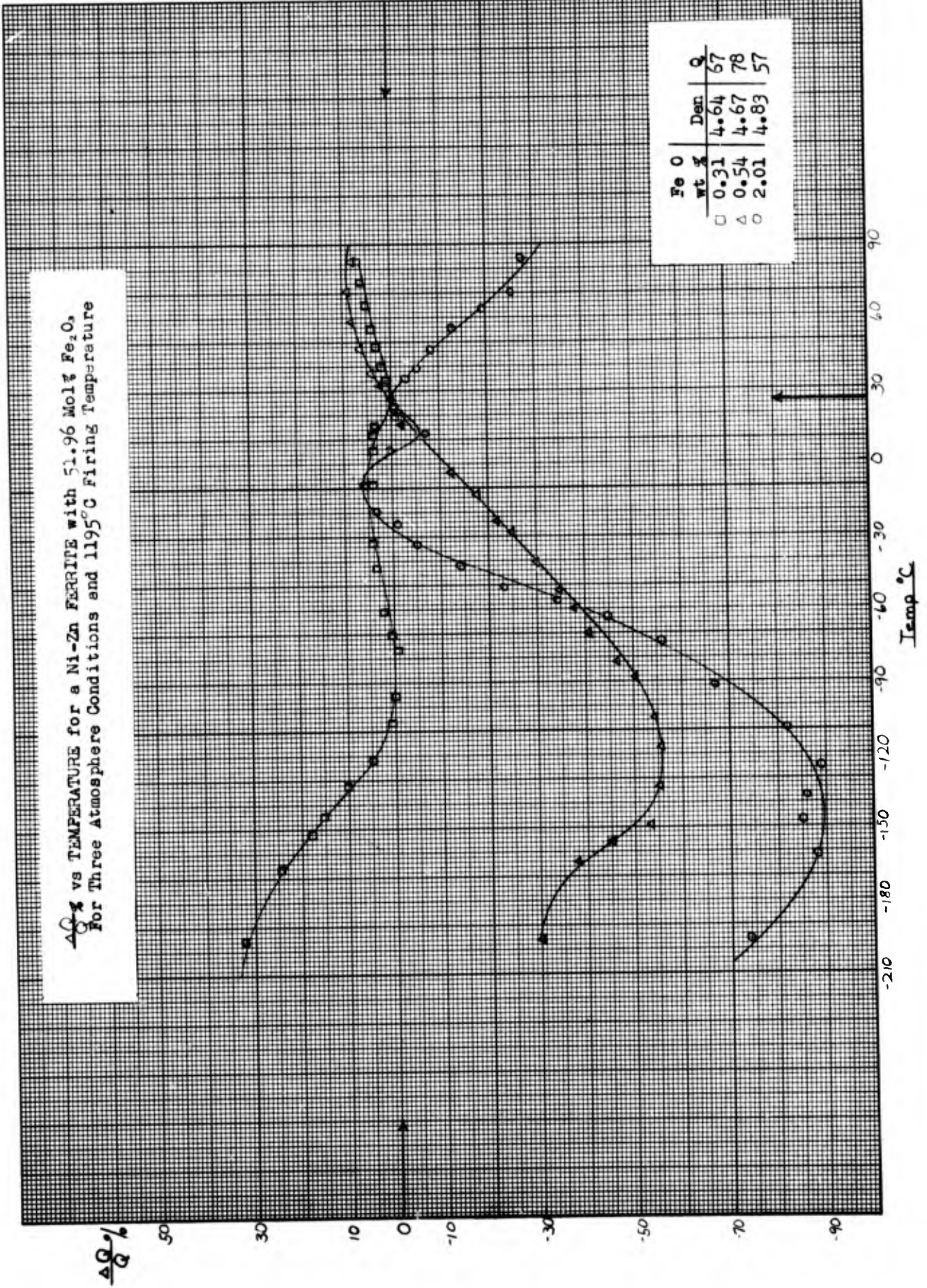


Fe O wt %	Den	Q
□ 0.08	4.57	75
△ 0.08	4.63	116
○ 0.85	4.89	58

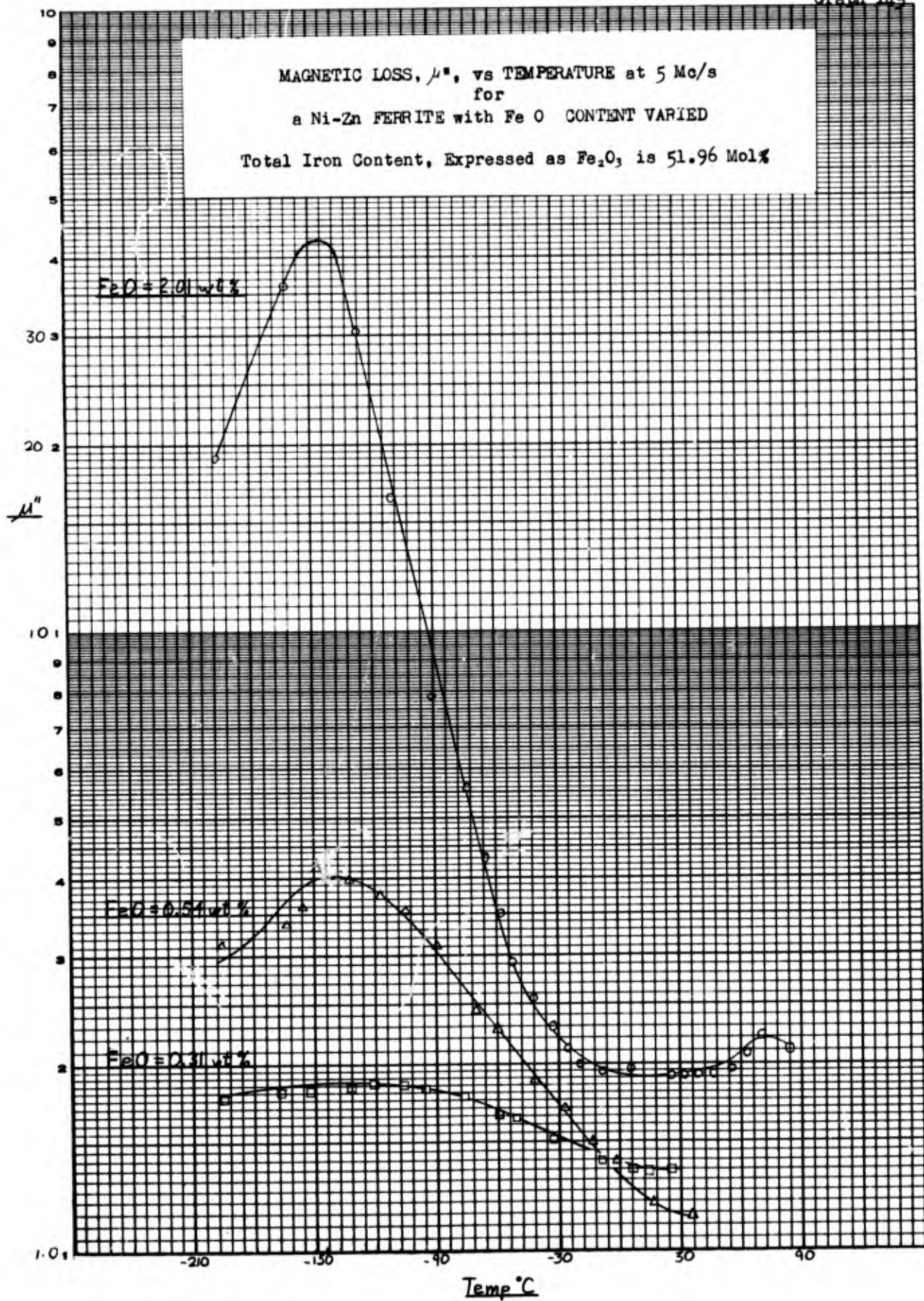
Temp.°C

$\frac{\Delta Q}{Q}$  %

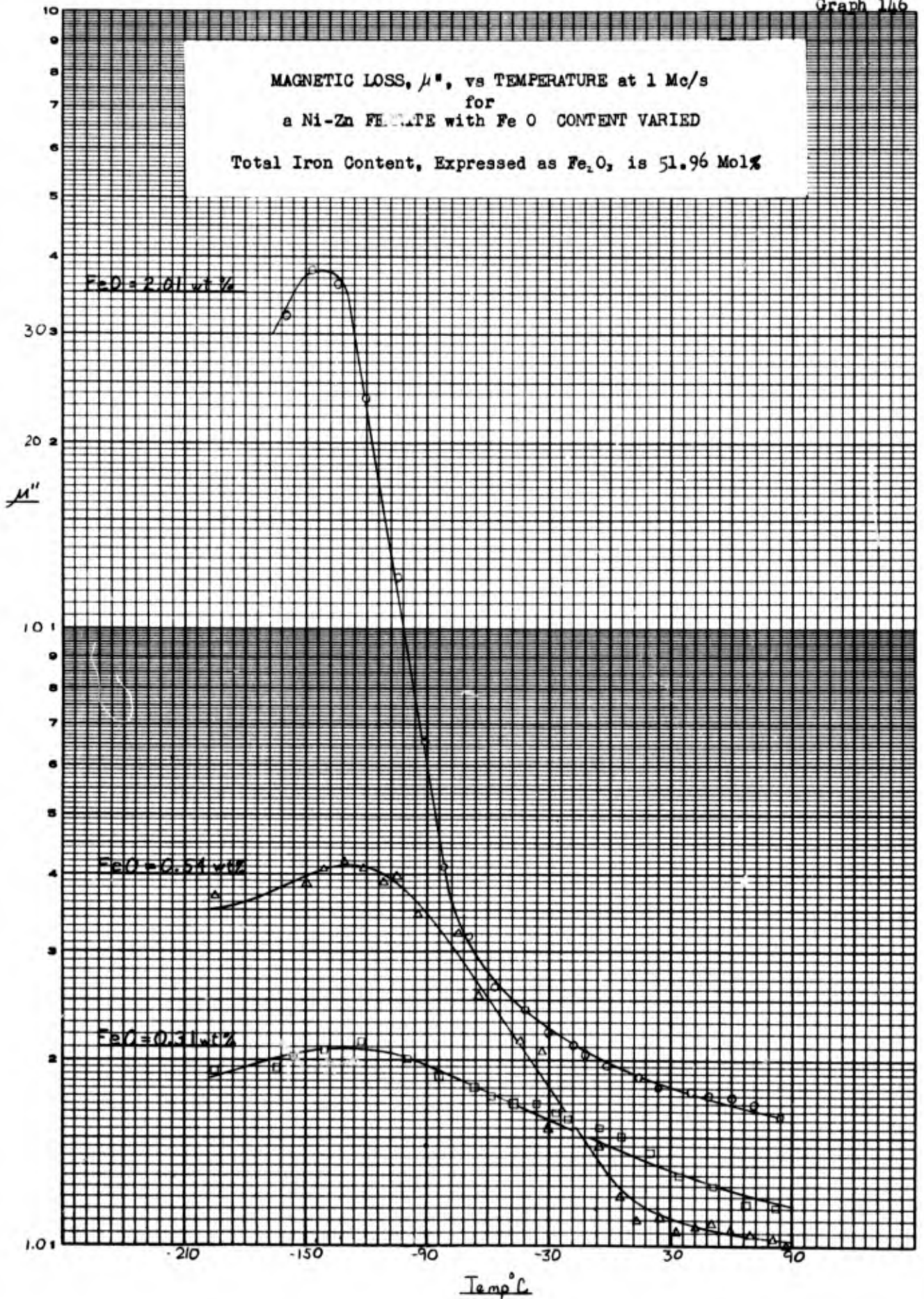
$\frac{\Delta Q}{Q} \%$  vs TEMPERATURE for a Ni-Zn FERRITE with 51.96 Mol%  $Fe_2O_3$   
 For Three Atmosphere Conditions and 1195°C Firing Temperature



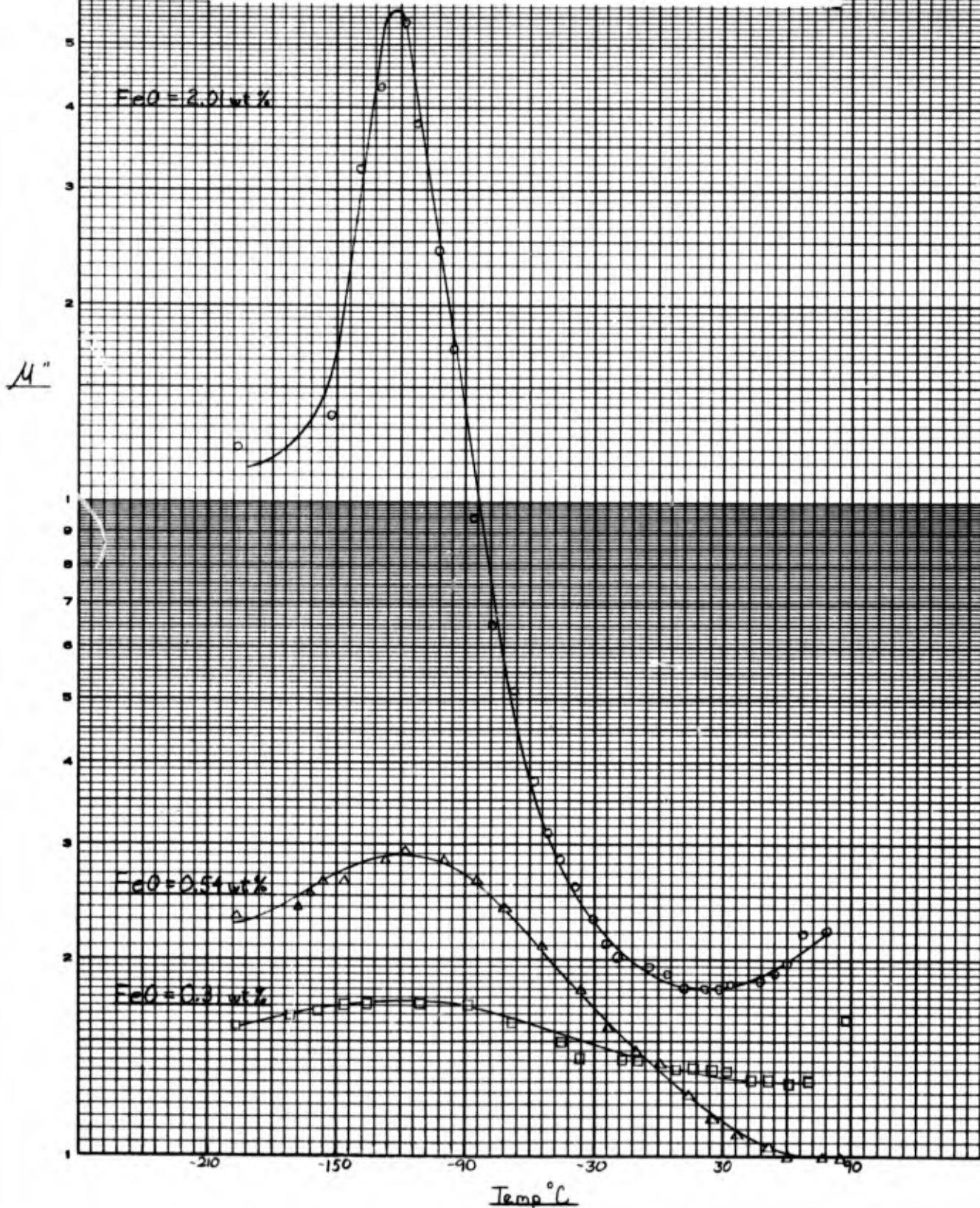
MAGNETIC LOSS,  $\mu''$ , vs TEMPERATURE at 5 Mc/s  
for  
a Ni-Zn FERRITE with Fe O CONTENT VARIED  
Total Iron Content, Expressed as  $Fe_2O_3$ , is 51.96 Mol%



MAGNETIC LOSS,  $\mu''$ , vs TEMPERATURE at 1 Mc/s  
 for  
 a Ni-Zn FERRITE with FeO CONTENT VARIED  
 Total Iron Content, Expressed as  $Fe_2O_3$ , is 51.96 Mol%

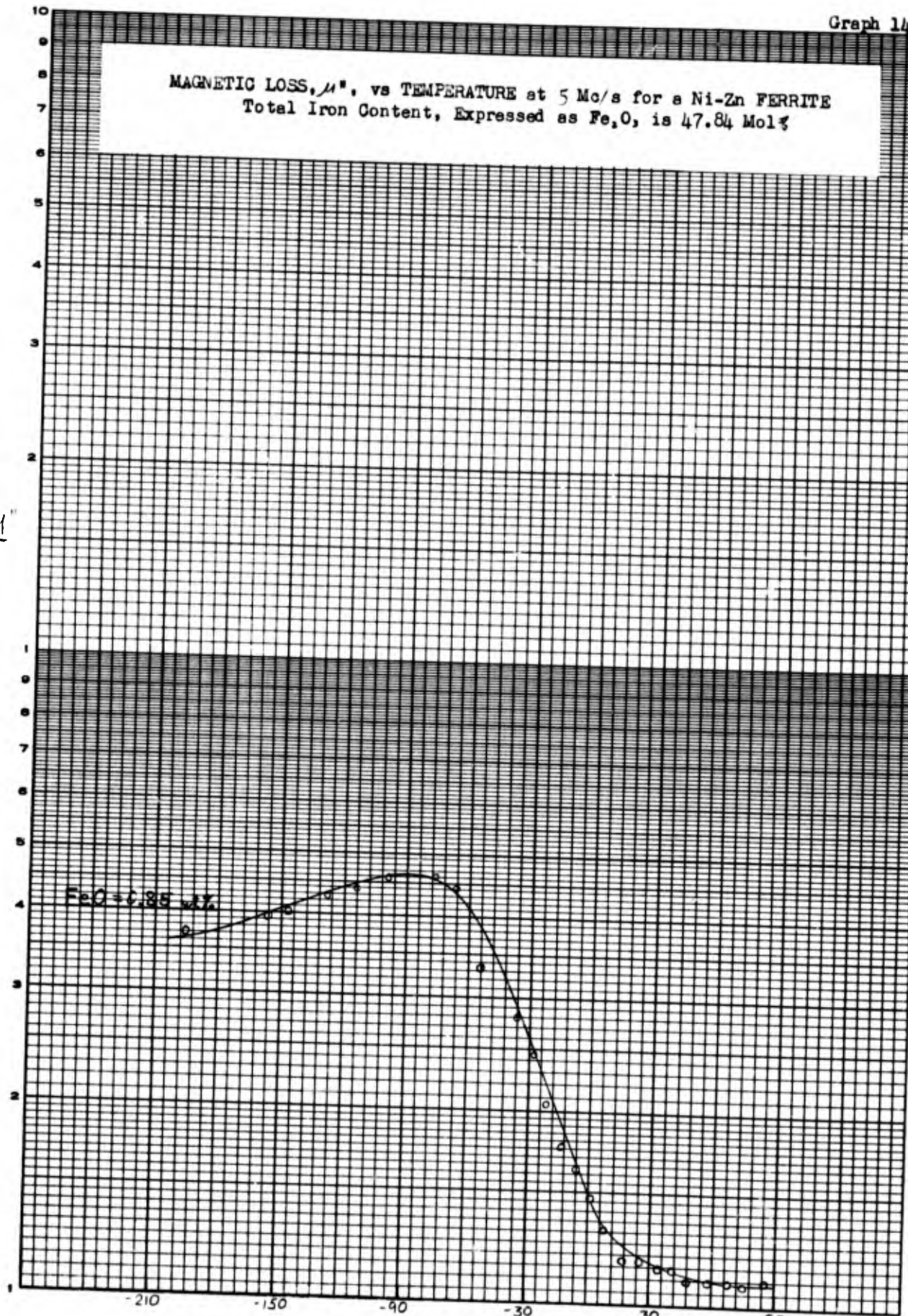


MAGNETIC LOSS,  $\mu''$ , vs TEMPERATURE at 10 Mc/s  
for  
a Ni-Zn FERRITE with FeO CONTENT VARIED  
Total Iron Content, Expressed as  $Fe_2O_3$ , is 51.96 Mol%



MAGNETIC LOSS,  $\mu''$ , vs TEMPERATURE at 5 Mc/s for a Ni-Zn FERRITE  
Total Iron Content, Expressed as  $Fe_2O_3$ , is 47.84 Mol%

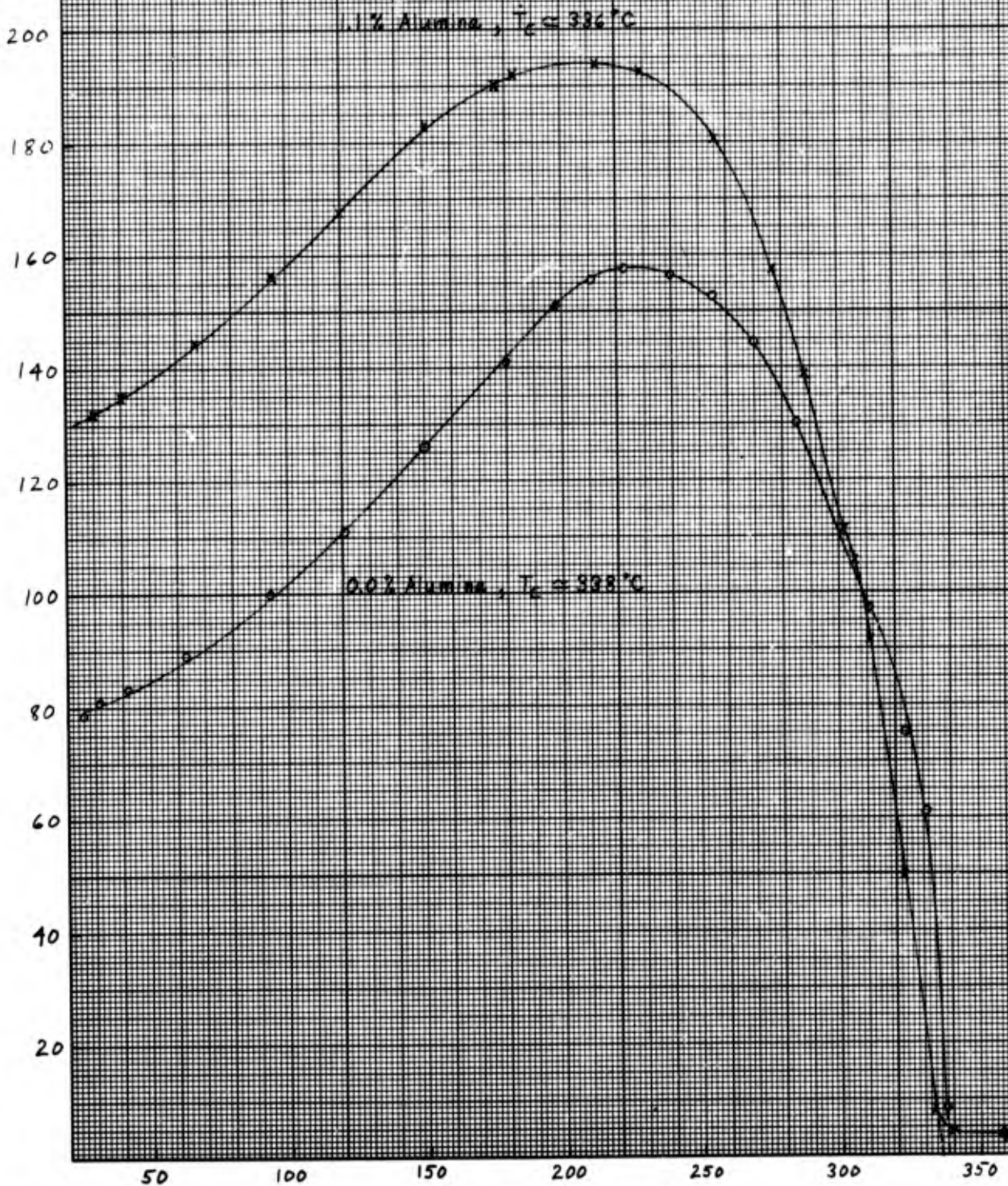
$\mu''$



Temp °C

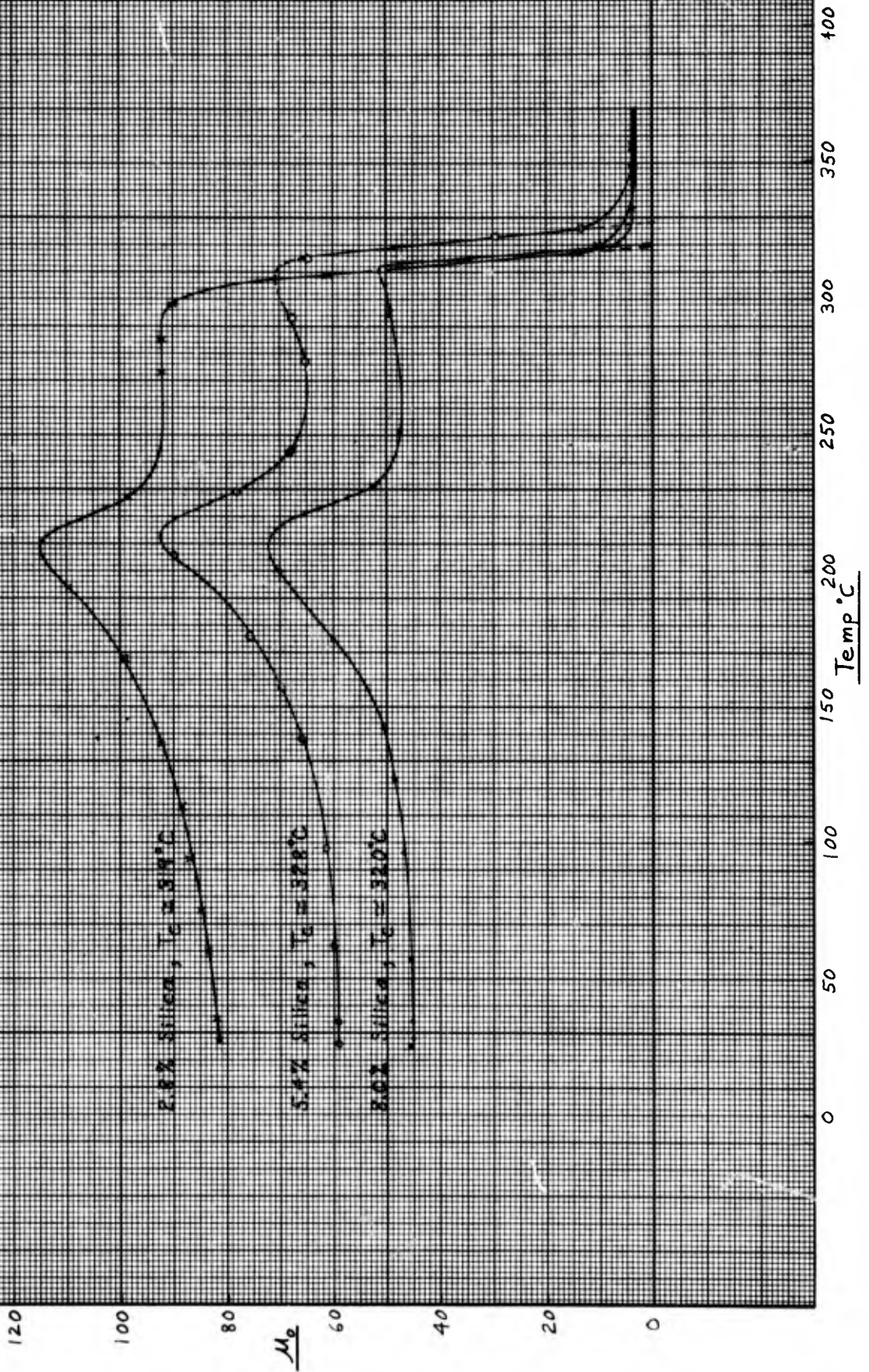
$\mu_o$  vs TEMPERATURE THROUGH  $T_c$   
for  
Material MF-9353 with 0.0 and 1.1 Weight % Alumina

$\mu_o$

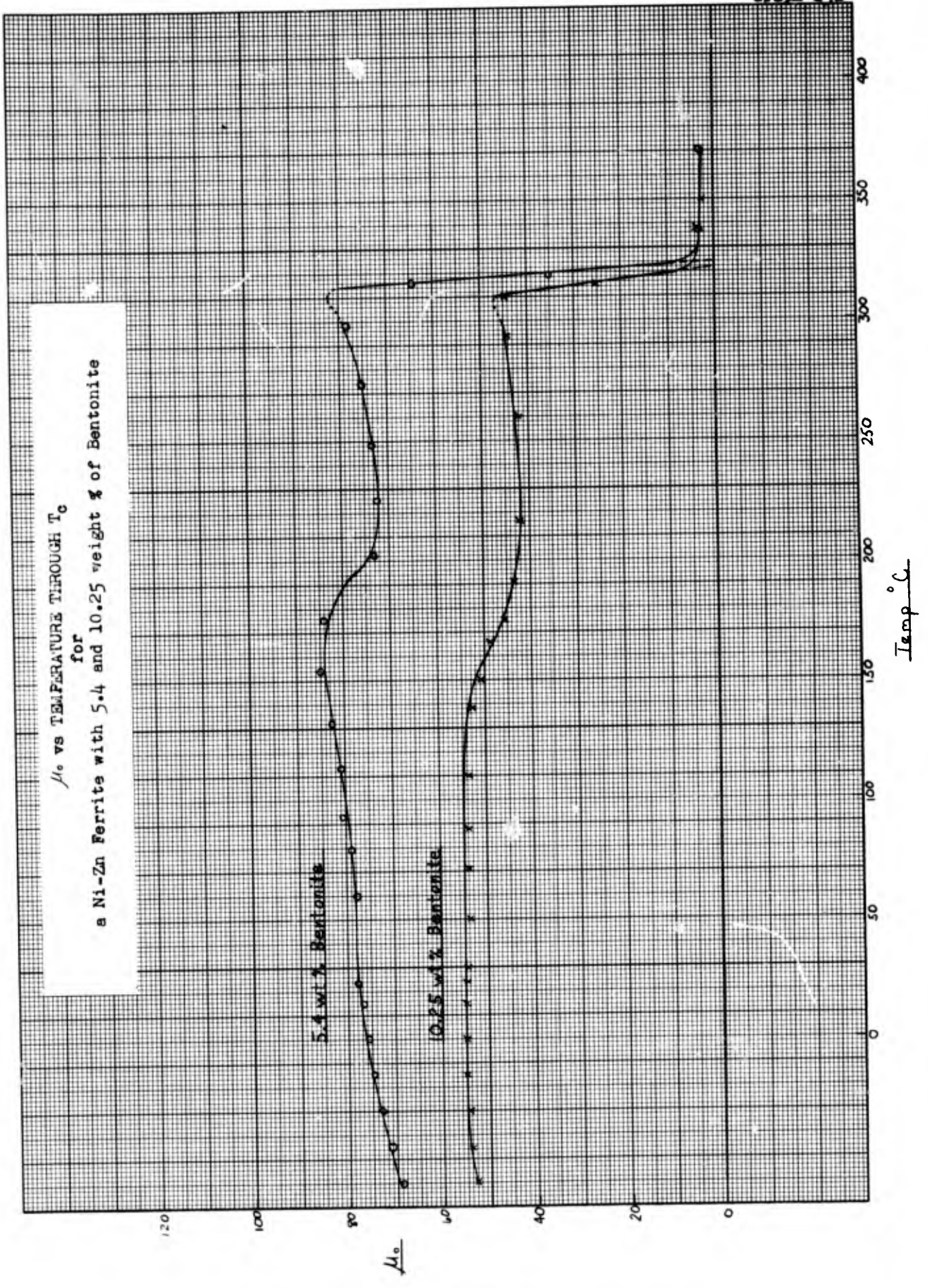


Temp  $^\circ\text{C}$

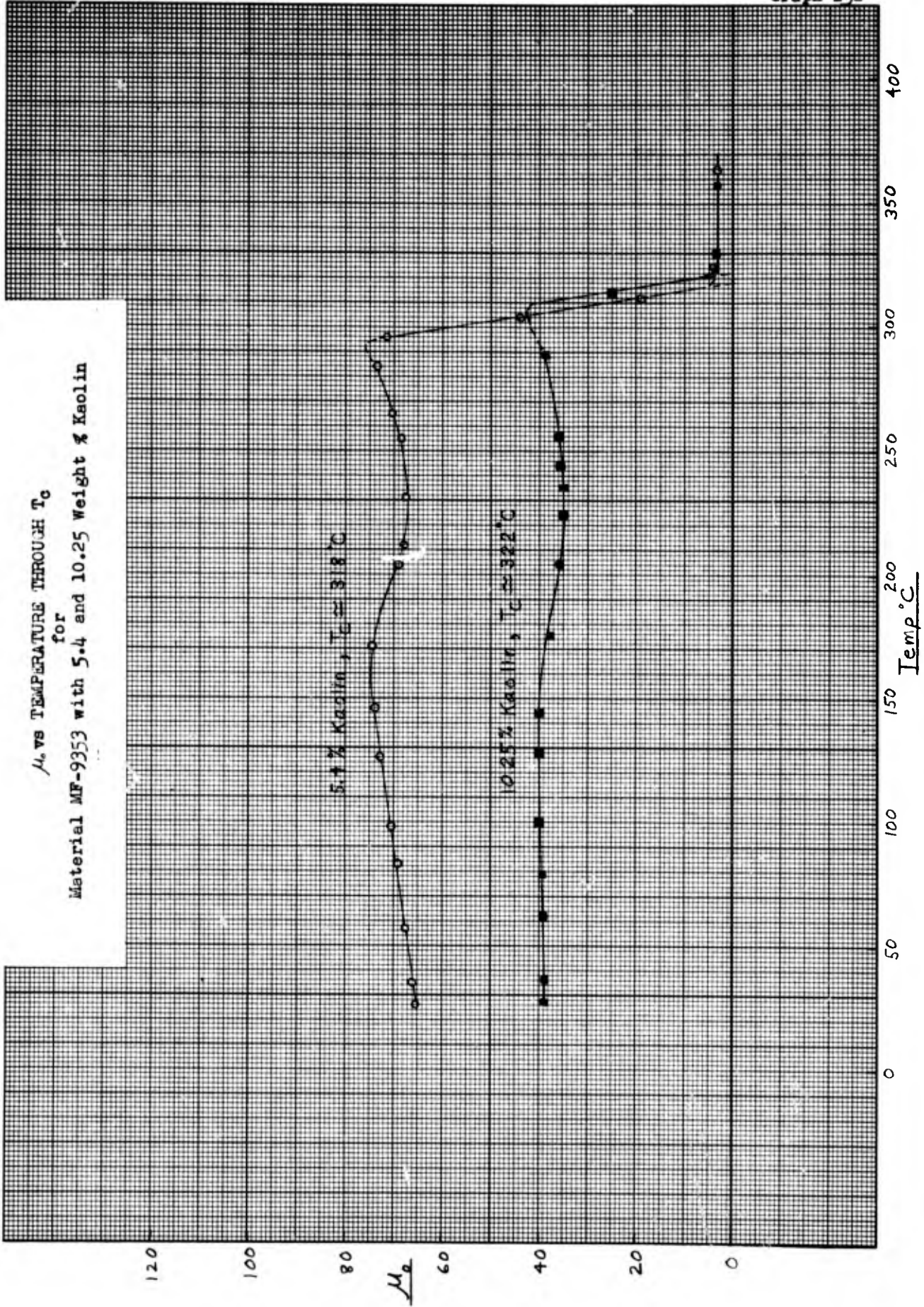
$\mu_e$  vs TEMPERATURE THROUGH  $T_g$   
for  
Material MF-9353 with 2.8, 5.4 and 8.0 Weight % Silica



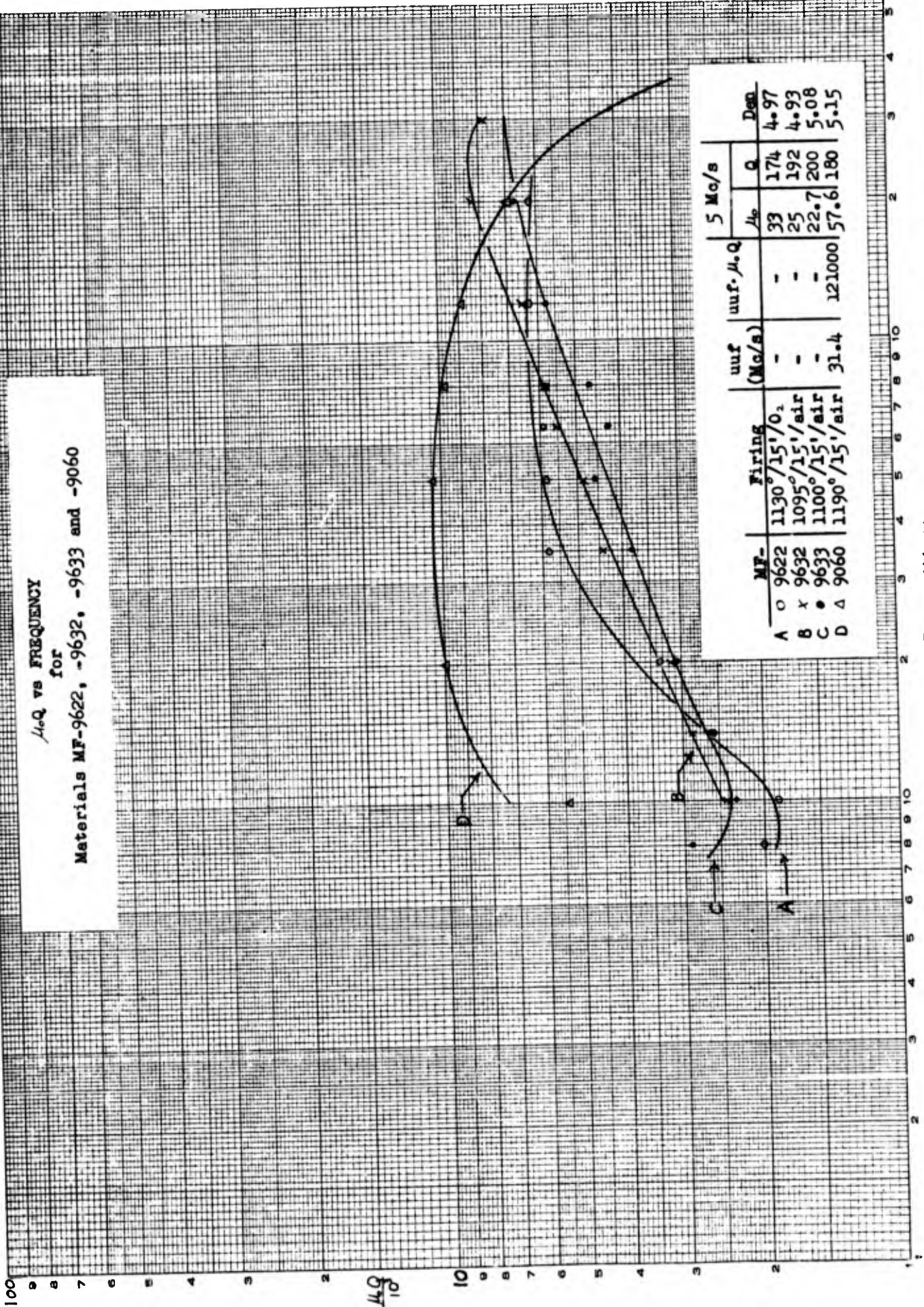
$\mu_o$  vs TEMPERATURE THROUGH  $T_c$   
for  
a Ni-Zn Ferrite with 5.4 and 10.25 weight % of Bentonite



$\mu_e$  vs TEMPERATURE THROUGH  $T_c$   
for  
Material MF-9353 with 5.4 and 10.25 Weight % Kaolin



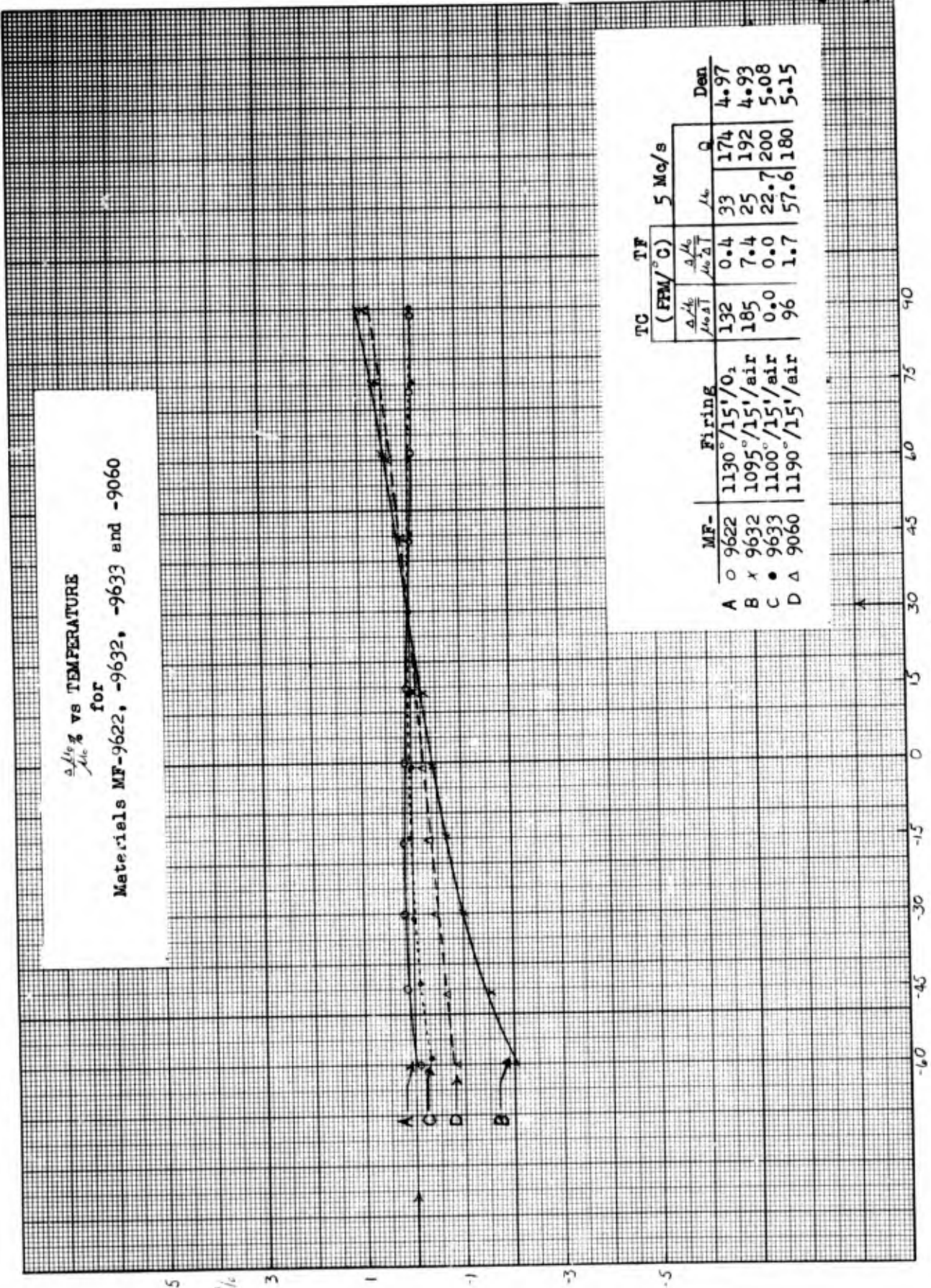
$\mu_c Q$  vs FREQUENCY  
for  
Materials MF-9622, -9632, -9633 and -9060



Freq (Mc/s)

$\frac{\Delta \mu_c}{\mu_c} \%$  vs TEMPERATURE

for  
Materials MF-9622, -9632, -9633 and -9060

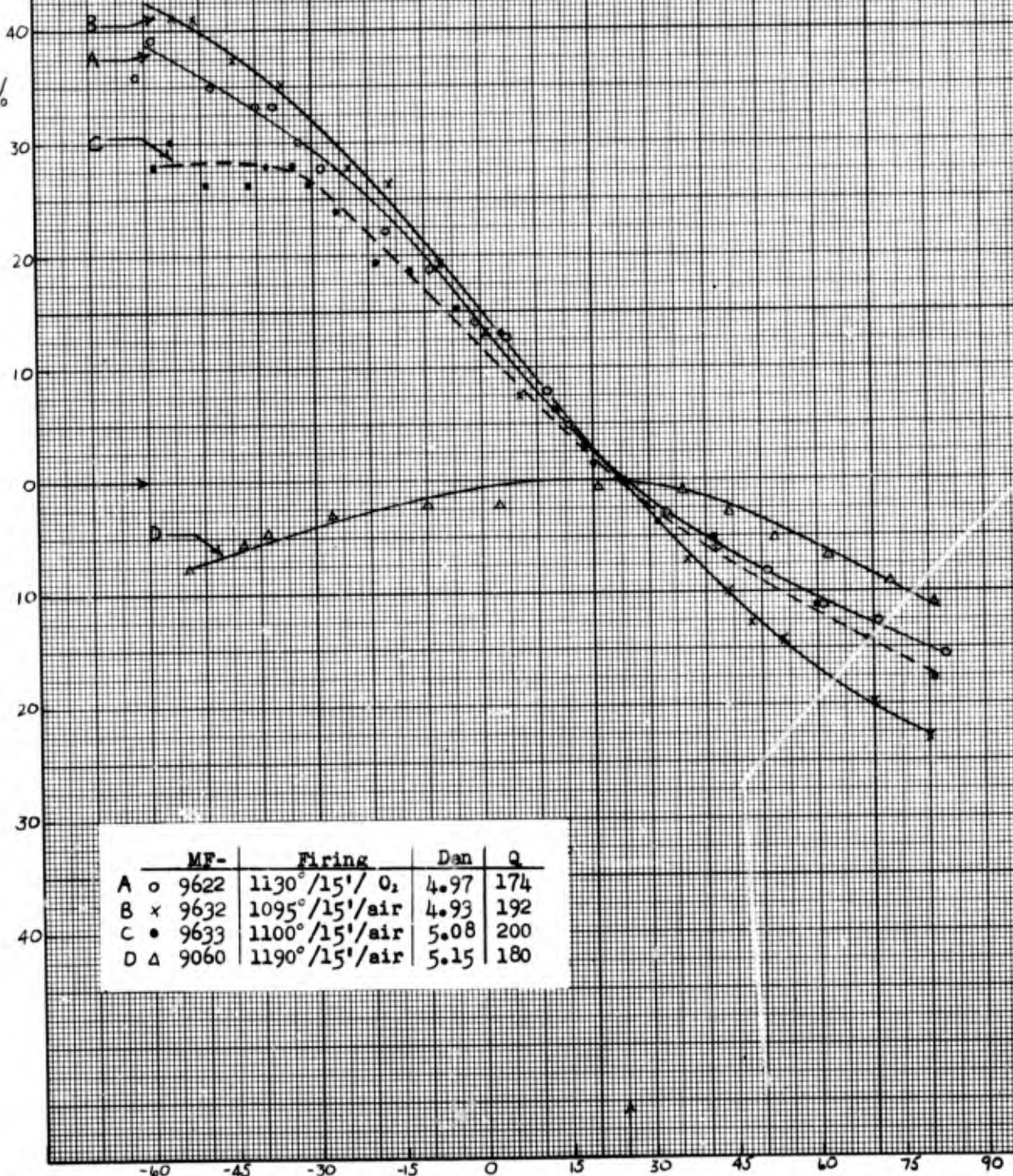


MF-	Firing	TC		TF		Den
		$\frac{\Delta \mu_c}{\mu_c} \%$	(FPM/°C)	$\frac{\Delta \mu_c}{\mu_c} \%$	(Mq/s)	
A ○	1130°/15'/O <sub>2</sub>	132	0.4	33	174	4.97
B ×	1095°/15'/air	185	7.4	25	192	4.93
C ●	1100°/15'/air	0.0	0.0	22.7	200	5.08
D △	1190°/15'/air	96	1.7	57.6	180	5.15

Temp. C

$\frac{\Delta Q}{Q} \%$  vs TEMPERATURE  
for  
Materials MF-9622, -9632, -9633 and -9060

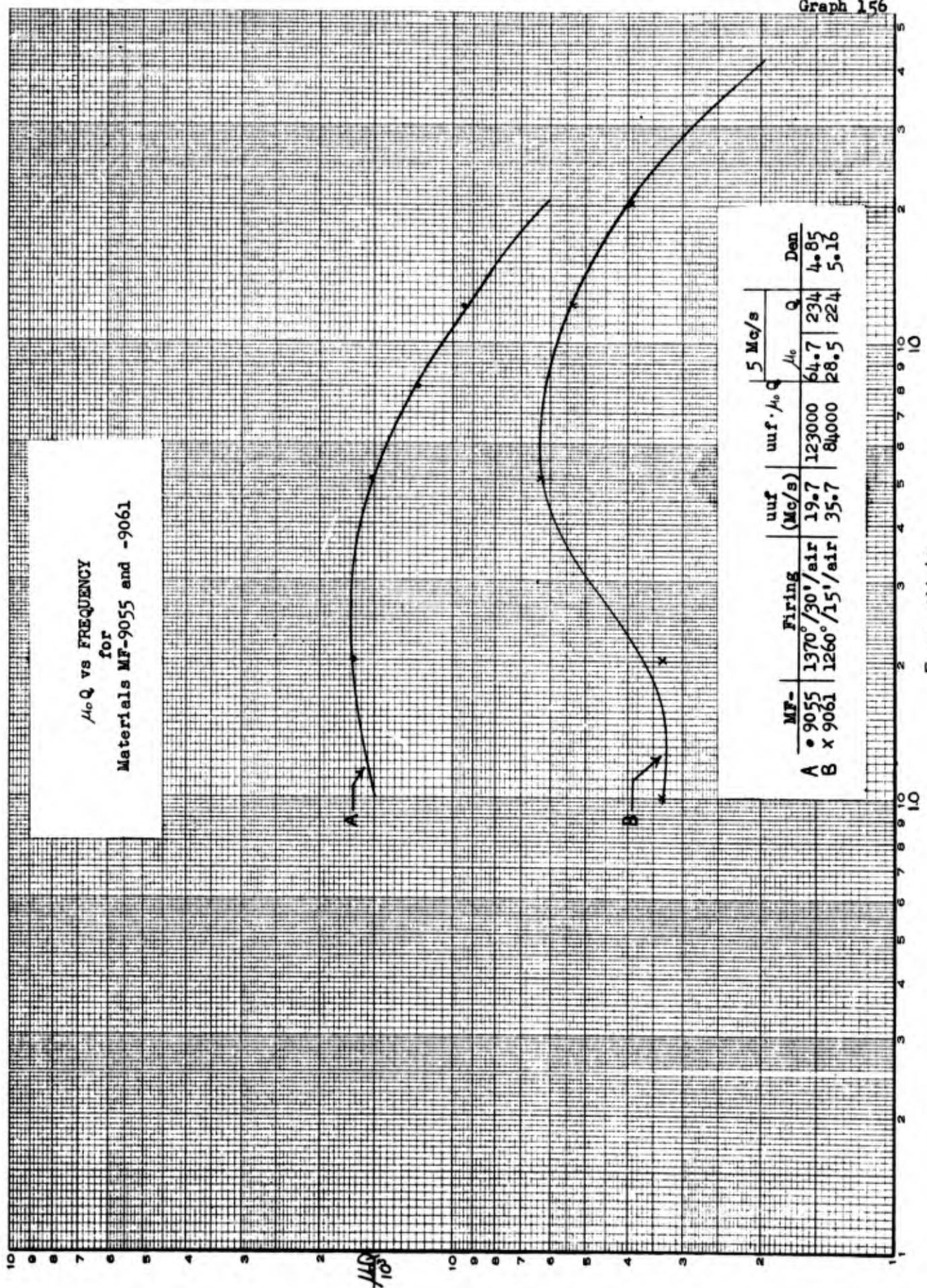
$\frac{\Delta Q}{Q} \%$



	MF-	Firing	Dan	Q
A	○ 9622	1130°/15'/ O <sub>2</sub>	4.97	174
B	× 9632	1095°/15'/air	4.93	192
C	• 9633	1100°/15'/air	5.08	200
D	△ 9060	1190°/15'/air	5.15	180

Temp °C

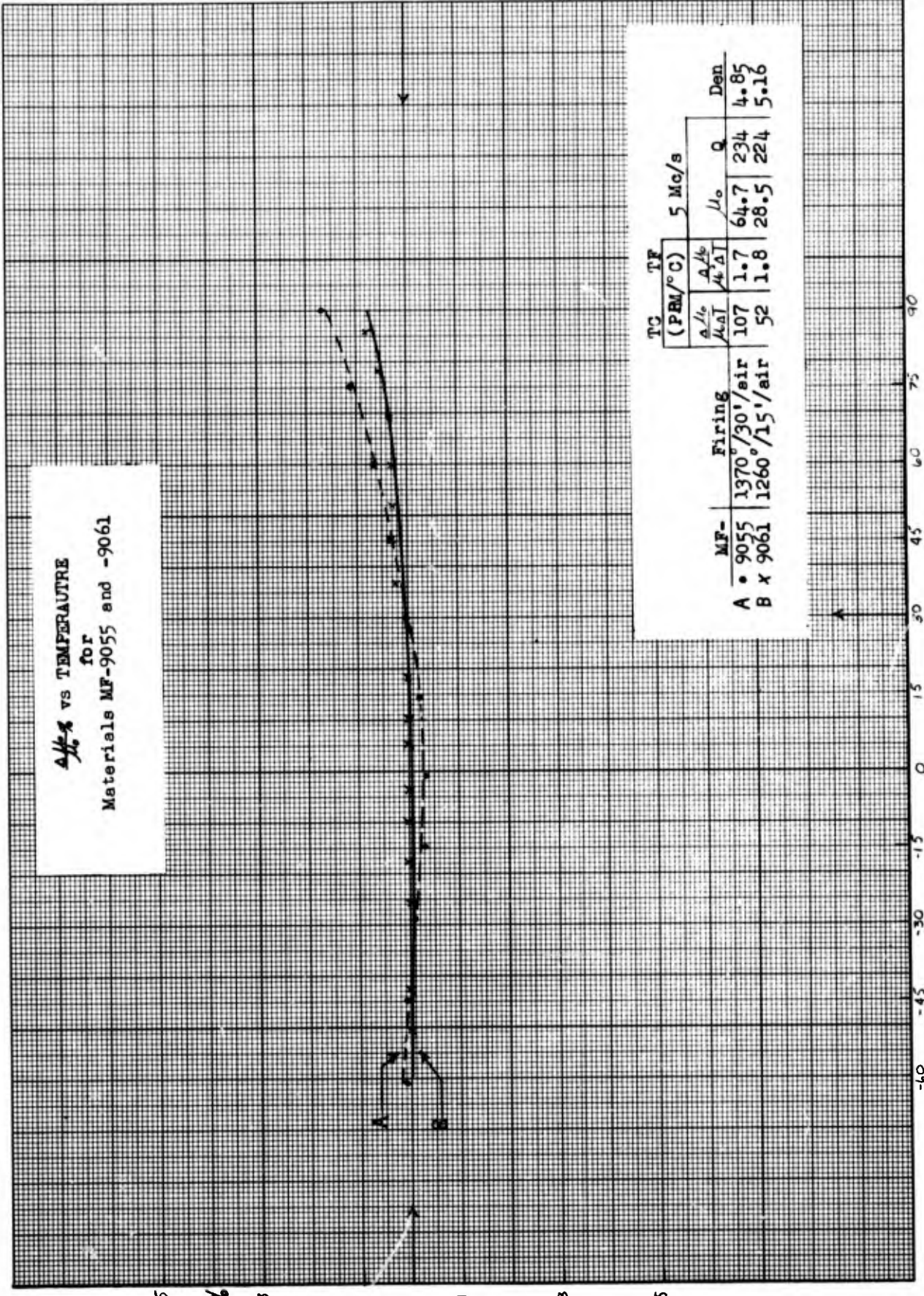
$\mu_c Q$  vs FREQUENCY  
for  
Materials MF-9055 and -9061



MF-	Firing	uuf (Mc/s)	uuf / $\mu_c Q$	5 Mc/s	Den	
				$\mu_c Q$		
A	• 9055 1370°/30'/air	19.7	123000	64.7	234	4.85
B	x 9061 1260°/15'/air	35.7	84000	28.5	224	5.16

Freq (Mc/s)

$\frac{\Delta \mu}{\mu}$  vs TEMPERATURE  
for  
Materials MF-9055 and -9061

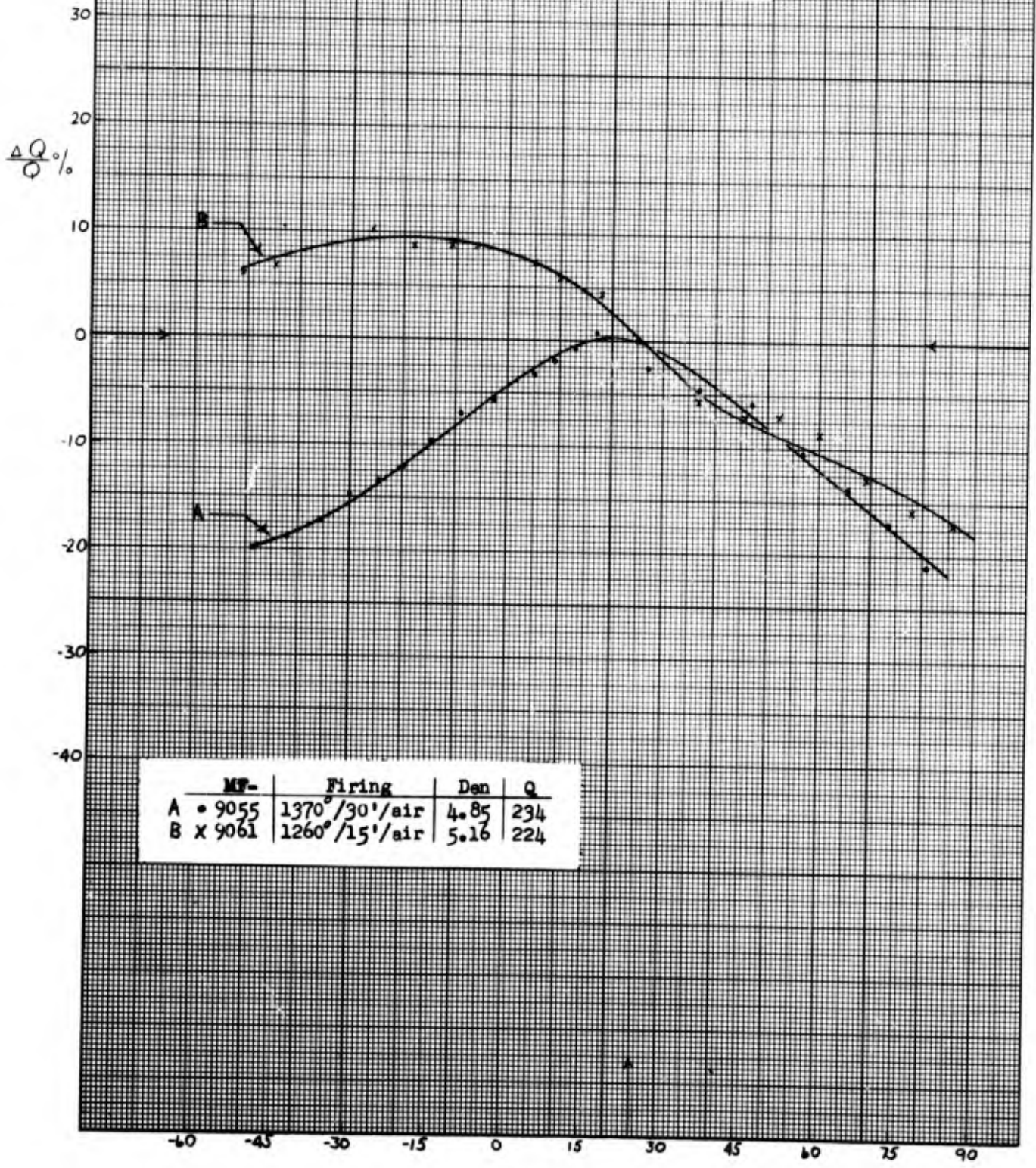


MF-	Firing	TC TF (PRM/°C)		5 Mc/s		Den
		$\frac{\Delta \mu}{\mu}$	$\frac{\Delta \mu}{\Delta T}$	$\mu_0$	Q	
A	1370°/30'/air	107	1.7	64.7	234	4.85
B	1260°/15'/air	52	1.8	28.5	224	5.16

$\frac{\Delta \mu}{\mu}$

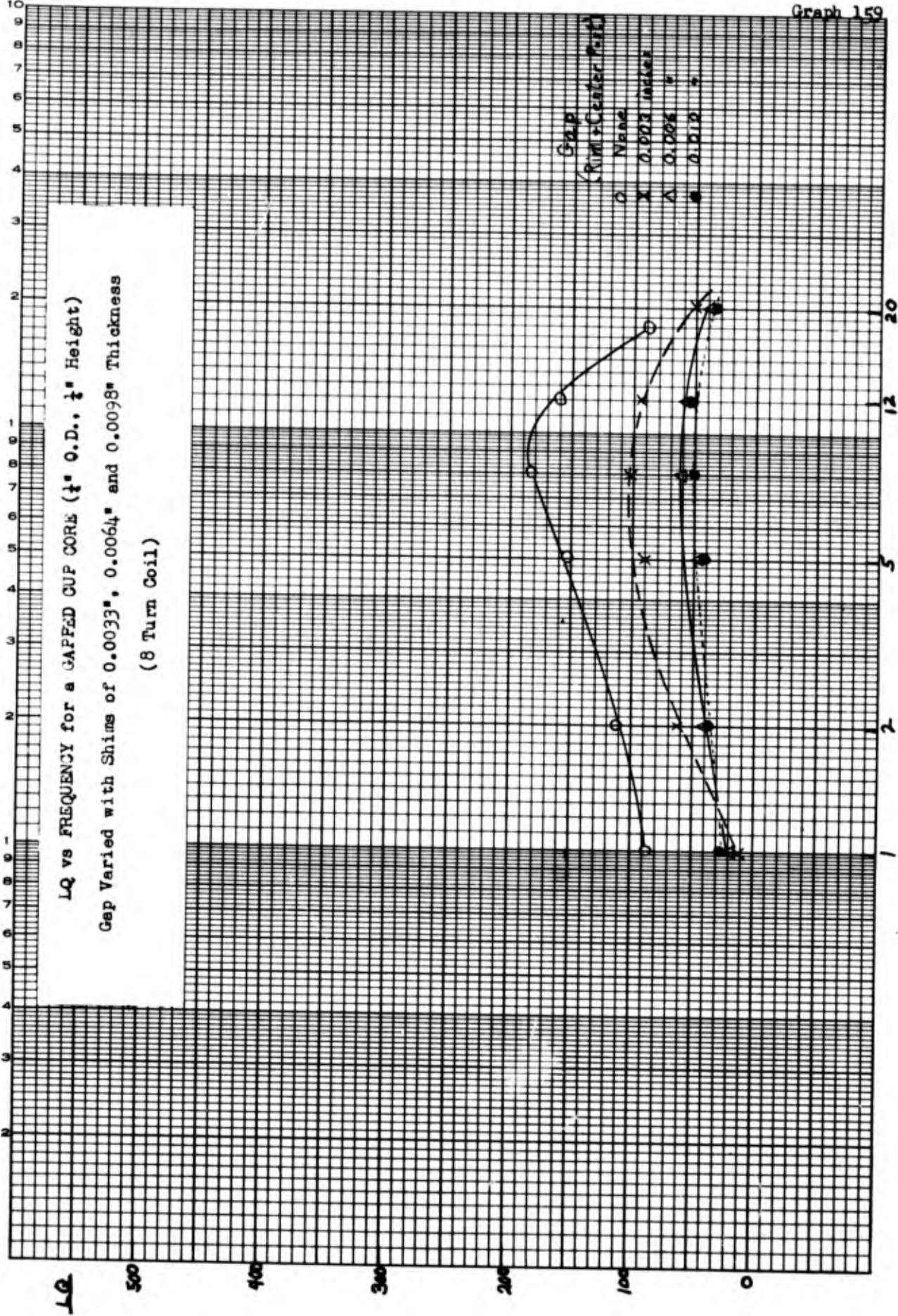
Temp °C

$\frac{\Delta Q}{Q}$  vs TEMPERATURE  
for  
Materials MF-9055 and -9061



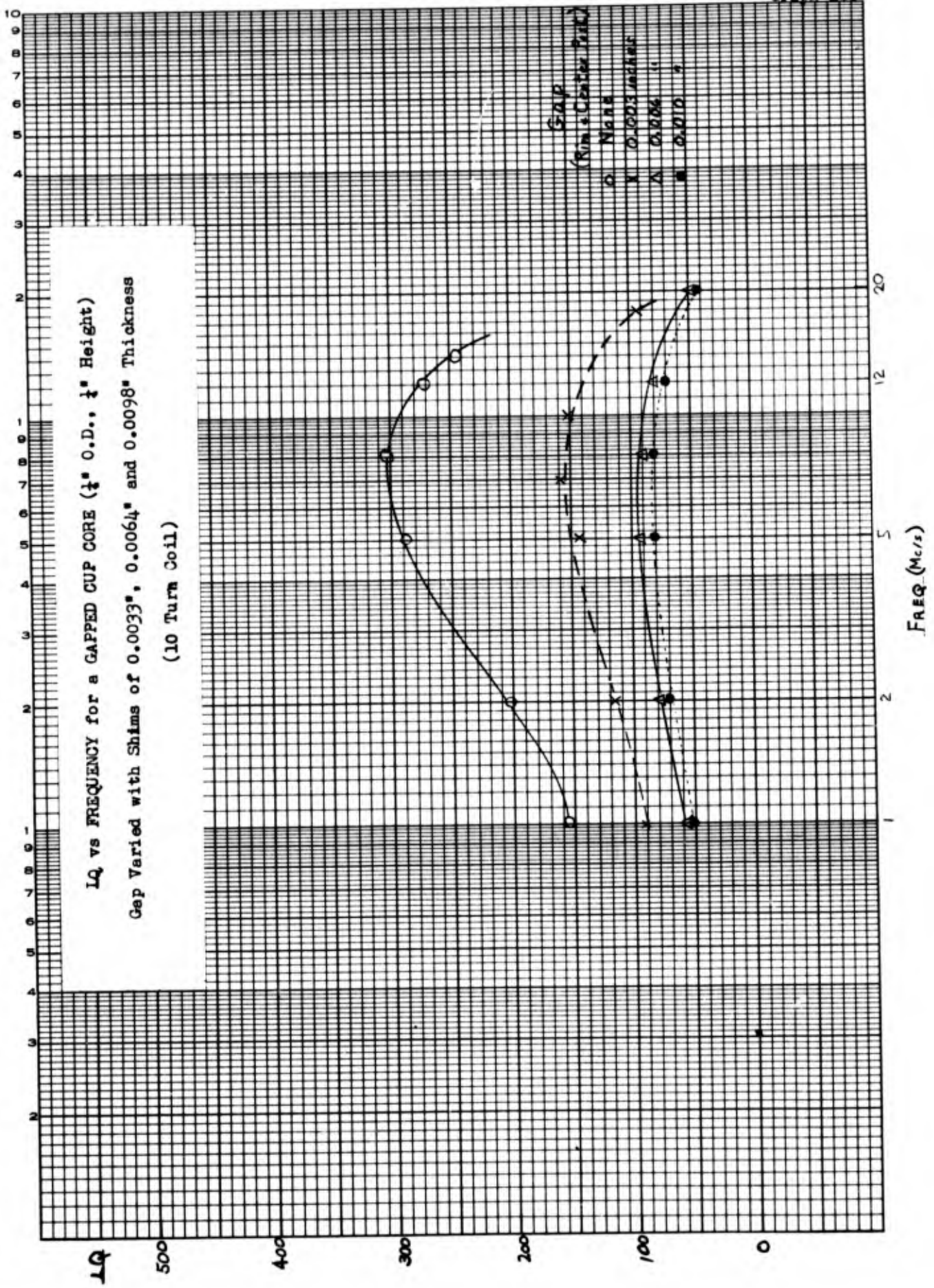
MF-	Firing	Den	Q
A • 9055	1370°/30'/air	4.85	234
B x 9061	1260°/15'/air	5.16	224

Temp °C



FREQ. (Mc/s)

**LQ vs FREQUENCY for a GAPPED CUP CORE ( $\frac{1}{4}$ " O.D.,  $\frac{1}{4}$ " Height)**  
 Gap Varied with Shims of 0.0033", 0.0064" and 0.0098" Thickness  
 (10 Turn Coil)



Gap  
 (Rim & Center Post)

- O 0.0033 inches
- X 0.0064 "
- Δ 0.0098 "

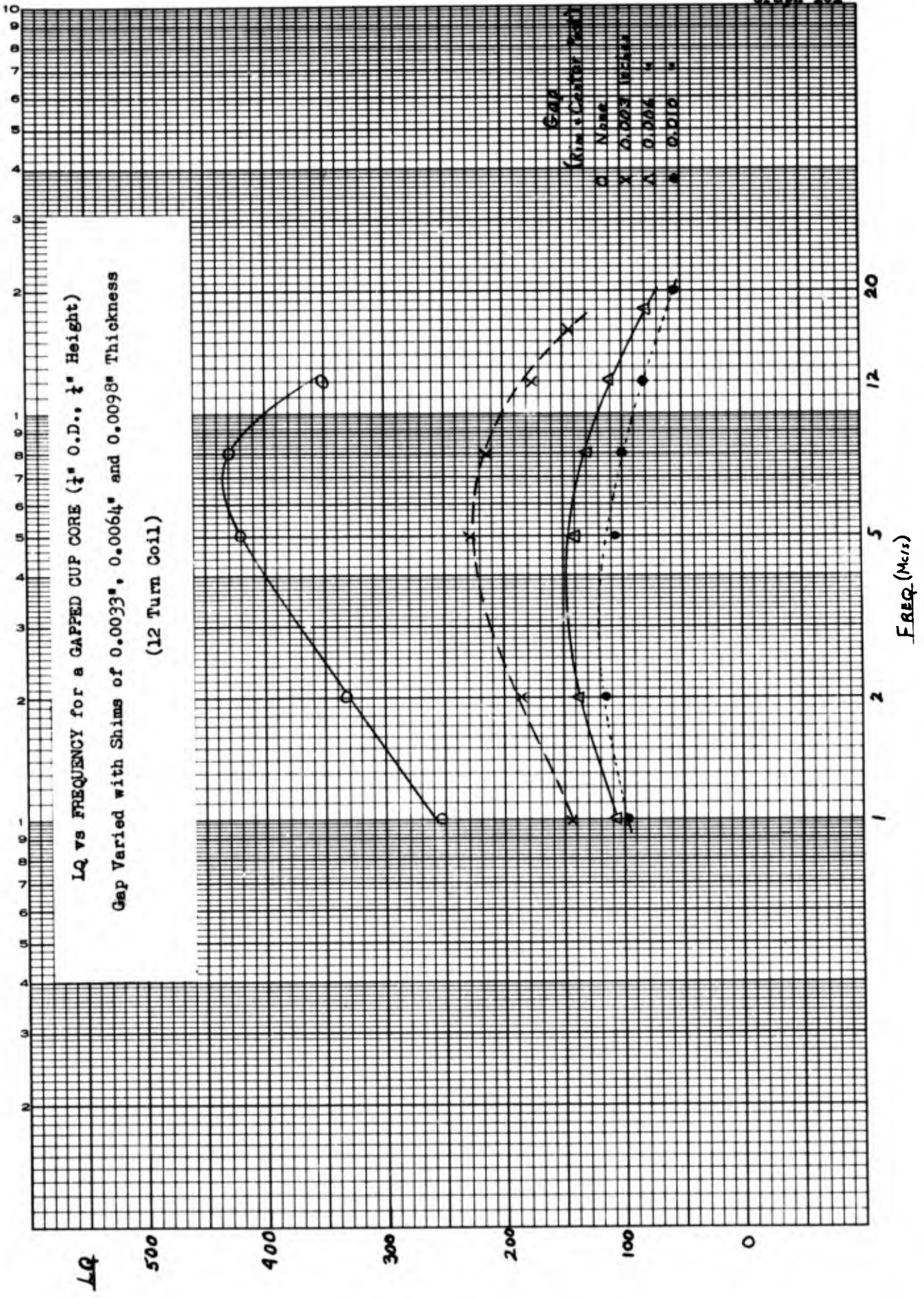
FREQ (Mc/s)

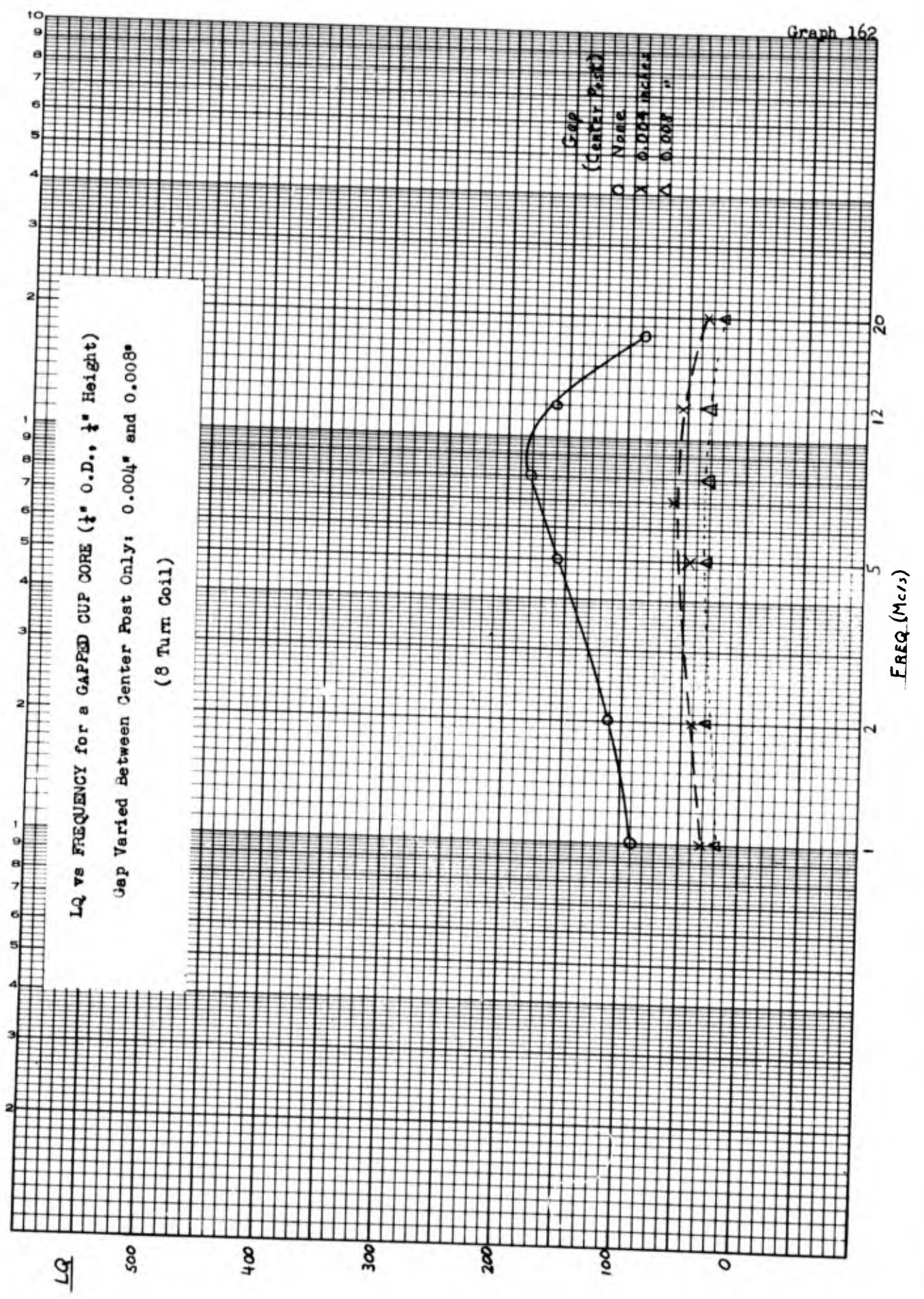
LQ

**LQ vs FREQUENCY for a GAPPED CUP CORE ( $\frac{1}{4}$ " O.D.,  $\frac{1}{2}$ " Height)**  
 Gap Varied with Shims of 0.0033", 0.0064" and 0.0098" Thickness  
 (12 Turn Coil)

Gap  
( $\frac{1}{4}$ " O.D. Center Post)

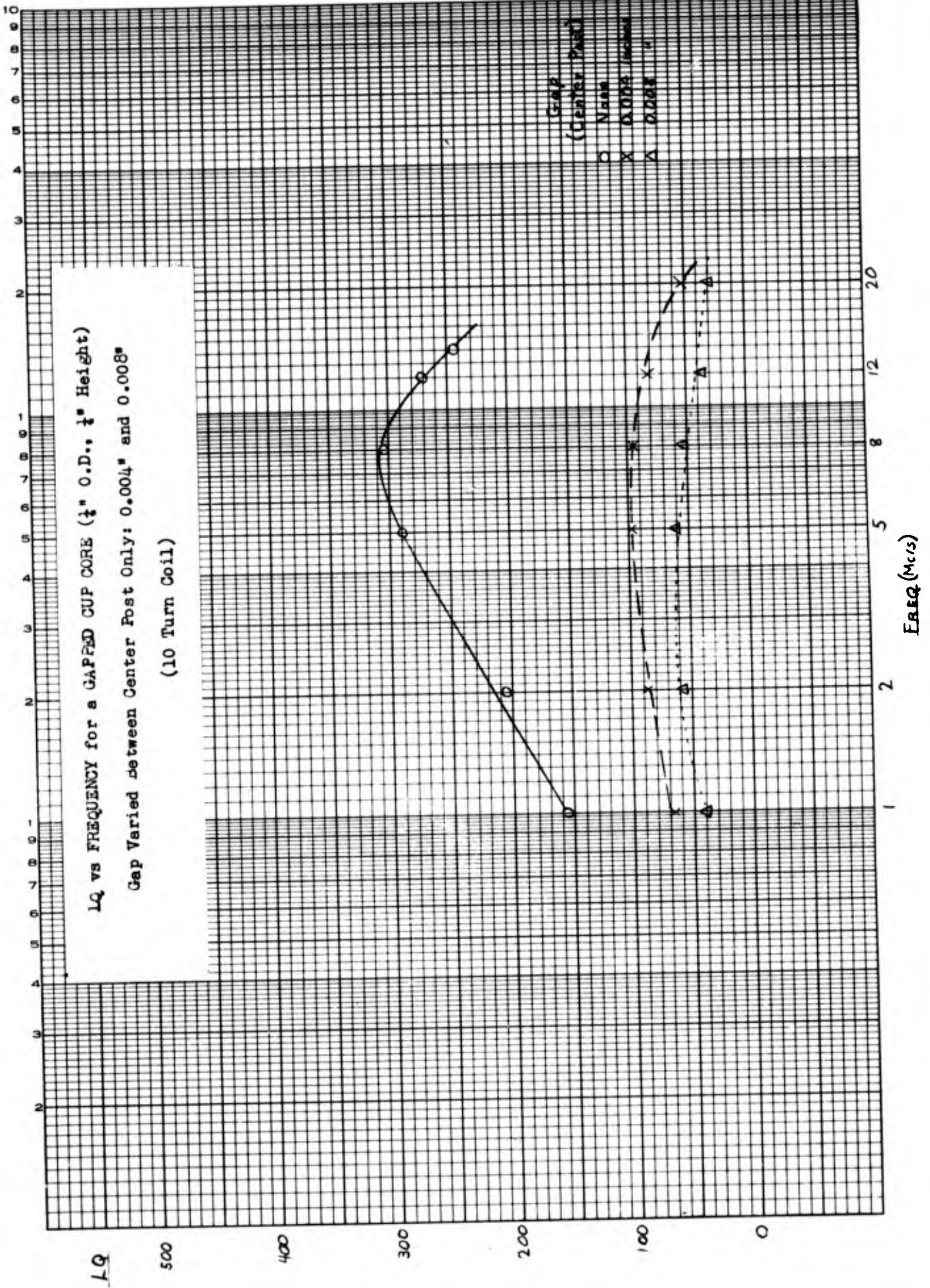
Symbol	Name	Value
O	None	0.0000
X	0.0033	0.0033
Δ	0.0064	0.0064
●	0.0098	0.0098

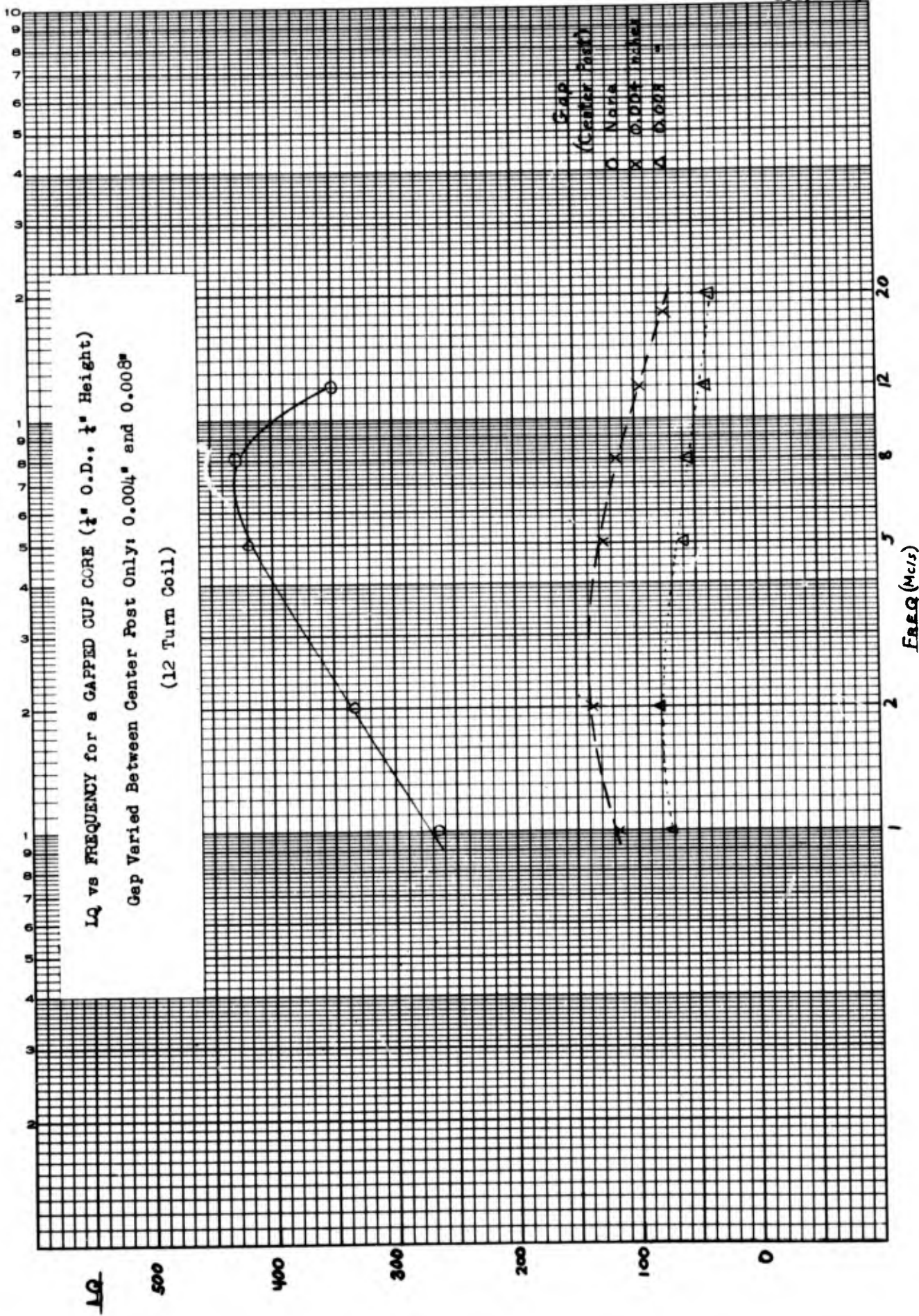




LQ vs FREQUENCY for a GAPPED CUP CORE ( $\frac{1}{2}$ " O.D.,  $\frac{1}{2}$ " Height)  
 Gap Varied between Center Post Only: 0.004" and 0.008"

(10 Turn Coil)





UNITED STATES ARMY ELECTRONICS LABORATORIES  
STANDARD DISTRIBUTION LIST  
RESEARCH AND DEVELOPMENT CONTRACT REPORTS

Copies

- 20 Defense Documentation Center, ATTN: DDC-IRS, Cameron Station (Bldg. 5), Alexandria, Virginia - 22314
- 1 Office of Assistant Secretary of Defense, (Research and Engineering), ATTN: Technical Library, RM 3E1065, Washington, D. C. - 20301
- 1 Chief of Naval Research, ATTN: Code 427, Department of the Navy, Washington, D. C. - 20325
- 1 Naval Ships Systems Command, ATTN: Code 6312 (Technical Library), Main Navy Building, Room 1528, Washington, D. C., 20325
- 1 Naval Ships Systems Command, ATTN: Code 6454, Department of the Navy, Washington, D. C. - 20360
- 2 Director, U. S. Naval Research Laboratory, ATTN: Code 2027, Washington, D. C. - 20390
- 1 Commanding Officer and Director, U. S. Navy Electronics Laboratory, ATTN: Library, San Diego, California - 92101
- 1 Commander, U. S. Naval Ordnance Laboratory, ATTN: Technical Library, White Oak, Silver Spring, Maryland - 20910
- 1 AFSC STLO (RTSND), Naval Air Development Center, Johnsville, Jarminster, Pa. - 18974
- 1 Rome Air Development Center (EMILD), ATTN: Documents Library, Griffiss Air Force Base, New York - 13440
- 1 Systems Engineering Group (SEPIR), Wright-Patterson Air Force Base, Ohio - 45433
- 1 Headquarters, Research & Technology Division, ATTN: RTTC, Bolling AFB, Washington, D. C. - 20332
- 1 Director, Air Force Materials Laboratory, ATTN: MAAM, Wright-Patterson AFB, Ohio - 45433
- 1 Air University Library (3T), Maxwell Air Force Base, Alabama - 36112

(continued)

Copies

- 2 Chief of Research and Development, Department of the Army, Washington, D. C. - 20315
- 2 Commanding General, U. S. Army Materiel Command, ATTN: R&D Directorate, Washington, D. C. - 20315
- 3 Redstone Scientific Information Center, ATTN: Chief, Document Section, U. S. Army Missile Command, Redstone Arsenal, Alabama - 35809
- 1 Headquarters, U. S. Army Munitions Command, Dover, New Jersey - 07801
- 3 Commanding Officer, U. S. Army Combat Developments Command, Communications-Electronics Agency, Fort Monmouth, New Jersey - 07703
- 1 Commander, U. S. Army Research Office (Durham), Box CM-Duke Station, Durham, North Carolina - 27706
- 1 Commanding Officer, U. S. Army Sec Agcy Combat Dev Actv, Arlington Hall Station, Arlington, Virginia - 22212
- 1 U. S. Army Security Agency, ATTN: OACofS, DEV (CDA), Arlington Hall Station, Arlington, Virginia - 22212
- 1 U. S. Army Security Agcy Processing Ctr, ATTN: IAVAPC-R&D, Vint Hill Farms Station, Warrenton, Virginia - 22186
- 1 Harry Diamond Laboratories, ATTN: Library, Connecticut Avenue and Van Ness Street, Washington, D. C. - 20438
- 1 Commanding General, U. S. Army Satellite Comm Agency, ATTN: Technical Documents Center, Fort Monmouth, New Jersey - 07703
- 1 Commanding General, U. S. Army Electronic Proving Ground, ATTN: Technical Information Center, Fort Huachuca, Arizona - 85613
- 1 Asst Secretary of the Army (R&D), Department of the Army, ATTN: Deputy Asst for Army (R&D), Washington, D. C. - 20315
- 1 Commanding Officer, U. S. Army Materials Research Agency, ATTN: Technical Information Center, Watertown, Massachusetts - 13601

Copies

(continued)

- 1 CG, U. S. Army Electronics Command, ATTN: AMSEL-MR,  
225 South 18th Street, Philadelphia, Pa. - 19103
- 1 Chief, Mountain View Office, Electronic Warfare Lab., USAECOM,  
P. O. Box 205, Mountain View, California - 94042
- 1 Chief, Missile Electronic Warfare Tech Area, EW Lab, USA Elec-  
tronics Command, White Sands Missile Range, N. M. - 88002
- 1 Chief, Willow Run Office, CSTA Lab, USAECOM, P. O. Box 618,  
Ann Arbor, Michigan - 48107
- 1 USAECOM Liaison Officer, MIT, Bldg 26, Rm 131, 77 Massachusetts  
Avenue, Cambridge, Massachusetts - 02139
- 1 USAECOM Liaison Officer, Aeronautical Systems Division, ATTN:  
ASDL-9, Wright-Patterson AF Base, Ohio - 45433
- 1 USAECOM Liaison Officer, Rome Air Development Center, ATTN:  
EMPL, Griffiss Air Force Base, New York - 13440

Commanding General, U. S. Army Electronics Command, Fort Mon-  
mouth, New Jersey - 07703

ATTN: 1 AMSEL-TE  
1 AMSEL-PP  
1 AMSEL-IO-T  
1 AMSEL-RD-MAT  
1 AMSEL-RD-MAF (Record Copy)  
1 AMSEL-RD-LNA  
1 AMSEL-RD-LNR  
1 AMSEL-XL-D  
1 AMSEL-NL-D  
1 AMSEL-WL-D  
1 AMSEL-VL-D  
1 AMSEL-HL-CT-D  
1 AMSEL-BL-D  
1 AMSEL-KL-DT  
3 AMSEL-KL-EM

- 2 Advisory Group on Electron Devices, 346 Broadway, 8th Floor, New  
York, New York - 10013
- 1 Project SETE, NYU College of Engineering & Science, 401 W. 205th  
Street (Rsch Bldg 2), New York, New York - 10034
- 2 NASA Scientific & Technical Info Facility, ATTN: Acquisitions  
Branch (S-AK/DL), P. O. Box 33, College Park, Maryland - 20740

UNCLASSIFIED

Security Classification

DOCUMENT CONTROL DATA - R&D		
<i>(Security classification of title, body of abstract and indexing annotation must be entered when the overall report is classified)</i>		
1. ORIGINATING ACTIVITY (Corporate author) Indiana General Corporation Electronics Division Keasbey, New Jersey 08832		2a. REPORT SECURITY CLASSIFICATION Unclassified
3. REPORT TITLE Stable Ferrites for R.F. Applications		2b. GROUP
4. DESCRIPTIVE NOTES (Type of report and inclusive dates) Final Report 1 July 1966 to 31 Dec 1966		
5. AUTHOR(S) (Last name, first name, initial) O'Neill, Charles F. Tenzer, R. K.		
6. REPORT DATE April 1967	7a. TOTAL NO. OF PAGES 92	7b. NO. OF REFS 1
8a. CONTRACT OR GRANT NO. DA 28-043 AMC-00264(E) b. PROJECT NO. 1CO 24401 A 348 00 c. 1CO 24401 A 348 00 03 d.	9a. ORIGINATOR'S REPORT NUMBER(S) 9 9b. OTHER REPORT NO(S) (Any other numbers that may be assigned this report) ECOM-00264-9	
10. AVAILABILITY/LIMITATION NOTICES Each transmittal of this document outside the Department of Defense must have prior approval of CG, US Army Electronics Command, Ft. Monmouth, N.J. Attn: AMSEL-KL-EM.		
11. SUPPLEMENTARY NOTES	12. SPONSORING MILITARY ACTIVITY US Army Electronics Command Fort Monmouth, New Jersey 07703 Attn: AMSEL-KL-EM	
13. ABSTRACT Material MF-9003 originally investigated under a previous Government contract was further developed under the present one. The more or less normal development techniques improved the material somewhat but in regards to stability of $U_0$ and $Q$ , serious deficiencies existed. Silicate additives, notably bentonite, were found to generally improve the stability of $U_0$ and $Q$ ; e.g., one material with 10.25 weight percent bentonite was found capable of yielding a temperature curve of $U_0$ with a TF of 0.7 PPM/°C. This sort of success prompted extensive investigation into additions of the silicate type, and another silicate, lead silicate, was found to give useful and promising results. Evidence is presented supporting the theory that these silicate materials are actually two phase systems. A major problem found associated with the silicate additions was a severe change of $Q$ with temperature. This problem was studied thoroughly and it was found that divalent iron was very closely related to it. Too much divalent iron results in a considerable loss of $Q$ with decreasing temperature and too little divalent iron results in a considerable increase in $Q$ with decreasing temperature. The best $Q$ behavior can be obtained by controlling both the total iron content and the amount of divalent iron. The hypothesis is made that there exists a loss mechanism dependent principally on the thermal energy of the ions and that a second loss mechanism exists which is related to the divalent iron content. The second loss mechanism is apparently dependent on the measuring frequency and total iron content. (see attached sheet)		

DD FORM 1473  
1 JAN 64

UNCLASSIFIED  
Security Classification

UNCLASSIFIED

Security Classification

14. KEY WORDS	LINK A		LINK B		LINK C	
	ROLE	WT	ROLE	WT	ROLE	WT
Ferrite Processing Reliable R.F. Inductors Temperature Stability of $U_0$ and Q Disaccommodation D.C. Field Effects A. C. Field Effects Divalent Iron Effect on Loss Excess Iron Effect on Loss Silicate Additives						

INSTRUCTIONS

1. **ORIGINATING ACTIVITY:** Enter the name and address of the contractor, subcontractor, grantee, Department of Defense activity or other organization (*corporate author*) issuing the report.
- 2a. **REPORT SECURITY CLASSIFICATION:** Enter the overall security classification of the report. Indicate whether "Restricted Data" is included. Marking is to be in accordance with appropriate security regulations.
- 2b. **GROUP:** Automatic downgrading is specified in DoD Directive 5200.10 and Armed Forces Industrial Manual. Enter the group number. Also, when applicable, show that optional markings have been used for Group 3 and Group 4 as authorized.
3. **REPORT TITLE:** Enter the complete report title in all capital letters. Titles in all cases should be unclassified. If a meaningful title cannot be selected without classification, show title classification in all capitals, in parenthesis immediately following the title.
4. **DESCRIPTIVE NOTES:** If appropriate, enter the type of report, e.g., interim, progress, summary, annual, or final. Give the inclusive dates when a specific reporting period is covered.
5. **AUTHOR(S):** Enter the name(s) of author(s) as shown on or in the report. Enter last name, first name, middle initial. If military, show rank and branch of service. The name of the principal author is an absolute minimum requirement.
6. **REPORT DATE:** Enter the date of the report as day, month, year, or month, year. If more than one date appears on the report, use date of publication.
- 7a. **TOTAL NUMBER OF PAGES:** The total page count should follow normal pagination procedures, i.e., enter the number of pages containing information.
- 7b. **NUMBER OF REFERENCES:** Enter the total number of references cited in the report.
- 8a. **CONTRACT OR GRANT NUMBER:** If appropriate, enter the applicable number of the contract or grant under which the report was written.
- 8b, 8c, & 8d. **PROJECT NUMBER:** Enter the appropriate military department identification, such as project number, subproject number, system numbers, task number, etc.
- 9a. **ORIGINATOR'S REPORT NUMBER(S):** Enter the official report number by which the document will be identified and controlled by the originating activity. This number must be unique to this report.
- 9b. **OTHER REPORT NUMBER(S):** If the report has been assigned any other report numbers (*either by the originator or by the sponsor*), also enter this number(s).

10. **AVAILABILITY/LIMITATION NOTICES:** Enter any limitations on further dissemination of the report, other than those imposed by security classification, using standard statements such as:

- (1) "Qualified requesters may obtain copies of this report from DDC."
- (2) "Foreign announcement and dissemination of this report by DDC is not authorized."
- (3) "U. S. Government agencies may obtain copies of this report directly from DDC. Other qualified DDC users shall request through \_\_\_\_\_."
- (4) "U. S. military agencies may obtain copies of this report directly from DDC. Other qualified users shall request through \_\_\_\_\_."
- (5) "All distribution of this report is controlled. Qualified DDC users shall request through \_\_\_\_\_."

If the report has been furnished to the Office of Technical Services, Department of Commerce, for sale to the public, indicate this fact and enter the price, if known.

11. **SUPPLEMENTARY NOTES:** Use for additional explanatory notes.
12. **SPONSORING MILITARY ACTIVITY:** Enter the name of the departmental project office or laboratory sponsoring (*paying for*) the research and development. Include address.
13. **ABSTRACT:** Enter an abstract giving a brief and factual summary of the document indicative of the report, even though it may also appear elsewhere in the body of the technical report. If additional space is required, a continuation sheet shall be attached.

It is highly desirable that the abstract of classified reports be unclassified. Each paragraph of the abstract shall end with an indication of the military security classification of the information in the paragraph, represented as (TS), (S), (C), or (U).

There is no limitation on the length of the abstract. However, the suggested length is from 150 to 225 words.

14. **KEY WORDS:** Key words are technically meaningful terms or short phrases that characterize a report and may be used as index entries for cataloging the report. Key words must be selected so that no security classification is required. Identifiers, such as equipment model designation, trade name, military project code name, geographic location, may be used as key words but will be followed by an indication of technical context. The assignment of links, rules, and weights is optional.

UNCLASSIFIED

Security Classification

Document Control Data - R&D  
Indiana General Corporation, cont'd

Abstract

The silicate containing materials were further improved by adding thorium nitrate. Q values were generally increased and the dependence of Q on temperature was lowered. In the case of lead silicate additions, the value of Q at frequencies below 5 Mc/s was greatly improved; sufficient in fact to make the material MF-9060 the most promising material investigated.

Cup core properties were evaluated in comparison with toroidal properties and a very favorable correlation was found.  $\mu_0$  and Q values equal to those of toroids can be attained in an ungapped cup core shape. Gapping was found to result in lower Q values and in lower inductances.

Overall, material MF-9060 (containing lead silicate and thorium nitrate), is probably the best material developed. Although MF-9060 hasn't been fully evaluated from a stability point of view, its  $\mu_0$  and Q properties are good; it has a relatively low temperature dependence of Q, which can undoubtedly be made smaller; and it has a temperature dependence of  $\mu_0$  which is relatively small and linear (96 PPM/°C). The fact that it is linear means that compensation techniques can be employed. In the case of the body discussed in the report, a ceramic capacitor with a temperature coefficient of -96 PPM/°C could be used.

In summary, while materials were developed which meet some of the contract requirements, none of the materials completely fulfill the requirements as specified.

ERRATA SHEET

Indiana General Corp.  
Final Report  
DA 28-043 AMC-00264(E)

Eighth Quarterly Report 1 Apr 66 to 30 June 66

On cover and title page:

"Technical Report ECOM-00246-8" and  
"Contract DA-28-043-AMC-00246(E)"

should read

"Technical Report ECOM-00264-8" and  
"Contract DA-28-043-AMC-00264(E)", respectively.